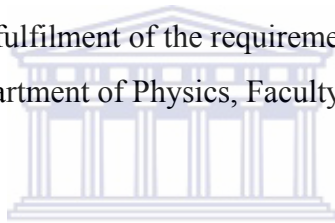


# **RADON ESCAPE FROM WATER**

MASHINGA JOHANNES MVELASE

A thesis submitted in partial fulfilment of the requirements for the degree of Magister  
Scientiae at the Department of Physics, Faculty of Natural Sciences,



UNIVERSITY *of the*  
WESTERN CAPE

University of the Western Cape,  
Private Bag X17,  
Bellville,  
7535

Supervisor: Prof. R. Lindsay

November 2010

## KEYWORDS

### RADON ESCAPE FROM WATER

Mashinga Johannes Mvelase



Radon

Degassing

Transfer velocity

Ostwald coefficient

Radon detection

Pressure effects

Temperature effects

Alpha detection

Diffusion

## DECLARATION

I, the undersigned, declare that the work contained in this thesis, ***RADON ESCAPE FROM WATER***, is my original work and has not previously in its entirety or part been submitted at any university for a degree, and that all the sources I have used or quoted have been indicated and acknowledged by complete references.

**Signature:**.....

**Date:**.....



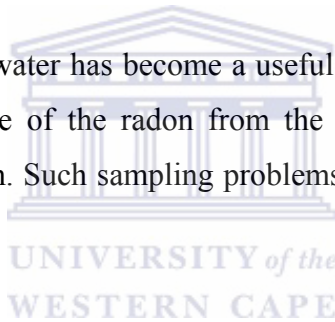
# ABSTRACT

## RADON ESCAPE FROM WATER

Mashinga Johannes Mvelase

M.Sc. full thesis, Department of Physics, University of the Western Cape

The measurement of radon in water has become a useful tool in the application of radon as a natural tracer. The escape of the radon from the water before the radon can be measured is a constant problem. Such sampling problems have been of major concern in the use of radon a tracer.



This thesis aims to measure the rate of radon loss from water in a systematic way. The dependence on surface area, temperature and concentration will be investigated. The experiments were done at UWC by creating radon using radium sources and then measuring the radon concentrations inside a vacuum chamber to obtain the speed of radon escape from the water.

The results are compared to a model [Cal 2002] where the radon concentration in the air and hence the transfer rate is measured using a RAD7 radon detector. Since the equations cannot be solved analytically, a numerical solution is employed. The radon transfer velocity coefficient is found to be  $(1.9 \pm 0.5) \times 10^{-6} \text{ m/s}$ . This value indicates that the escape of radon should not be a problem when a sample is open to the air for a minute or two.

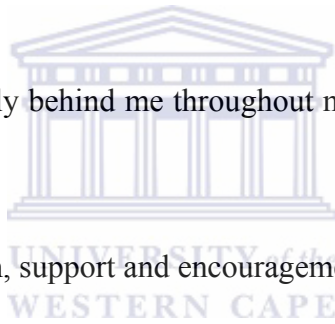
November 2010

## ACKNOWLEDGEMENTS

I would like to acknowledge with gratitude the following highlighted people and departments for making my studies a real success:

**Prof Robbie Lindsay**, my supervisor, for his guidance, his availability in times of need and willingness to help.

My **family** for remaining solidly behind me throughout my studies and for their patience and undying support.



My **friends** for their motivation, support and encouragement throughout my studies.

The financial contribution from the **National Research Foundation** through the **Department of Labour Scarce Skills Master's Scholarship**.

The **Physics Department of UWC**, for selecting me to be part of this programme and for the kind support and assistance from the beginning right to the end of the study. The support by **University Work-Study programme** is worth mentioning since it really helped me.

# TABLE OF CONTENTS

|   |             |
|---|-------------|
| <b>RADON ESCAPE FROM WATER.....</b>                               | <b>I</b>    |
| <b>KEYWORDS.....</b>  | <b>II</b>   |
| <b>DECLARATION.....</b>   | <b>III</b>  |
| <b>ABSTRACT.....</b>  | <b>IV</b>   |
| <b>ACKNOWLEDGEMENTS .....</b>                                     | <b>V</b>    |
| <b>TABLE OF CONTENTS .....</b>                                    | <b>VI</b>   |
| <b>LIST OF FIGURES .....</b>                                      | <b>VIII</b> |
| <b>LIST OF TABLES .....</b>                                       | <b>X</b>    |
| <b>CHAPTER 1 – BACKGROUND AND MOTIVATION.....</b>                 | <b>1</b>    |
| 1.1. Introduction.....  | 1           |
| 1.1.1. Radon in water .....                                       | 1           |
| 1.2. Thesis outline.....  | 4           |
| 1.3. Background to radon.....                                     | 4           |
| 1.3.1. Physical and chemical properties of radon .....            | 4           |
| 1.4. Radiation in general .....                                   | 7           |
| 1.4.1. The background to radiation .....                          | 7           |
| 1.4.2. Alpha Radiation .....                                      | 8           |
| 1.4.3.1. Beta minus decay .....                                   | 11          |
| 1.4.3.2. Beta plus decay .....                                    | 11          |
| 1.4.4. Gamma Radiation .....                                      | 11          |
| 1.5. The Attenuation of radiation by matter.....                  | 12          |
| 1.6. The radioactive decay laws.....                              | 15          |
| <b>CHAPTER 2 - THE APPLICATIONS AND DANGERS OF RADON.....</b>     | <b>16</b>   |
| 2.1. Radon and research in groundwater.....                       | 16          |
| 2.1.1. Formation of radon in groundwater .....                    | 16          |
| 2.1.2. The use of radon as a hydro-geochemical tracer .....       | 18          |
| 2.1.3. Radiological effects of radon to humans .....              | 19          |
| 2.1.3.1. Natural exposure to background radiation.....            | 19          |
| 2.1.3.3. Health effects of radon progenies and tobacco smoke..... | 20          |
| 2.2. The sources of radon.....                                    | 21          |

|   |           |
|---|-----------|
| 2.3. Radon accumulation in houses.....                                      | 22        |
| <b>CHAPTER 3 – INSTRUMENTS AND INTRODUCTION TO MODELLING.....</b>           | <b>24</b> |
| 3.1. The RAD7.....  | 24        |
| 3.2. RAD-H <sub>2</sub> O.....  | 25        |
| 3.3. Vacuum Chamber.....  | 27        |
| 3.4. Laboratory prepared water samples.....                                 | 29        |
| 3.4.1. The collection of water samples.....                                 | 29        |
| 3.4.2. Alpha emitting source.....   | 29        |
| 3.5. Modelling of radon escape from water.....                              | 30        |
| 3.5.1. Background to diffusion.....   | 30        |
| 3.5.2. Theory and parameters considering diffusion of radon from water..... | 32        |
| 3.5.3. The diffusion equation.....  | 33        |
| 3.5.4. The development of the numerical model.....                          | 36        |
| <b>CHAPTER 4 – EXPERIMENTAL METHODS AND RESULTS.....</b>                    | <b>38</b> |
| 4.1. Radon measurement using the Vacuum Chamber method.....                 | 38        |
| 4.1.1. Example of radon escape from water to air.....                       | 39        |
| 4.1.2. The effect of the area of water/air interface on radon escape.....   | 43        |
| 4.1.3. The effect of temperature on radon escape from water.....            | 51        |
| 4.2. Field water samples measured with the RAD-H <sub>2</sub> O.....        | 55        |
| <b>CHAPTER 5 - MODELLING THE DIFFUSION OF RADON.....</b>                    | <b>59</b> |
| 5.1. Modelling the experimental data.....                                   | 59        |
| 5.1.1. The curves of the numerical model.....                               | 59        |
| 5.1.2. The results of the numerical modelling.....                          | 60        |
| 5.2. Results and uncertainty analysis.....                                  | 63        |
| 5.3. Results and Discussion.....  | 64        |
| 5.3.1. Results.....   | 64        |
| 5.3.2. Discussion.....  | 66        |
| <b>CHAPTER 6 - RESULTS AND DISCUSSION.....</b>                              | <b>68</b> |
| 6.1. Results from measurements.....   | 68        |
| 6.1.1. Vacuum Chamber.....  | 68        |
| 6.1.1.1. The effect of the water-air interface area on radon escape.....    | 68        |
| 6.1.1.2. The effect of temperature on radon escape from water.....          | 69        |
| 6.1.2. RAD-H <sub>2</sub> O.....  | 69        |
| 6.2. Results from numerical modelling.....                                  | 70        |
| <b>CHAPTER 7 - CONCLUSION.....</b>  | <b>71</b> |
| 7.1. Experimental results.....  | 71        |
| 7.2. Modelling result.....  | 72        |
| APPENDICES.....   | 73        |
| REFERENCES.....   | 87        |
| NOMENCLATURE.....   | 96        |
| GLOSSARY.....   | 97        |

## LIST OF FIGURES

|  |    |
|--|----|
| <b>Figure 1.1:</b> Sources and average distributions of background exposure. ....  | 7  |
| <b>Figure 1.2:</b> Plot of proton number (Z) versus neutron number (N). ....   | 10 |
| <b>Figure 1.3:</b> The intensity of radiation reduces after passing through the matter .....                                       | 13 |
| <b>Figure 1.4:</b> The diagram showing penetrating strength of radiation.....  | 14 |
| <b>Figure 2.1:</b> The cross section of crust showing of hydrogeological formation. ....   | 17 |
| <b>Figure 2.2:</b> The path of radon into a building.....  | 23 |
| <b>Figure 3.1:</b> The RAD7 and a printer .....  | 25 |
| <b>Figure 3.2:</b> The RAD-H <sub>2</sub> O connected to RAD7.....   | 26 |
| <b>Figure 3.3:</b> The example of solubility of radon at different temperatures.....   | 28 |
| <b>Figure 3.4:</b> The experimental set up of the Vacuum Chamber method.....   | 28 |
| <b>Figure 3.5:</b> The preparation of alpha emitting source.....   | 30 |
| <b>Figure 4.1:</b> Radon at water-air interface in the container .....   | 38 |
| <b>Figure 4.2:</b> The diffusion of radon atoms from water to air in the chamber .....   | 40 |
| <b>Figure 4.3 (a):</b> The radon activity concentration in the air versus time with error bars ..                                  | 41 |
| <b>Figure 4.3 (b):</b> The radon activity concentration in the air without error bars.....   | 41 |
| <b>Figure 4.4 (a):</b> The radon activity concentration in the air above a vial versus time. ....                                  | 45 |
| <b>Figure 4.4 (b):</b> The ratio of the radon flux ( $\lambda/\beta$ ) from the vial versus the time. ....                         | 45 |
| <b>Figure 4.4 (c):</b> The radon flux divided by $\beta C_0$ versus time for escape from the vial. ....                            | 46 |
| <b>Figure 4.5 (a):</b> The radon activity concentration in the air above the 500 mL Al can<br>versus the time. ....                | 46 |
| <b>Figure 4.5 (b):</b> The ratio of the radon flux ( $\lambda/\beta$ ) from the Al can versus time.. ....                          | 47 |
| <b>Figure 4.6 (a):</b> The radon activity concentration in the air above a beaker versus time..                                    | 47 |
| <b>Figure 4.6 (b):</b> The radon flux( $\lambda/\beta$ ) from the beaker versus the time for three initial<br>concentrations. .... | 48 |



**Figure 4.7:** Examples of the radon activity concentration from each container versus time ..... 48

**Figure 4.8:** The ratio of radon flux to  $\beta$  from three containers versus time..... 49

**Figure 4.9 (a):** The radon experiment before the introduction of the ice ..... 52

**Figure 4.9 (b):** The whole Vacuum Chamber immersed in ice in bowl ..... 53

**Figure 4.10:** The water temperature and radon concentration versus time..... 54

**Figure 5.1 (a):** The experimental and model radon concentration values for the  $\beta$  value that best fits the experimental data..... 60

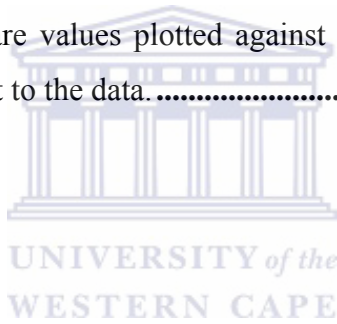
**Figure 5.1 (b):** Same as **Fig. 5.1(a)** for a different initial radon concentration ..... 61

**Figure 5.1 (c):** Same as **Fig. 5.1(a)** for a different initial radon concentration..... 61

**Figure 5.1 (d):** Same as **Fig. 5.1(a)** for a different initial radon concentration ..... 62

**Figure 5.1 (e):** Same as **Fig. 5.1(a)** for a different initial radon concentration..... 62

**Figure 5.2:** The total chi-square values plotted against the beta values for Fig. 5.1(b). The curve is a quadratic fit to the data..... 65



## LIST OF TABLES

|  |           |
|--|-----------|
| <b>Table 1:</b> The uranium-238 decay series and its radiation types.....  | <b>6</b>  |
| <b>Table 2:</b> Tabulated data on radiation characteristics.....   | <b>14</b> |
| <b>Table 3:</b> Radioactive gas types in heavy metal transformation .....  | <b>22</b> |
| <b>Table 4:</b> Radon concentration in water samples .....   | <b>57</b> |
| <b>Table 5:</b> The parameters used in the numerical modelling and the results obtained. See discussion in section 5.2 on uncertainties..... | <b>63</b> |
| <b>Table 6:</b> The transfer velocity coefficient of radon deduced from model fits. ....   | <b>66</b> |
| <b>Table 7:</b> The approximate areas and volumes of the containers used in the study .....  | <b>73</b> |
| <b>Table 8:</b> Experimental data for graphs shown on Fig. 4.3 .....   | <b>74</b> |
| <b>Table 9:</b> Experimental data for use in modelling Fig. 5 (a).....   | <b>76</b> |
| <b>Table 10:</b> Experimental data for use in modelling Fig 5 (b).....   | <b>78</b> |
| <b>Table 11:</b> Experimental data for use in modelling Fig. 5 (c).....  | <b>80</b> |
| <b>Table 12:</b> Experimental data for use in modelling Fig 5 (d).....   | <b>82</b> |
| <b>Table 13:</b> Experimental data for use in modelling Fig. 5(e).....   | <b>84</b> |



UNIVERSITY *of the*  
WESTERN CAPE

# CHAPTER 1 – BACKGROUND AND MOTIVATION

## 1.1. Introduction

### 1.1.1. Radon in water

The applications of radon span many research fields. The importance of the knowledge regarding radon in water is not only confined to radiation protection issues but also in its use for studying geological and hydrogeological characteristics of the environment (Somlai *et al.*, 2007). The study of submarine groundwater discharge involves the use of radon as a natural tracer (Burnett *et al.*, 2006; Waska. *et al.*, 2008; Lee *et al.*, 2006). Since the groundwaters are rich in radon as compared to surface waters (Burnett *et al.*, 2010; Dulaiova *et al.*, 2007; Marques *et al.*, 2004), the discharge of groundwaters into open water bodies like oceans, lakes and rivers can be noted by high concentration of radon in water. This thesis studies the escape of radon from water, an important issue for radon in water measurements.

The investigations of the exchange of surface water and groundwater using natural radioactive isotope techniques have recently become increasingly common (Wu *et al.*, 2004). The expanding concern about the radiological health risks posed by waterborne radon progenies attracts many researchers to this field of research, as does the use of radon as a fresh water tracer (Waska *et al.*, 2008; Burnett *et al.*, 2010) in groundwater discharge.

Radon is a naturally occurring radioactive noble gas that forms in rocks and soils from the decays of  $^{238}\text{U}$  via  $^{226}\text{Ra}$ . The significant radon concentrations in seawater may signal the seepage of groundwater into the sea. It is therefore important that proper knowledge of the radon transfer velocity from water to air during measurement is understood, to

avoid overestimation or underestimation of the gas in the water sample. The applications of radon imply that good techniques for measuring radon are required. This thesis discusses the escape of radon from water, which influences such measurements.

Radium, the predecessor of radon, is soluble in water and it decays to radon. Radium spends much time in contact with water as it is embedded in rocks and dissolves in the water occupying the fracture spaces. Radon from the decay of radium in the soil grains can also enter the pore space in the soil and dissolve in the groundwater. As a result, most groundwaters are highly enriched in  $^{222}\text{Rn}$  as compared to open water bodies of water from which radon escapes into the atmosphere. This notion is applied to identify groundwater inputs to surface waters based on their  $^{222}\text{Rn}$  concentration differences (Pates *et al.*, 2007).

The radium in groundwater, which decayed from  $^{238}\text{U}$  in rocks (Schmidt *et al.*, 2008) ultimately reaches houses with groundwater (Aghamiri *et al.*, 2006) when water is pumped from boreholes for household activities. Radon also diffuses from the soils and enters houses through foundation cracks. Its radiations are the main cause of radiological risk indoors. The exposure to high radon radiation has a carcinogenic effect to human organs thus radon dissolved in groundwaters brings concern to the residents (Waska. *et al.*, 2008) since it delivers both inhalation and ingestion radiological risks. The radiation from radon and radon progenies pose the largest radiation exposure to the population in the world among all the naturally existing radiation sources (Picolo *et al.*, 2000; Jones and Childers, 1990; Prasad *et al.*, 2008).

The noble gases are a reliable tool for studying the origin and processes involving fluids during their ascent to the surface (Walia *et al.*, 2005). Radon is used to study hydrological and geological events taking place in the crust. Since radon is chemically inert, it is used as an environmental tracer in hydrology, geochemistry and oceanography to track the influx of fresh water that discharges into the coastal ocean (Dimova *et al.*, 2007).

The applications described above, indicate the importance of accurate radon in water measurements. Knowledge of the rate of radon loss from water is thus very important. In this thesis, water samples were pumped from boreholes, fetched from a river and prepared in a laboratory to be able to study the  $^{222}\text{Rn}$  escape from water. The preparation of water samples in the laboratory saved time and effort. In boreholes, the stagnant water column, where radon had decayed, was flushed for 80 minutes before collecting the characteristic water samples containing more radon. Those water samples were then taken to the laboratory within a short time to avoid too much decay of radon before analysis.

The laboratory-preparation of water samples was conducted in the Physics Laboratory at the University of the Western Cape. Three  $^{226}\text{Ra}$  sources, each of activity 185 kBq, were tied together and attached to the wall of a 500 mL aluminium can, and suspended over the water. The can was then tightly closed to avoid radon leakage during the period of accumulation. The sample was kept for about two days to make a water sample of high radon activity concentration. As the radium decays, the released radon enters the air and partly dissolves in the water in the container. The typical values of dissolved radon activity concentrations in the water that were reached were in the range 10-1600 kBq/m<sup>3</sup>. These radon activities are similar or higher than those found in drilled wells and groundwaters (Cosma *et al.*, 2008; Amrani *et al.*, 1999; Nazaroff *et al.*, 1987).

The radon activity concentration in water was measured with different methods. The RAD-H<sub>2</sub>O measurement method, and by measuring radon in the air in a vacuum chamber which was the main method since the objective was to measure radon that escapes from water to air. In that way, the radon escape from water to air could be monitored for many hours. The borehole and river water samples were analyzed using a RAD-H<sub>2</sub>O system that uses the internal pump of the RAD7 radon detector (see Chapter 3) to strip radon from a 250 mL vial and circulate it back to the counter for measurement. The RAD-H<sub>2</sub>O analyses the samples and produces the results within 30 minutes. However, the lengthy measurements using the vacuum chamber method were preferred to monitor the radon escape.

In this study, the main objectives are to measure dissolved radon activity concentration in water samples, mainly from laboratory-prepared, groundwater and surface waters and to estimate the transfer velocity coefficient of radon across the water-air partition. Mathematical models, based on Fick's diffusion laws, are developed to simulate (1) radon behaviour with time (2) the diffusive transport of radon from the water to air and (3) radon decay within the vacuum chamber. Numerical modelling techniques have to be applied since the equations are not analytically solvable.

## 1.2. Thesis outline

The remaining parts of this thesis are as follows: Chapter 1 describes and illustrates the interaction of radiation with matter, basic theories, and formulae in radiation. The research on radon radioactivity and the intensive use of radon in hydrogeological studies are introduced in Chapter 2. The radiological risk correlated with radon and tobacco smoke and the entrance of radon into houses are discussed. The experimental set-ups, sample preparations, measurement instruments and introduction to modelling are discussed in Chapter 3.

Chapter 4 describes the experimental methods pursued in this study and presents the results while Chapter 5 presents the results of the modelling part of the study and the fitting of radon concentration by numerical models. The estimation of the escape rate of radon from water to air is also discussed in this chapter. Chapter 6 and Chapter 7 present the general discussion and the overall outcomes of the study and a summary.

## 1.3. Background to radon

### 1.3.1. Physical and chemical properties of radon

Radon, whose chemical symbol is Rn, is a naturally occurring radioactive gas, which is invisible, tasteless and odourless with a half-life of 3.82 days (Lee *et al.*, 2006). It is an

immediate decay product of radium-226 ( $^{226}\text{Ra}$ ). Both  $^{226}\text{Ra}$  and  $^{222}\text{Rn}$  are in the decay series of uranium-238 ( $^{238}\text{U}$ ). Radon concentrations vary from place to place depending on the underlying geology. Radon has many other isotopes with very short half-lives and thoron ( $^{220}\text{Rn}$ ) and actinon ( $^{219}\text{Rn}$ ) are the most common among them. Their half-lives are so short that the only isotope that reaches the earth surface in noticeable amounts is  $^{222}\text{Rn}$  (Al-Kazwini and Hasan, 2003).

Radon is the element with atomic number 86 in the Periodic Table, one of the noble gases. The electrons completely fill the outer shell of radon so there are no free electrons. Contrary to most gases, the noble gases are monatomic. They have stable electron configurations and for that reason, under normal conditions they do not react with other elements. In the text below, radon always means  $^{222}\text{Rn}$ ; radium means  $^{226}\text{Ra}$ , and uranium means  $^{238}\text{U}$ .

All soil contains naturally occurring primordial radionuclides such as  $^{238}\text{U}$ ,  $^{232}\text{Th}$  and  $^{40}\text{K}$ . These radionuclides have long half-lives and were present from the time the earth was formed, thus radioactivity has always been part of life. These radionuclides pose a radiological health hazard externally due to their gamma-ray emissions from progeny and internally due to alpha radiation emissions from radon and its progenies (Al-Hamarneh *et al.*, 2009; Papastefanou *et al.*, 2009). Many research projects are carried out on radon from a radiation perspective as well as on the use of radon as an environmental tracer.

Radon in water studies complement the use of long-lived isotopes such as  $^3\text{H}$  with a half live of 12.43 years and  $^{14}\text{C}$  with a half-life of 7530 years that are used to measure the hydrological cycle of groundwater from several months to thousands of years. The concentration differences between groundwater and surface water can be used to assess the exchange of groundwater and surface waters (Wu *et al.*, 2004).

The consumption of water with elevated amounts of radon pose a radiological hazard to the public using private wells (Singh *et al.*, 2008). Radon is a gaseous descendant of radioactive  $^{238}\text{U}$  that undergoes a series of decay steps before it ultimately reaches the



stable  $^{206}\text{Pb}$ , which is the final product. In the uranium-238 series shown in **Table 1**, the radiations are emitted in the form of alpha particles, beta particles, and gamma rays and in the process, many daughter products form. These emissions are the basis by which radioactivity is measured by the radiation detectors.

**Table 1:** The uranium-238 decay series and its radiation types

| The decay series of uranium-238 |                  |                   |                     |  |
|---------------------------------|------------------|-------------------|---------------------|--|
| Nuclide                         | Name             | Half-life         | Radiation type      | Reference  |
| $^{238}\text{U}$                | Uranium-238      | 4.5 billion a     | Alpha               | (Kaplan, 1955;<br>Semat, 1954;Lapp<br>& Andrews, 1972) |
| $^{234}\text{Th}$               | Thorium-234      | 24.1days          | Beta, gamma         |  |
| $^{234\text{m}}\text{Pa}$       | Protactinium-234 | 1.0 min           | Beta, gamma         |  |
| $^{234}\text{U}$                | Uranium-234      | 245000 a          | Alpha, gamma        |  |
| $^{230}\text{Th}$               | Thorium-230      | 76000 a           | Alpha, gamma        |  |
| $^{226}\text{Ra}$               | Radium-226       | 1600 a            | Alpha, gamma        |  |
| $^{222}\text{Rn}$               | <b>Radon-222</b> | <b>3.82 days</b>  | <b>Alpha, gamma</b> |  |
| $^{218}\text{Po}$               | Polonium-218     | 3.0 min           | Alpha, gamma        |  |
| $^{214}\text{Pb}$               | Lead-214         | 27 min            | Beta, gamma         |  |
| $^{214}\text{Bi}$               | Bismuth-214      | 20 min            | Beta, gamma         |  |
| $^{214}\text{Po}$               | Polonium-214     | 160 $\mu\text{s}$ | Alpha, gamma        |  |
| $^{210}\text{Pb}$               | Lead-210         | 22 a              | Beta, gamma         |  |
| $^{210}\text{Bi}$               | Bismuth-210      | 5 days            | Beta, gamma         |  |
| $^{210}\text{Po}$               | Polonium-210     | 138 days          | Alpha, gamma        |  |
| $^{206}\text{Pb}$               | Lead-206         | Stable            | N/A                 |  |

Radon is the highest contributor of natural background radiation. Radon is the daughter product of uranium and radium that are found in soils and rock everywhere but in varying amounts. It accounts for more than 50 % of the background radiation dose to which an average person is exposed (Jones and Childers 1990). Some background radiation comes from synthetic radiation, like nuclear medicines, consumer products like smoke detectors

and some comes from X-rays used in hospitals and industry. The pie chart below shows the approximate percentage contribution of each of these to the annual radiation dose.

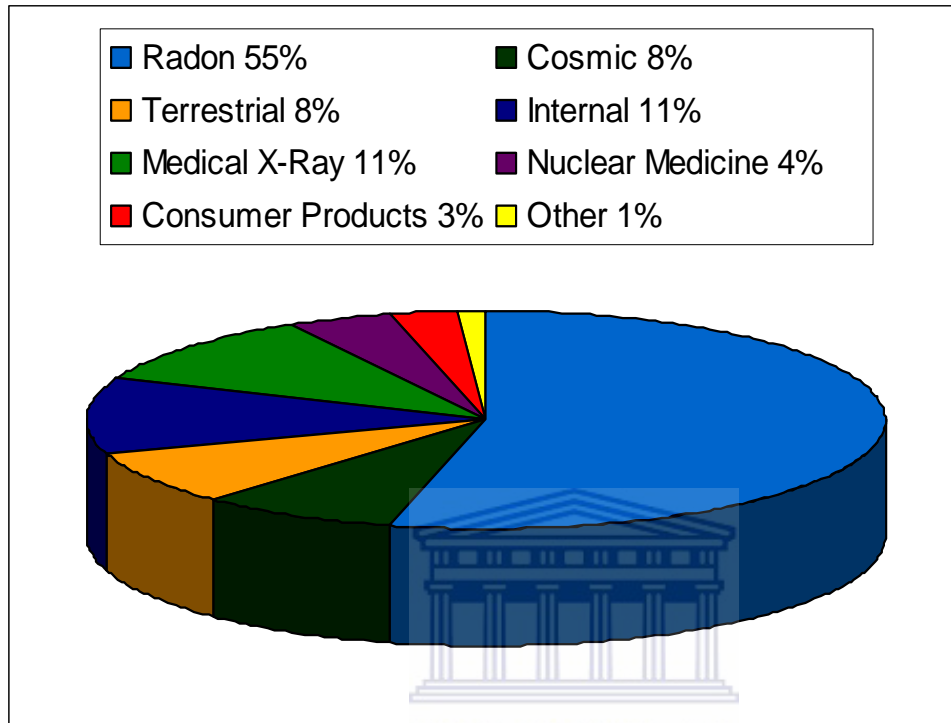


**Figure 1.1:** Sources and average distributions of background exposure. (Adapted from Jones and Childers, 1990)

## 1.4. Radiation in general

### 1.4.1. The background to radiation

The sources of radiation divide into two categories. These are the natural radiation and synthetic radiation. The natural background radiation divides into cosmic radiation, terrestrial radiation and internal radiation. The earth and all in it are constantly bombarded with radiation from outer space. The charged particles from the sun and stars interact with the atmosphere and earth magnetic field to generate a shower of radiation. The amount of cosmic radiation varies from place to place depending on the altitude.

The earth itself has been radioactive ever since its formation. The radioactive materials are common throughout nature in soil, rocks, water, and vegetation. The radioactive nuclides include ubiquitous uranium-238, thorium-232, potassium-40 (Chang *et al.*, 2008) and their progenies. Some radioactive materials, like trace uranium absorbed by plants while growing, in cooking water and C-14, are ingested with food and water and radon gas is inhaled. In addition, the amount of terrestrial radiation varies in different parts of the world due to different concentrations of uranium and thorium in soil.

Humans are exposed to radiation from radioactive materials inside their bodies. Besides radon and its progenies, the most common internal radioactive isotope is naturally occurring potassium-40 ( $^{40}\text{K}$ ) and carbon-14 ( $^{14}\text{C}$ ). Potassium-40 and Carbon-14 are the main constituent of internal radiation exposure to humans, but the exposure of an individual varies because of radon exposure, which differs from place to place.

### 1.4.2. Alpha Radiation

Alpha particles are  $^4_2\text{He}$  nuclei, usually energetic, positively charged particles consisting of two protons and two neutrons. They are usually emitted in the decay of the unstable heavy radionuclides. An example of alpha decay is



Following this transition, if the daughter nucleus is left in an excited state, the emission of the gamma ray will follow almost immediately (Lapp and Andrews, 1972). Two protons and neutrons leave the nucleus in an assembly known as an alpha particle. The measurements of alphas are used to measure radon in the RAD7 detector, the main instrument used in this thesis.

### 1.4.3. Beta Radiation

There are around 270 stable atoms of elements. The stability of these elements is dictated by the configuration of their protons and neutrons. The ratio of the number of neutrons to the number of protons ( $N/Z$ ) is an indicator of the nuclear stability. For small atomic numbers, the ratio is close to unity. This is the case for all lightweight radionuclides but for heavy nuclei, the ratio goes up to 1.6. The plot of atomic numbers versus neutron numbers of all nuclides is shown on **Fig. 1.2**. All stable nuclides are concentrated around the line of stability.

Beta radiation is the nuclear process by which unstable radionuclide attains its stability by either changing a neutron into a proton or vice versa. Beta decay comprises minus and plus decay. Beta plus particles are fast moving positive electrons called positrons. Beta minus particles are fast moving negative electrons ejected from the nuclear disintegration.

If a radionuclide is neutron deficient, positron emission occurs whereas if it is neutron rich, beta emission occurs (Lilley, 2001). All isotopes with proton and neutron numbers higher than 83 and 126 are radioactive in nature. Each black dot in **Fig. 1.2** represents a stable nuclide. The nuclear decays by beta radiations are briefly detailed below.

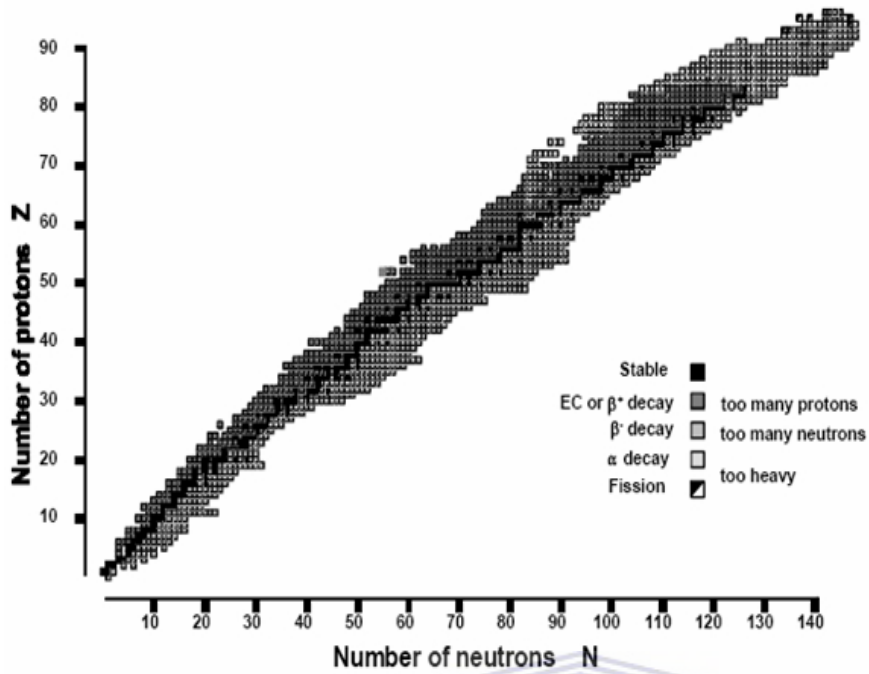
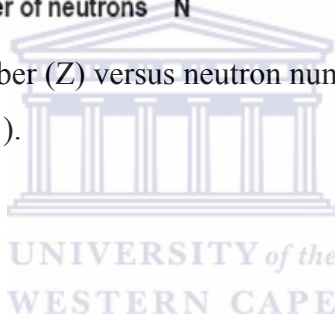


**Figure 1.2:** Plot of proton number ( $Z$ ) versus neutron number ( $N$ ). (Adapted from Semat and Albright 1973, Lilley, 2001).



### 1.4.3.1. Beta minus decay

The neutron converts into a proton and an electron. As an electron cannot exist inside the nucleus, it is ejected. For instance, Lead-214 transforms into Bismuth-214 in this way:



In this decay, not only an electron is emitted but also an antineutrino, symbolized by the Greek letter nu ( $\bar{\nu}$ ). The atomic number of the daughter nucleus increases by a unit. The electron-antineutrino pair is a characteristic of beta minus decay. Neutrinos ( $\nu$ ) and anti-neutrinos ( $\bar{\nu}$ ) are electrically neutral and travel close to the speed of light.



### 1.4.3.2. Beta plus decay

A proton converts into a neutron and a positively charged electron, the positron, is emitted. Sodium-22 decays to Neon-22 by emission of a positron in this way.



The atomic number of the daughter nucleus reduces by a unit. The positron-neutrino pair is a characteristic of beta plus decay.

## 1.4.4. Gamma Radiation

Gamma radiation is the emission of high-energy electromagnetic waves from a radionuclide. Gamma rays often accompany the emission of particulate radiation. They are also produced in annihilation reactions. They internally and externally present radiation hazard to the entire body. When  ${}^{222}\text{Rn}$  decays by alpha emission, the radon is

formed in an excited state that then decays by gamma emission giving off a gamma ray with energy 186 keV:



The asterisk (\*) in Eqn (4) indicates that the radionuclide is in an excited state and the gamma ( $\gamma$ ) indicates that an amount of energy is released in the form of electromagnetic radiation by the nucleus to achieve its stability. The gamma rays can easily pass completely through the human body or be absorbed by tissue, thus constituting a radiation hazard for the entire body. A very thick wall of concrete or a few centimetres of lead may be required to block the energetic gamma radiation.

The gamma rays pass through almost all matter. The shielding for gamma rays is usually provided by making use of lead shields. Since lead is a common element with high atomic number, the gamma rays spend more time interacting with the protons and even getting absorbed by the lead shield and in the process, the intensity of incident radiation is in that way attenuated. The thicker the lead shield the better the attenuation.

## 1.5. The Attenuation of radiation by matter

Charged particles do not penetrate far in matter because they lose more energy interacting with electrical interaction induced by electrons in atoms of the matter. The gamma radiation can only be attenuated by matter through the processes of Photoelectric Effect, Compton scattering, and pair production, which dominates at different energy levels. The photoelectric effect dominates at lower energies of less than 0.1 MeV.

The Compton Effect dominates at intermediate energies of about 1.0 MeV whereas the pair production predominantly takes place at higher energies (Knoll, 2000). Among the three types of radiation, alpha particles create the greatest ionization density per path length. Since the ionization of atoms requires energy, all three types of radiations lose

energy as they pass through matter and depending on the type of material and its thickness, these radiations could be blocked or absorbed completely.

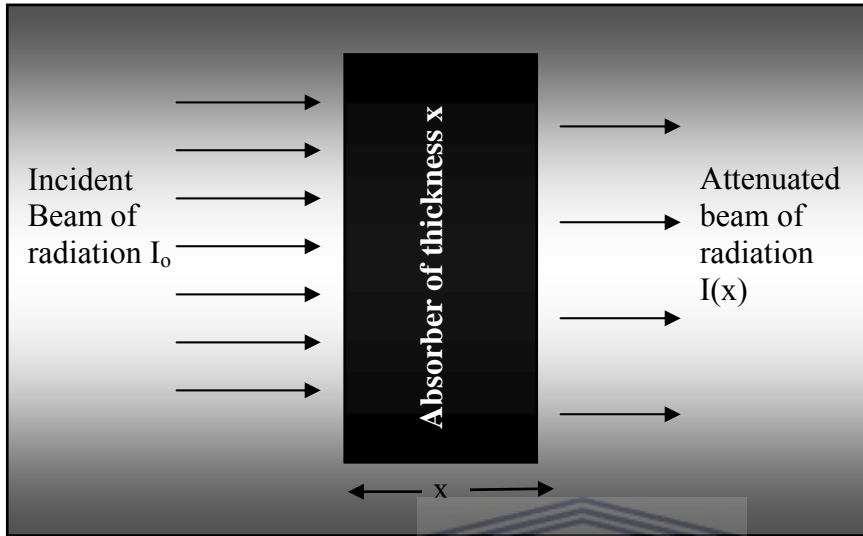


**Figure 1.3:** The intensity of radiation reduces after passing through the matter.

The intensity of radiation decreases exponentially with distance as it passes through matter. The intensity of radiation decreases because the incident radiation interacts with the particles making up the matter and it thus loses energy. The intensity is given by:

$$I(x) = I_0 e^{-\mu x} \quad (5)$$

where  $I_0$  incident radiation beam,  $I(x)$  the attenuated radiation beam,  $\mu$  is the mass absorption or attenuation coefficient in units inverse to meters and  $x$  is the thickness of the absorber. The total gamma ray intensity, after passing through the absorber, obeys Eqn (5) as is illustrated on **Fig. 1.3**.

The information about different radiations and their attenuations are collected and tabulated. The information presented in **Table 2** is very important from a radiation protection perspective. The attenuation of radiation as it passes through matter is important for topics such as shielding radiation sources, X-rays, and tumour irradiation.



Different radiations have different penetrating power in matter. The penetrating strengths of different radiation in matter are depicted in **Fig. 1.4**.

**Table 2: Tabulated data on radiation characteristics (Knoll, 2000)**

| <b>The characteristics of radiation</b> |                               |                        |                           |                  |
|---|-------------------------------|------------------------|---------------------------|------------------|
| <b>Characteristics</b>                  | <b>Alpha particle</b>         | <b>Beta particle</b>   | <b>Neutrons</b>           | <b>Gamma ray</b> |
| Symbol                                  | $\alpha$ or ${}^4_2\text{He}$ | $\beta^-$ or $\beta^+$ | ${}^1_0n$                 | ${}^0_0\gamma$   |
| Mass (a m u)                            | 4                             | 0.0005                 | 1                         | 0                |
| Charge                                  | +2                            | $\pm 1$                | 0                         | 0                |
| Speed                                   | Fast                          | Very Fast              | Fast                      | Speed of light   |
| Ionizing ability                        | High                          | Medium                 | Low or zero               | Low              |
| Penetrating power                       | Low                           | Medium                 | Very High                 | High             |
| Radiation type                          | Particulate                   | Particulate            | Particulate               | Photon           |
| Shielding                               | Paper/hand                    | Aluminium              | Concrete/H <sub>2</sub> O | Lead             |

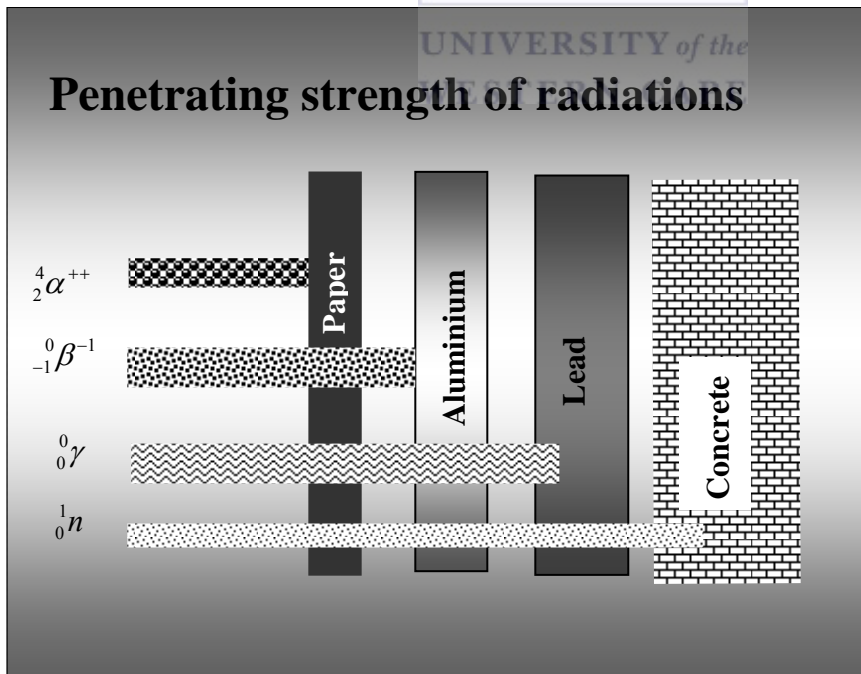


**Figure 1.4:** The diagram showing penetrating strength of radiation.

## 1.6. The radioactive decay laws

The radioactive decay laws are derived below. Each isotope has a distinct decay constant,  $\lambda$ . The activity  $A$  of a sample of  $N$  nuclei decays proportionally to the decay constant.

$$A = \lambda N \quad (6)$$

The average number  $dN$  that will disintegrate in a short time  $dt$  is proportional to the number of atoms  $N$  present, that is:

$$dN = -\lambda N dt \quad (7)$$

Eqn (7) can be integrated by separating variables to give formulae that after some mathematical manipulation give:

$$N(t) = N_0 e^{-\lambda t} \quad (8)$$

where  $N(t)$  and  $N_0$  represent the radioactive nuclei present at time  $t$  and initial number of radioactive nuclei respectively. Half the amount of the radioactive atoms decays within one half-life. The decay constant,  $\lambda$  is related to the half-life:

$$T_{1/2} = \frac{0.693}{\lambda} \quad (9)$$

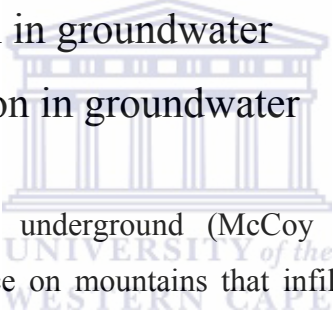
The activity of a radioactive sample is expressed in Becquerel (Bq), the number of disintegrations per second.

# CHAPTER 2 - THE APPLICATIONS AND DANGERS OF RADON

This chapter focuses on the ways by which radon and its progenies are used for the benefit of research. Radon is a trace element that can be used in hydrological studies and be used to localise the fresh water inflows into oceans. It has also been explored as an earthquake precursor. The chapter also focuses on the carcinogenic effect that radon and its progenies pose to humans in their lifetime exposure to significant amounts of the gas indoors or to miners in uranium mines, and uranium processing facilities.

## 2.1. Radon and research in groundwater

### 2.1.1. Formation of radon in groundwater



Groundwater describes water underground (McCoy *et al.*, 2009) resulting from rainwaters, hail and melting ice on mountains that infiltrate into the ground and seep downward through fractures, pores, and other spaces in soils and rocks. High surface pressure drives water downwards. The process whereby water flows into an aquifer is called recharge. The water seeping into the ground does not pass through the layer of bedrock, which lies beneath the soil, and therefore groundwater usually accumulates above this barrier of rock. The water table lies just above the zone of saturation. During rainy seasons, the soil becomes soaked with water and the water table rises closer to the surface of the soil, and during the dry weather, it falls closer to the zone of saturation.

As rainwaters are partially acidic, they tend to dissolve minerals in the soil and rocks covering the aquifer. Since the rocks contain different minerals, the groundwaters in contact with these minerals will have different degrees of contamination (Singh *et al.*, 2008). A confined aquifer is overlain and underlain by confining impermeable rocks as shown in **Fig.2.1**. An unconfined aquifer is situated just beneath the water table.

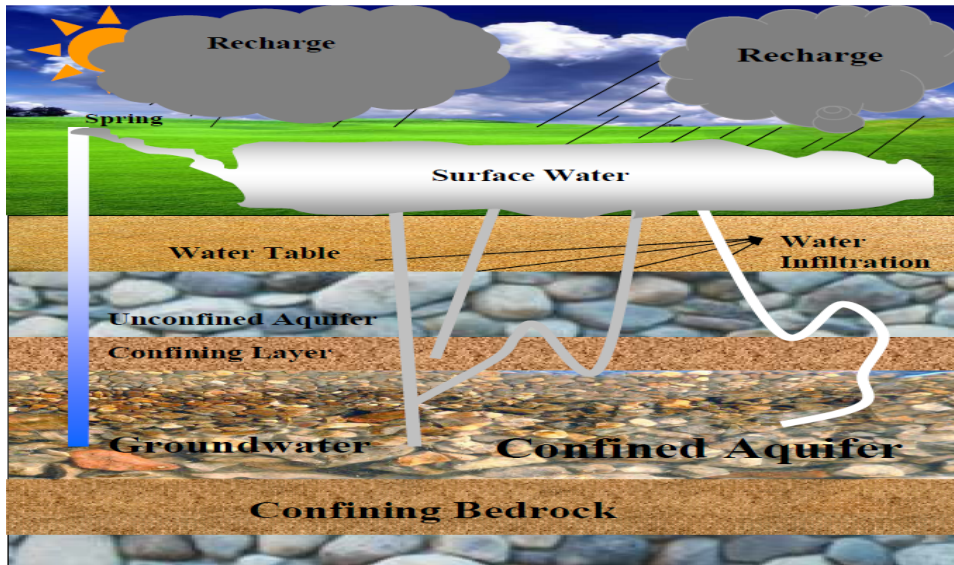


**Figure 2.1:** The cross section of crust showing of hydrogeological formation. (Adapted from Hydrogeology by Davies, 1966)

The groundwater is contained in rock fractures and soils that have uranium and radium content since the earth crust is enriched with these radionuclides (Nain *et al.*, 2008). The source of radon in groundwater can be in the water itself or in the rock formation in contact with groundwater or in both. The content of dissolved minerals in groundwater is enhanced by the time water spends in contact with those minerals.

The infiltrating precipitation washes chemicals down into the ground. This is another reason groundwater is enriched in nutrients. The influx of these chemicals improves the radium (Gainon *et al.*, 2007) dissolution in groundwater thus enhancing the groundwater with much higher concentrations of radon than surface waters. In addition to that, the higher solubility of radium in water than uranium further enhances the radon content in groundwater (Savidou *et al.*, 2006; Aghamiri *et al.*, 2006). Furthermore radon that enters the pore space as a result of radium decay in soil grains dissolve in groundwater. These are the main ways by which groundwaters have higher concentrations of radon than surface waters and this makes it easy to characterise the seepage of the groundwater into the open water body.

### 2.1.2. The use of radon as a hydro-geochemical tracer

The measurement of radon in water has become a useful tool in the application of radon as a natural tracer. Radon, just like other tracers, is used to characterize the physical hydrology, geophysics and geochemistry (Schiavo *et al.*, 2009). Radon can be used as a natural tracer in the study of submarine groundwater discharge (SGD) (Ghose *et al.*, 2003; Burnett *et al.*, 2007; Waska *et al.*, 2008) due to its higher concentration of radon (Marques *et al.*, 2004), thus significant radon concentrations may signal that groundwater seeps into the sea. SGD may also refer to seeping of groundwater into the coastal oceans, flowing out along most shorelines (Schiavo *et al.*, 2007) and it occurs wherever an aquifer is connected to the sea. The coastal hydrology is studied by making investigations using the combinations of stable, long-lived and short-lived radioisotopes.

The proper understanding of the SGD gives a good platform in the knowledge and sustainable management of coastal fresh water aquifers in populated coastal places worldwide. Many essential nutrients come to the coastal environments with SGD and in that sense; the SGD serves as a pathway of both organic and inorganic contaminants (Schiavo *et al.*, 2009) that may pollute the marine environment from land-based activities. The groundwater carries tracers, and nutrients therefore studying the hydrogeology and geochemistry of environmental tracers and their ground-to-water movement are vital. As the groundwater temperature at the discharge zone is high, then temperature, electrical conductivity, and pH can be also used to assess the contamination of the environment (Taniguchi *et al.*, 2003).

The groundwater could be contaminated by surface water depending on how the surface water is contaminated and how fast it infiltrates into groundwater. A proper knowledge of infiltration velocity would be useful for the management and exploitation of quality groundwater (Van Giap, 2003). The expanding human population and their activities always generate waste, and the poor management of that waste contaminates water, soil and atmosphere, which has a negative effect on public health.

Understanding the inert gas geochemistry is regarded as a reliable tool for investigating the origin and processes involving fluids during their ascent to the surface. Knowledge about the nature and evolution of the deep fluids give a platform for understanding geological events (Walia *et al.*, 2005) occurring deep underground. Radon has been studied as a possible precursor of earthquakes (Elmaghraby *et al.*, 2009) and changes in the soil gas concentrations can be correlated with volcanic-seismic activity (Williams-Jones *et al.*, 2000; Eff-Darwich *et al.*, 2008).

### 2.1.3. Radiological effects of radon to humans

#### 2.1.3.1. Natural exposure to background radiation

Radon is an immediate daughter of a ubiquitous  $^{226}\text{Ra}$  isotope in the earth crust (Chang *et al.*, 2008), therefore significant amounts of radon are also prevalent in groundwaters. This makes radon a source of radiological health risks to humankind received by both ingestion and inhalation. The death of underground miners from lung cancer led to the identification of radon as a health hazard (Mohamed *et al.*, 2008; Othman *et al.*, 2007; Lehnert *et al.*, 1997; Prasad *et al.*, 2008). The laboratory animals exposed to significant amounts of radon and its progenies display lung carcinoma. The cancer deaths in miners who also smoke suggest a synergistic effect of alpha radiation and smoke (Field, 1999; Prueitt *et al.*, 2009).

The International Agency for Research on Cancer classifies radon as a human carcinogen primarily because of the research findings on miners exposed to high levels of radon progenies. The lung cancer has been examined in populations of underground miners from the United States, Canada, Australia, China, and Europe. The research findings emphasized that the radon progenies had the causative effect of lung cancers in miners (Field, 1999).

The background radiation is divided into two categories. There are terrestrial and cosmic radiations. Terrestrial radiation is produced from the earth whereas cosmic is a major

outdoor source of natural radiation from space, which varies with altitude. The metallic radon progenies attach to air, and are inhaled and settle within the lungs (Barros-Dios *et al.*, 2002; Field, 1999). Food and water are the only source of human exposure that leads to internal radiological dose (Nain *et al.*, 2008; Chen *et al.*, 2005). Naturally, the primordial radionuclides like  $^{238}\text{U}$ ,  $^{232}\text{Th}$  and  $^{40}\text{K}$  are prevalent in the soil (Al-Hamarneh *et al.*, 2009; Papastefanou *et al.*, 2009) and in fertilizer workers they pose radiological risk externally due to their gamma-ray emissions and internally due to the radon and the alpha emission of its progenies (Al-Hamarneh *et al.*, 2009).

### 2.1.3.3. Health effects of radon progenies and tobacco smoke

The high concentration of radon in indoor air increases the risks of developing lung cancer and the risk increases by up to ten times for smokers (Chang *et al.*, 2008). The radon progenies and tobacco smoke enter the lungs attached to aerosol particles and deposit on the walls of alveolar parenchyma (Prueitt *et al.*, 2009). The smoker is exposed to about 50 times more dose than non-smokers (Carvalho *et al.*, 2006; Yngveson *et al.*, 1999; Prueitt *et al.*, 2009). As much as radon can cause cancer, its risk is far less than that for smoking. The mechanisms or actions by which tobacco smoke and radon cause damage to the epithelium are similar. The generation of free radicals and oxidative stress are the common early phase of both processes (Alavanja, 2002).

When the tobacco smoke is inhaled, smokers expose their lungs to the  $^{210}\text{Pb}$  and  $^{210}\text{Po}$  and this may increase the probability of lung cancer (Carvalho *et al.*, 2006) induction. As  $^{210}\text{Pb}$  and  $^{210}\text{Po}$  are metallic particles that lodge in lungs, they serve as a localized source of internal radiation in the lungs.  $^{210}\text{Pb}$  and  $^{210}\text{Po}$  become very volatile at burning temperatures of  $500^{\circ}\text{C}$  to  $800^{\circ}\text{C}$  of cigarettes and they are inhaled with smoke in the vapour phase (Savidou *et al.*, 2006). The lead ( $^{210}\text{Pb}$ ) deposits on the surfaces of bones while  $^{210}\text{Po}$  deposits in the liver, kidney, and spleen. The liver, kidney and spleen cancers may result from smoking because of this internal radiation source. The phosphate fertilizers enhance radiation in tobacco and the NORM enhances the level of

radionuclides accumulating in leaves of the tobacco plant while the plant grows (Prueitt *et al.*, 2009; Savidou *et al.*, 2006).

The tobacco smoke and radon have a synergistic effect of lung cancer induction. The cancer inception may be noticed after many years. The interaction between radon exposure and tobacco smoking with regard to lung cancer exceeds additivity and is close to a multiplicative effect. Plant roots absorb some uranium and radium as minerals from the soil. The sticky leaves of tobacco trap the progenies of radon (Lauria *et al.*, 2009; Prueitt *et al.*, 2009; Papastefanou *et al.*, 2009) while the plant grows.

## 2.2. The sources of radon

The primary sources of radon are the rocks in the earth crust, soils on the ground and groundwater and natural gas. The rocks in the earth crust, which break into soil during weathering, contain the element uranium. The weathering of rocks gives rise to soils hence the soils also have uranium content. The uranium has a long half-life therefore the uranium that existed during weathering still exists in soil. Groundwaters are contained in aquifers and rocks. The  $^{238}\text{U}$  makes up 99.274 % of the uranium present in the crust whereas  $^{235}\text{U}$  makes up only about 0.7205 %. Its decay means the beginning of a series of 14 decays (see **Table 1**) that ends at  $^{206}\text{Pb}$  after 8 alpha and 6 beta emissions and many gamma decays.  $^{222}\text{Rn}$  ( $T_{1/2}=3.82$  days) is the only gas in the decay series of  $^{238}\text{U}$ .

Radon is a noble gas and generally lacks reactivity towards other chemical agents (Stieglitz, 2005). Considering its short half-life, the radon naturally occurring in the environment comes from proximal distances beneath the ground. The isotopes thoron  $^{220}\text{Rn}$  ( $T_{1/2}=56$  s) and actinon  $^{219}\text{Rn}$  ( $T_{1/2}=4$  s) decay soon after production because they have very short half-lives. In this study their contribution is insignificant and the only isotope of concern is  $^{222}\text{Rn}$  ( $T_{1/2}=3.82$  days). The natural radioactive series and gases produced in the decays are presented in **Table 3**.



**Table 3:** Radioactive gas types in heavy metal transformation

| Series Name | Parent nuclide    | Half-life ( $\times 10^9$ years) | Final stable isotope | Gas produced                  |
|-------------|-------------------|----------------------------------|----------------------|-------------------------------|
| Uranium     | $^{238}\text{U}$  | 4.47                             | $^{206}\text{Pb}$    | Radon [ $^{222}\text{Rn}$ ]   |
| Thorium     | $^{232}\text{Th}$ | 14.1                             | $^{208}\text{Pb}$    | Thoron [ $^{220}\text{Rn}$ ]  |
| Actinium    | $^{235}\text{U}$  | 0.71                             | $^{207}\text{Pb}$    | Actinon [ $^{219}\text{Rn}$ ] |

Radon responds to temperature and pressure gradients like other gases. It is very soluble in organic solvents, such as toluene and xylene, and moderately in cold water and this property leads to higher concentrations of radon in hydrocarbon contaminants (Surbeck, 2007; Field, 1999).

### 2.3. Radon accumulation in houses

The soil, groundwater supply and building material are the three main sources of radon in the indoor air. Radon enters buildings through cracks in solid foundations, construction joints through the process of molecular diffusion and the water supply (Loureiro *et al.*, 1990). Sealing windows with the intention to save energy also enriches the house with more radon (Urosevic *et al.*, 2008) therefore a poorly ventilated house will attain large radon concentrations compared to a well-ventilated house and outside air.

Air pressure inside the house is usually lower than the pressure in the soil around the foundation of a house. Due to this pressure gradient, the house acts like a vacuum, thus it traps radon into its space (Mohamed *et al.*, 2008). In this process, warm air inside the building is replaced by cool radon-containing air from the ground. High soil temperatures and lower soil moisture can improve radon seepage into houses (Zhuo *et al.*, 2008). Since atmospheric pressure and temperature, soil temperature and wind speeds are environmental factors affecting the radon flux (Eff-Darwich *et al.*, 2008); it is usually possible to have more radon at lower wind speeds, high pressure and higher temperature.

For homes using the groundwater or well water supply, the activities such as showering, bathing, laundry, dishwashing (Singh *et al.*, 2008), and cooking agitate water thus easily releasing radon into the house (Vinson *et al.*, 2008). The illustration in **Fig. 2.2** shows that not only soil air and groundwater are the sources of radon but the building materials also contribute (Nazaroff *et al.*, 1987; Faheema *et al.*, 2008).

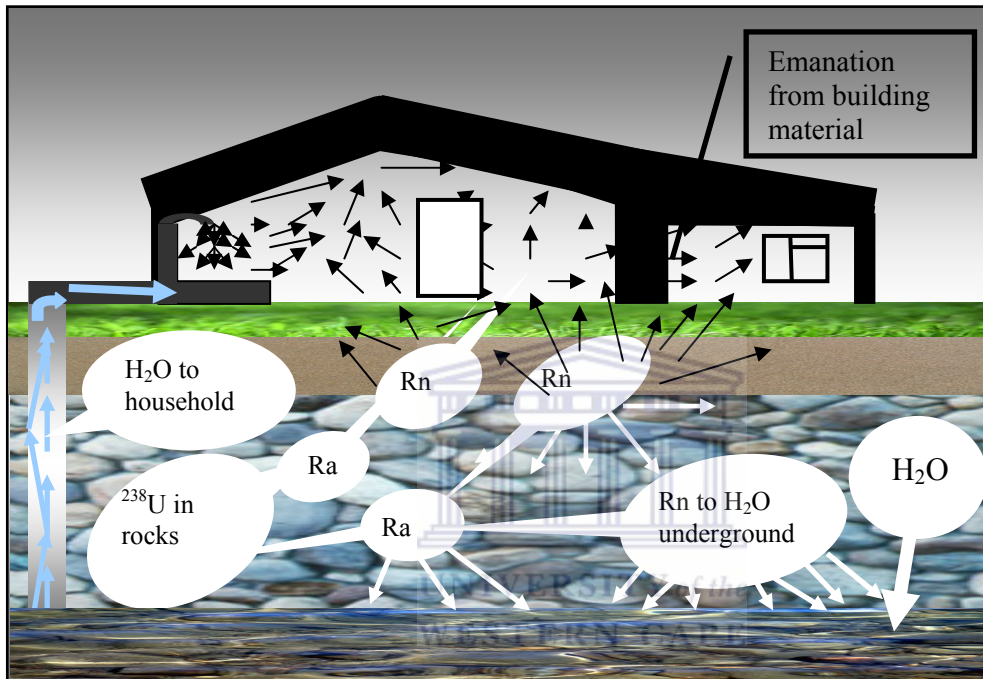


**Figure 2.2:** The path of radon into a building

The radon entering the house through the soil poses a health risk, especially if the house has a poor air exchange rate. The radiological hazard is enhanced when radon groundwater is a water supply (Loureiro *et al.*, 1990) in a house with a poor air exchange rate since that water is enriched in radionuclides that decay to radon. As groundwater is richer in radon than surface water (Dulaiova *et al.*, 2007; Marques *et al.*, 2004), the inhalation of waterborne radon and ingestion of dissolved radon in water pose a radiological risk in the lungs and stomach. Therefore, the assessment of the radon concentration in water and air is of vital importance towards reducing radiation exposure (Lee *et al.*, 2006) but this also requires that the transfer velocity coefficient of radon from water to air is well known so that better corrections are made to the values determined.

# CHAPTER 3 – INSTRUMENTS AND INTRODUCTION TO MODELLING

This chapter focuses on the apparatus and measuring instruments used to measure radon in this work and introduces the modelling formulae to be used in this study. In conducting the experiments, the RAD7 continuous radon monitor was the main instrument used with a Drierite desiccant column. More details about the operation of the instruments are briefly discussed below.

## 3.1. The RAD7

The RAD7 manufactured by DurrIDGE ([www.durrIDGE.com](http://www.durrIDGE.com)) operates on the principle of the electrostatic collection of charged alpha-emitters on the surface of a silicon solid-state detector and their subsequent detection through spectroscopic analysis. The RAD7 system shown on **Fig. 3.1**, detects  $\alpha$ -particles emitted by the radon progenies,  $^{218}\text{Po}$  and  $^{214}\text{Po}$  (Schubert *et al.*, 2008; RAD 7 Manual DurrIDGE company Inc. downloadable at [www.durrIDGE.com](http://www.durrIDGE.com)). An electric field above a silicon semiconductor detector at ground potential attracts the positively charged daughter of radon,  $^{218}\text{Po}$ , which is counted as a measure of the radon concentration in air (Stieglitz, 2005, Waska *et al.*, 2008). The RAD7 has an internal pump that pumps air at the flow rate of  $1 \text{ Lmin}^{-1}$  (Lee *et al.*, 2006). The RAD7 is purged for one hour to minimize the relative humidity (RH) and to get rid of the alpha emitters that could have adsorbed on the inside of the RAD7.

The RAD7 has a test chamber with high voltage that contains a detector. This high voltage charges the entire chamber in that way creating an electric field. The radon in air is sucked inside and it decays into the positive ions of  $^{218}\text{Po}^+$  ( $t_{1/2} = 3.05 \text{ min}$ ; alpha-energy = 6.00 MeV) and  $^{214}\text{Po}^+$  ( $t_{1/2} = 164 \mu\text{s}$ ; alpha-energy = 7.67 MeV), which are attracted by the electric field and may be deposited on to the detector, which is at ground potential, before they are neutralized. The humidity inside the chamber must be kept low

to attract nearly all positive ions. This explains the need for the desiccant, a laboratory-drying unit that is made of  $\text{CaSO}_4$  granules, which have a high affinity for water, therefore; it absorbs moisture before it reaches the RAD7. In the detector, the alpha particles hit the active surface of the detector thus producing the signals equivalent to the energy of the alpha energy. In this operation, the RAD7 is able to differentiate different radionuclides by their alpha energy using alpha-spectroscopy.

The operating panel of the RAD7 detector must not be exposed to excess moisture. The connection tubes should be connected in the right way to avoid any unnecessary damage to the detector and to avoid the suction of liquids into the inlet tube of the RAD7 detector. Normally the RAD7 operates well at humidity less than 10 percent (Schubert *et al.*, 2008) and can measure below  $4 \text{ Bq/m}^3$ . In these experiments, the humidity was kept at less than 6 percent. The RAD7 with illustrations is shown on **Fig. 3.1**.



**Figure 3.1:** The RAD7 and a printer

### 3.2. RAD-H<sub>2</sub>O

The RAD-H<sub>2</sub>O is an accessory to the RAD7 to find the activity of the radon in a water sample in a short time. It measures the activity of the sample giving results in about 30

minutes. It is connected to a small desiccant and RAD7. In this system, air is bubbled through a vial of either 40 mL or 250 mL with a water sample in five minutes, so that the radon is removed from the water sample. The  $^{222}\text{Rn}$  diffusing from the water sample continuously circulates through a desiccant column, to the RAD7 detector, and then back to the water sample to establish equilibrium between the radon in the water and air.

As the RAD7 aerates the water sample, radon is stripped from the water. The radon in air and water establishes equilibrium in these five minutes. The system waits for another five minutes, making it 10 minutes after bubbling, so that  $^{218}\text{Po}$  and  $^{222}\text{Rn}$  are in equilibrium. After that, the RAD7 runs a further four five-minute counting cycles thus making the total analysis time to be 30 minutes. The HP printer shown on **Fig. 3.1** and **Fig. 3.2** is an infrared printer through which the analysis results of RAD7 are printed out every five minutes for the case of radon measurement using RAD-H<sub>2</sub>O or hourly in the case of the vacuum chamber method as described in the next section.



**Figure 3.2:** The RAD-H<sub>2</sub>O connected to RAD7

### 3.3. Vacuum Chamber

A vacuum chamber was used as an airtight chamber where the radon that escaped from a water sample to the air can be measured. A sample is placed inside the chamber, which is immediately closed tightly with bolts and nuts. The bolts and nuts squeeze an “O”-ring rubber band between the lid and the vacuum chamber thereby minimising the chances of radon leakage. This system is connected to a desiccant and the RAD7 using radon tight tubes. The air, from the chamber passes through a drying unit and then to the RAD7 and back in a closed loop. The measurement of radon in air can be used at equilibrium to calculate the radon in water using the Ostwald solubility coefficient,  $\alpha$ , which is temperature dependent. It is given by the Fritz Weigel equation (RAD AQUA Manual, [www.durridge.com](http://www.durridge.com)) as follows:

$$\alpha(T) = 0.105 + 0.405e^{-0.0502T} \quad (10)$$

where T is the temperature in degrees Celsius. At equilibrium at time, t and temperature, T the relationship between the radon concentrations,  $C_w(t, T)$  in water and,  $C_a(t, T)$  in air are given by

$$C_w(t, T) = C_a(t, T) \times \alpha(T) \quad (11)$$

Eqn (11) is the equation that is used to determine the radon concentration in water given radon concentration in air at equilibrium. The Ostwald coefficient decreases with an increase in temperature. This means that at higher temperatures the solubility of the radon gas decreases as shown by an example in **Fig. 3.3**. At room temperature, the value of  $\alpha$  is about 0.22 that gives an approximate five-to-one ratio of radon in air to water at equilibrium.

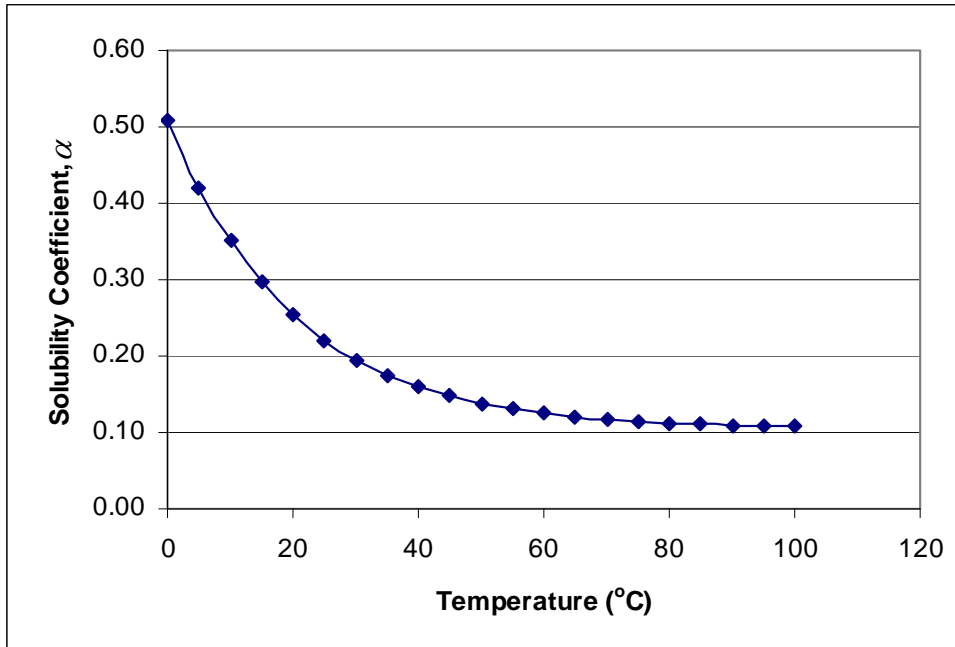


**Figure 3.3:** The example of solubility of radon at different temperatures.

The solubility of radon at typical temperatures is about 0.22. The temperatures in the vacuum chamber were in the range of 22-25°C. The set up using the vacuum chamber is shown in **Fig. 3.4**.

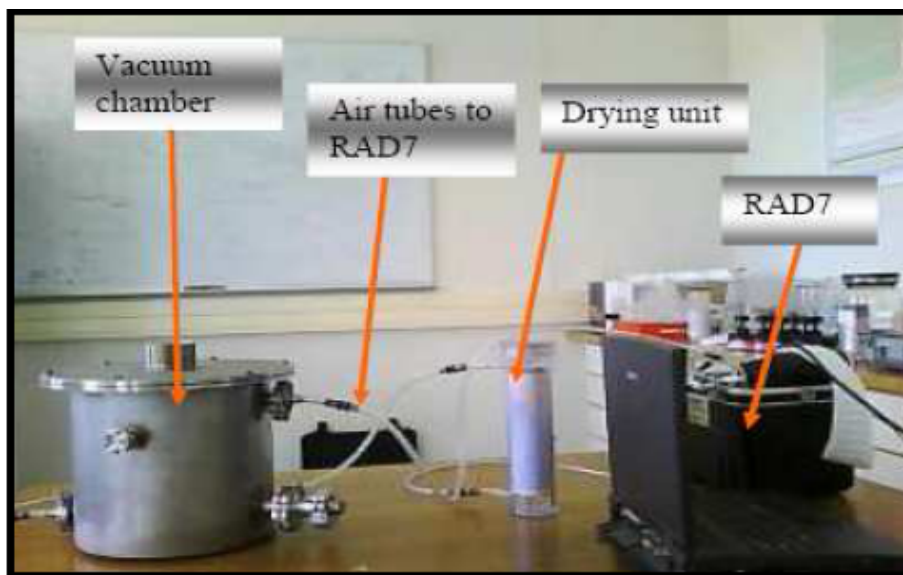
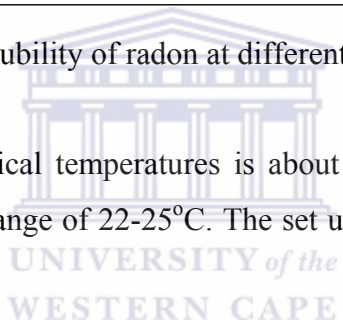


**Figure 3.4:** The experimental set up of the Vacuum Chamber method

## 3.4. Laboratory prepared water samples

### 3.4.1. The collection of water samples

The collection of water samples to analyse the radon content is done to study the radioactivity in water from rivers, groundwater, dams and shorelines. From the radiation point of view to assessing the SGD but the loss of radon during sampling remains a problem. The problem this study tries to solve. The groundwater was used as the source of radon in the first part of this study.

They were pumped from UWC and iThemba LABS boreholes. The water samples were pumped up, collected in containers, and immediately taken to the laboratory for analysis. To minimise radon loss the containers were closed under water. Later on in the study, the samples were prepared in the laboratory as mentioned above. The laboratory preparation of the water samples saved time and effort.

### 3.4.2. Alpha emitting source

The experiments in this thesis were conducted by placing a water sample with high radon concentration inside the vacuum chamber and measuring the radon in the air to find the rate of radon escape from water. The water samples were prepared in the Physics Laboratory at the University of the Western Cape. Three  $^{226}\text{Ra}$  sources, each of activity 185 kBq, were attached together with sticky tape and suspended over the water level in a 500 mL aluminium can with a rubber lid as shown on **Fig. 3.5**.

The sample is kept for about two days to make a radon-rich water sample with radon concentrations in the range of  $\text{kBq/m}^3$  and it can be kept longer to prepare a higher radon concentration in water sample. Radon dissolves in water in the container. The radon-rich water sample was usually divided into two samples. Out of the 500 mL water sample in the container, a 40 mL sample is measured with the RAD-H<sub>2</sub>O for an initial radon activity concentration in water.



The values can then be compared with the values found at equilibrium in the vacuum chamber. The remaining 450 mL is poured into containers of different volumes and areas depending on the specific experiment. The values of dissolved radon activity concentrations in the water samples covered a wide range, 10-1600 kBq/m<sup>3</sup>. The radon activities in the samples that are produced in this way are similar to or higher than those found in groundwater (Cosma *et al.*, 2008; Amrani *et al.*, 1999; Nazaroff *et al.*, 1987). The method of sample preparation is the same right throughout the study unless otherwise stated.

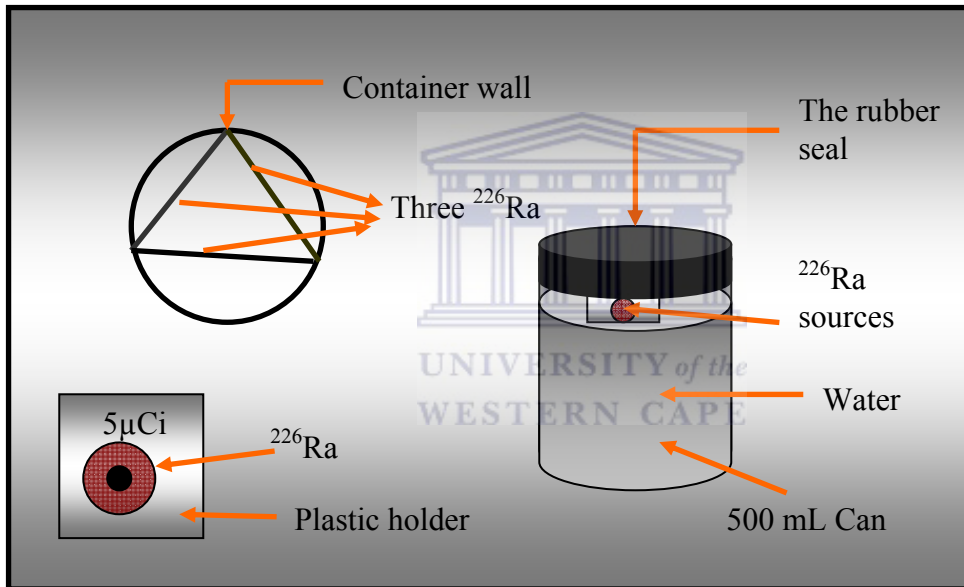


**Figure 3.5:** The preparation of alpha emitting source

### 3.5. Modelling of radon escape from water

#### 3.5.1. Background to diffusion

The term diffusion can be defined as a process of mass transfer of individual molecules of a substance brought about by random molecular motion under the influence of a driving force. The driving force could be pressure, temperature and or concentration gradient. The diffusion is caused by random molecular motion (Rebour *et al.*, 1997) that leads to complete mixing. The diffusion rate in gases is at a rate of about 5 cm/min, 0.05

cm/min in liquids, and only about 0.00001 cm/min in solids (Othman *et al.*, 2006; Masaro *et al.*, 1999). A fragrance of a perfume is a good example of molecular diffusion in gases.

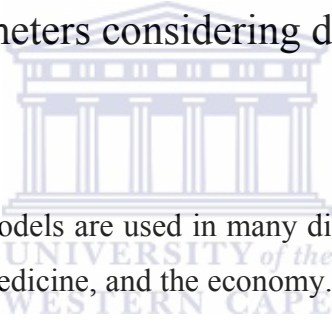
The atoms of a gas are constantly in motion at any temperature except at absolute zero. The motion of particles is random because the movement is associated with collisions. The diffusion process applies in many fields like in high-level nuclear repositories, in the drying of paper and textiles, and in agricultural processes and in medicine. In medicine, important diffusion-based processes incorporate drug absorption, distribution and elimination as it does in drug and nutrient transport in biological membranes in the vital organs. However, in this study, we look at the diffusion of radon gas from water to air in partial stagnant water in the chamber where turbulence is minimised.

The escape velocity of gases across the air-sea interface is regarded as the key in determining the gas exchange fluxes such as the absorption of anthropogenic carbon dioxide into the ocean. The understanding of the exchange of the gases across membranes is vitally important in many applications. The flux exchanges of CO<sub>2</sub> and other gases across the ocean-air interface are very important components in global climate dynamics, photosynthesis and respiration, and the absorption of the anthropogenically produced CO<sub>2</sub> (Kawabata *et al.*, 2003; Edson *et al.*, 2008). The transfer of gases between the ocean and the atmosphere can be studied in oceans, seas and be extended to lakes using radon and thoron.

The gas diffusion in the vacuum chamber is in a quiescent environment because the chamber is such that the experiment is running in a stagnant lake because the water is not disturbed by any external factor except air movement from the RAD7 detector. The experiments conducted in the vacuum chamber mimic the radon escape from the water sample exposed to the air. In oceans, the presence of waves limits the rate of gas exchange because the wave crests retain gases. In rivers or lakes, radon is easily lost from water when water flows over rocks or is moved by wind. A net transfer of <sup>222</sup>Rn occurs from the river to the atmosphere across the air-water interface through the process of molecular diffusion (Wu *et al.*, 2004).

In this study, the dissolved radon sample is placed in the container in a vacuum chamber and the chamber is tightly closed before the loss of much radon to air. The radon will escape the aqueous phase to a gaseous phase by the process of molecular diffusion. The process of molecular diffusion will be due to the difference in concentration between the phases, some air movement pumping from the RAD7, and temperature effects. These are the driving forces behind the escape of radon from water to air. The one-dimensional mathematical models, based on Fick's diffusion laws, are used to simulate the processes associated with the following: (1) radon behaviour with time, (2) the diffusive transport of radon within the water or air and (3) radon decay in the water and air within the vacuum chamber.

### 3.5.2. Theory and parameters considering diffusion of radon from water



Mathematical modelling and models are used in many disciplines in the natural sciences and engineering as well as in medicine, and the economy. It can be defined as the style of translating the problems from the application into mathematical formulations. The theoretical and numerical analysis gives the insight in the application. Mathematical modelling also refers to the derivation of appropriate equations that are solved using analytical or numerical methods. The major purpose of modelling is to approximate numerically the values of certain dependent variables for given independent variables. The independent variables are also called the input variables. Different variables can be used as a test to study the behaviour of the numerical model at different conditions.

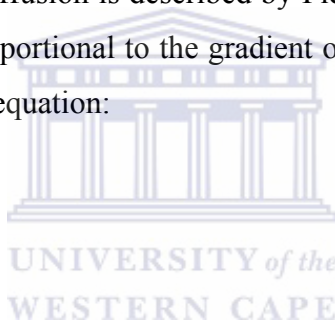
The model is tested with parameters. The parameters are independent variables because their values are also provided in studying the model. For example, in this study, the volume of the radon source, air volume and the Ostwald coefficient are the input parameters. The model produces the dependent variables. These are the output points of the numerical model. The values of the radon activity concentration in the air and water

as a function of the time are dependent variables. Numerical models are usually studied to observe the behaviour of the output variables with respect to changing input values.

### 3.5.3. The diffusion equation

In most experiments conducted during this study, the driving force behind the flow of radon gas was the concentration gradient. When a radon-rich water source is placed in a container large enough, there is an expectation that the radon will diffuse from high to lower concentration. In that way, the radon atoms are spontaneously leaving the liquid phase and accumulating in the gaseous phase and, at the same time, are decaying. As water is the source of radon, the air space is initially assumed to have negligible radon concentration. The theory of diffusion is described by Fick's diffusion Law. It states that the flux of concentration is proportional to the gradient of concentration in that direction as formulated in the following equation:

$$\vec{J} = -D\vec{\nabla} C \quad (12)$$



where  $\vec{J}$  is the effective flux density of radon activity ( $\text{Bq}\cdot\text{m}^{-2}\cdot\text{s}^{-1}$ ),  $D$  is the diffusion coefficient ( $\text{m}^2\cdot\text{s}^{-1}$ ) and  $C$  is the radon activity concentration ( $\text{Bq}\cdot\text{m}^{-3}$ ). For a normal diffusion process, the particles cannot be created or destroyed. This means that the flux of particles into one region must be the sum of particle flux flowing out of the surrounding regions.

This is stated mathematically by the continuity equation:

$$\frac{\partial C}{\partial t} + \vec{\nabla} \cdot \vec{J} = 0 \quad (13)$$

where the first term represents the change of concentration with time whereas the second term represents the gradient of flux  $J$ . Substituting Eqn (12) into Eqn (13) yields the diffusion equation

$$\frac{\partial C}{\partial t} = \vec{\nabla} \cdot (D \vec{\nabla} C) \quad (14)$$

If  $D$  does not vary with position, which is normally the case, then Eqn (14) becomes Fick's Second Law:

$$\frac{\partial C}{\partial t} = D \nabla^2 C \quad (15)$$

Eqn (15) can be expanded and be fully written in spatial coordinates as follows:

$$\frac{\partial C}{\partial t} = D \left( \frac{\partial^2 C}{\partial x^2} + \frac{\partial^2 C}{\partial y^2} + \frac{\partial^2 C}{\partial z^2} \right) \quad (16)$$

In the present study, we approximate to a one-dimensional problem. The x- and y-axis are ignored because radon is assumed to be diffusing along the vertical z-axis. The z-axis is chosen for the vertical column of water in the container, thus Eqn (16) reduces to this form (Thakre *et al.*, 2008):

$$\frac{\partial C}{\partial t} = D \left( \frac{\partial^2 C}{\partial z^2} \right) \quad (17)$$

As Eqn (17) stands, it does not characterize radon diffusion fully; another term is required to show the fact that radon decays. The inclusion of this term leads to the following equation.

$$\frac{\partial C}{\partial t} = D \left( \frac{\partial^2 C}{\partial z^2} \right) - \lambda C \quad (18)$$

where  $\lambda$  is the decay constant of radon. In our case, we look at a radon particle at a water-air interface when the particle diffuses from water to air as shown on **Fig 4.1**. The molecular diffusion governs the flux of radon atoms across the air-water interface as described by the following authors (Calugaru *et al.*, 2002; Burnett *et al.*, 2007; Wanninkhof *et al.*, 2009; Schmidt *et al.*, 2010):

$$F(t, T) = \beta \left( C_w(t, T) - \alpha(T) \times C_a(t, T) \right) \quad (19)$$

where  $F(t, T)$  is the flux of radon from water to air,  $\alpha(T)$ , is the Ostwald's coefficient and  $\beta$  ( $\text{m.s}^{-1}$ ) is the transfer velocity coefficient. The following diffusion models are proposed for the modelling of the radon gas as it escapes from aqueous to the air phase. The terms inside the brackets of Eqn (19) are defined as in the following:

$$C_a(t, T) = \frac{N_a(t, T)}{V_a} \quad (20a)$$

$$C_w(t, T) = \frac{N_w(t, T)}{V_w} \quad (20b)$$

where T and t represent temperature and time respectively. Eqn (20a) and (20b) represent radon activity concentrations in air and water respectively. In both equations,  $V_w$  and  $V_a$  represent the volumes of water and air respectively and  $N_w$  and  $N_a$  represent the radon atoms in water and in air respectively. Taking into account, that radon is decaying while it escapes from a phase to another, Eqn (19) can be expressed in terms of concentration to

give the following equation for radon activity concentration accumulated in air in analogy to Eqn (18).

$$\Delta C_a(t, T) = \frac{AF(t, T)\Delta t}{V_a} - \lambda C_a(t, T)\Delta t \quad (21a)$$

where A is the air-water interface area expressed in square meters (m<sup>2</sup>) and V<sub>a</sub> is the air volume. After substituting the Eqn (19) into Eqn (21a), the resulting equations can be written as follows.

$$\Delta C_a(t, T) = \frac{A\beta(C_w(t, T) - \alpha C_a(t, T))\Delta t}{V_a} - \lambda C_a(t, T)\Delta t \quad (21b)$$

Whereas the model for radon atoms diffusing from and decaying from water phase is given by this equation:

$$\Delta C_w(t, T) = -\frac{A\beta(C_w(t, T) - \alpha C_a(t, T))\Delta t}{V_w} - \lambda C_w(t, T)\Delta t \quad (21c)$$

Eqn (21b) governs radon concentration in air where as Eqn (21c) governs the change of radon concentration in water. Since diffusion is from the higher to lower concentration region, then the inclusion of a negative sign in Eqn (21c) is to indicate that radon atoms are diffusing from water.

### 3.5.4. The development of the numerical model

Now that the equations are in place, Eqn (21b) and Eqn (21c) can be expanded and written as finite difference equations. In this study, the equations to be used in numerical

modelling are expressed in terms of concentrations. Eqn (21a) and Eqn (21b) describe the behaviour of radon in the aqueous-gaseous system. Eqn (21a) and Eqn (21b) are written as finite difference equations:

$$C_a(t_i) = C_a(t_{i-1}, T) + \frac{A\beta(C_w(t, T) - \alpha(T)C_a(t, T))}{V_a}(t_i - t_{i-1}) - \lambda C_a(t, T)(t_i - t_{i-1}) \quad (22a)$$

Similarly, the change in the radon concentration in water is given by:

$$C_w(t_i, T) = C_w(t_{i-1}, T) - \frac{A\beta(C_w(t, T) - \alpha(T)C_a(t, T))}{V_w}(t_i - t_{i-1}) - \lambda C_w(t, T)(t_i - t_{i-1}) \quad (22b)$$

where  $C_a(t_{i-1}, T)$  and  $C_w(t_{i-1}, T)$  are the initial radon concentration in air and water at initial time  $(t_{i-1})$  respectively. The  $C_a(t_i, T)$  and  $C_w(t_i, T)$  are the iterated radon concentration in air and water at the step time  $(t_i)$ , respectively. The transfer velocity coefficient of radon may then be estimated from either Eqn (22a) or (22b) when compared to measured data. The intention is to find the velocity transfer coefficient at the air-water interface. Modifying Eqn (22a) algebraically and making the transfer velocity coefficient,  $\beta$  the subject of the formula and taking the absolute value help to obtain an appropriate model for estimating beta at the air-water interface.

$$\beta = \left| \frac{(C_a(t_i, T) - C_a(t_{i-1}, T) + \lambda C_a(t, T)(t_i - t_{i-1}))V_a}{A(C_w(t_i, T) - \alpha(T)C_a(t_i, T))(t_i - t_{i-1})} \right| \quad (23)$$

where  $i$  is an iteration number that is greater or equal to zero,  $i=0, 1, 2, \dots, N$

The mathematical models so far listed were used to estimate one-dimensional, vertical radon fluxes. A simple code can use Eqn (23) to estimate the value of the velocity transfer coefficient. Eqn (21a) and (21b) form two coupled first order differential equations that cannot in general be solved analytically.



# CHAPTER 4 – EXPERIMENTAL METHODS AND RESULTS

This chapter describes the protocols followed in conducting each of the experiments in this work. The following measurement methods are applied in many of the experimental investigations that are done in this study. The aim of the experiments is to measure the escape of radon from water. This is an important measurement since most radon in water measurements involve a sampling protocol during which radon can escape.

## 4.1. Radon measurement using the Vacuum Chamber method

The measurement of radon in the vacuum chamber will depend on the volume, the area of escape and the temperature. The experimental setup of the equipment used, is shown on **Fig. 3.4** for all the experiments using the vacuum chamber. The radon at the water-air interface is schematically shown on **Fig. 4.1** below.

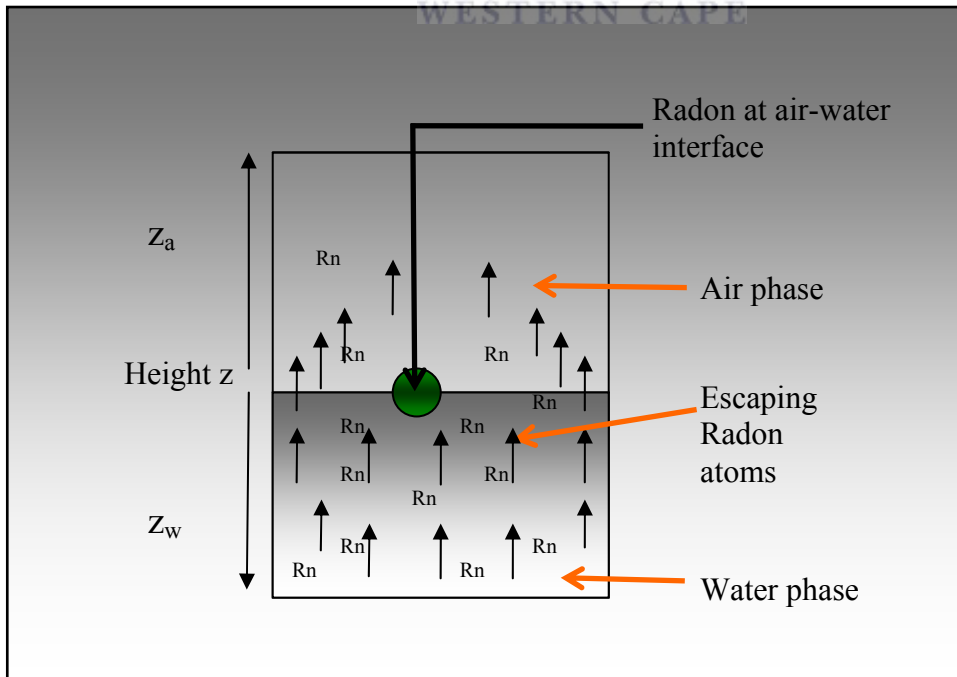


**Figure 4.1:** Radon at water-air interface in the container

## 4.1.1. Example of radon escape from water to air

### Introduction

This experiment describes a typical experiment of the radon release from water to air as performed in this work. In this case, a sample of 1.8 L is used instead of using the sample of 250 mL or 450 mL as in most experiments. A sample of 1.8 L was used to measure radon from a larger concentration container and to see if volume of the sample has any effect to the escape. The water sample is poured into a 2 L jar and placed in the vacuum chamber.

### Measurement of radon in air

The water sample was placed in the vacuum chamber as described earlier. The initial concentration is measured with RAD-H<sub>2</sub>O in a 250 mL vial and the remaining 1.8 L water sample is placed in the vacuum chamber. The vacuum chamber is immediately closed after putting the sample inside to avoid radon escape from water to air before measuring, which is the main issue of the thesis.

The objective is to measure the radon gas that diffuses from the water sample to the air. The water sample is placed in the vacuum chamber and the radon gas escapes from the water phase to the air phase in the container and the vacuum chamber as shown on **Fig. 4.2**. The RAD7 measures the radon concentration in the air. The data values are printed hourly and will be presented on the graph.

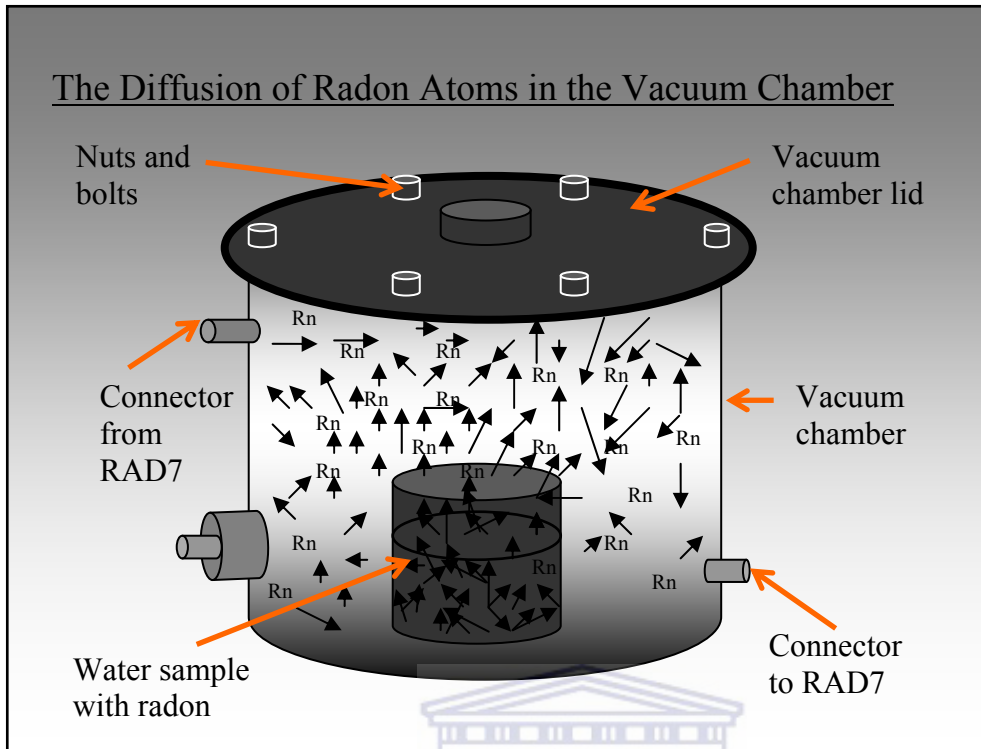
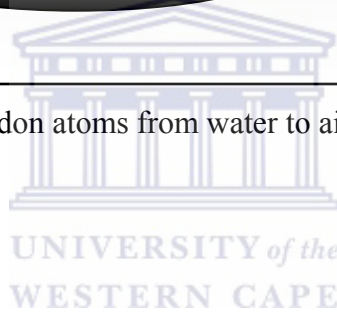


**Figure 4.2:** The diffusion of radon atoms from water to air in the chamber

## Results



The radon in air measurements and the uncertainties as given by the RAD7 are shown on **Fig. 4.3 (a)**. In most figures in this thesis, the error bars will not be shown for clarity. The results in Fig. 4.3 (a) indicate that the RAD7 probably overestimates the uncertainties, as the spread in values from the mean appears to be smaller than the error bars.

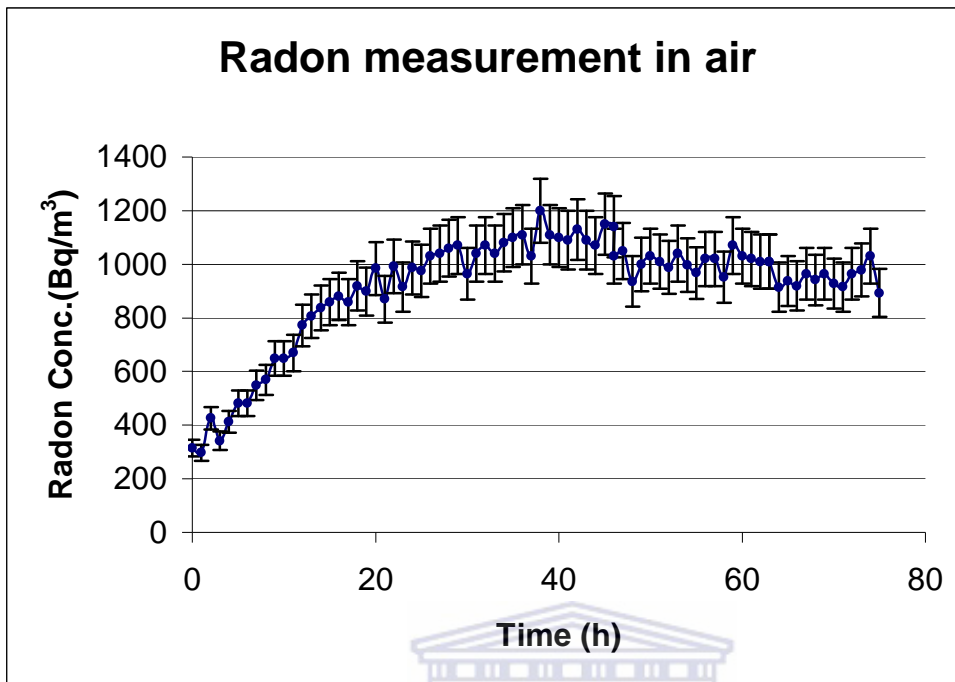


Figure 4.3 (a): The radon activity concentration in the air versus time with error bars

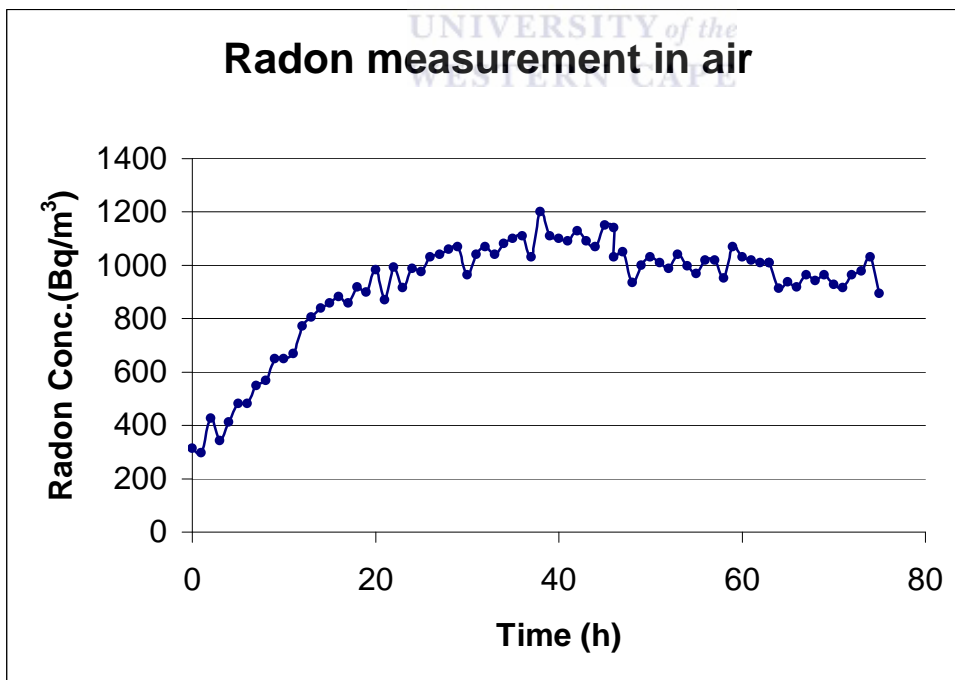


Figure 4.3 (b): The radon activity concentration in the air without error bars

## Discussion

The experiments require that the relative humidity be below 7% in order for the RAD7 detector to make reliable measurements. This experiment was conducted when the relative humidity inside the vacuum chamber was 5%, which is good enough to conduct the experiment of this nature. The radon concentration in air inside the vacuum chamber was measured. The temperature was recorded hourly and on average was 22°C without much change, which is good enough to run this experiment. According to **Fig. 3.3**, the solubility of radon in water is temperature dependent but the dependence at this temperature is small. This experimental set-up facilitates the measurement of radon gas that diffuses across the water–air interface.

The measurements show that radon builds up in the vacuum chamber for a number of hours before reaching equilibrium. The graphs show that the equilibrium is established at around 42 hours and the concentration seems to stabilize for several hours. At this time, the radon in water is nearly in equilibrium with radon in air. After the equilibrium is established, the radon concentration in air starts to reduce, as the radon decay becomes the main factor in the change in the radon level. **Fig. 4.3 (a)** shows the consistency of radon data points. The consistence of points indicates that the only sink for radon will be due to decay not radon leakage.

## 4.1.2. The effect of the area of water/air interface on radon escape

### Introduction

In this section, the area effect on the diffusion of radon from water to air will be investigated. Different escape areas are tested and the radon transfer for each area is studied. Different containers with different circular openings are used. The radius of each container will be used to calculate the escape area of radon from each container. The objective of this investigation is to study the radon escape from the water samples across the different normal areas. The initial concentrations are different since the experiments are conducted at different times. The water samples have nearly the same volume but different initial radon activity concentrations.

### Behaviour of the radon particles

The purpose of this experiment is to study the behaviour of the of radon particles that are passing across the normal area,  $A$  per unit time. The total flux,  $F$ , is dependent on the total activity of the system. This is given by the following formula.

$$C_w(t, T) \times V_w + C_a(t, T) \times V_a = A(t) = A_0 e^{-\lambda t} \quad (24)$$

where  $C_w$  and  $C_a$  are radon in water and air concentrations respectively and  $A_0 (= C_0(t, T) \times V_w)$  is the initial radon activity in the water sample. The values of  $C_0(t, T)$  are determined from the radon concentration at equilibrium and calculated back for cases where the initial concentration was not measured. The flux of the radon atoms depends on a proportionality constant  $\beta$ , which is the transfer velocity coefficient of radon across the water-air interface, and Eqn (19) gives:

$$F(t, T) = \beta [C_w(t, T) - \alpha(T) \times C_a(t, T)] \quad (25)$$

Eqn (24) can be used to eliminate  $C_w(t, T)$  in Eqn (25) and the resulting numerical model, taking into account that  $\beta$  is a constant, is given below:

$$F(t, T) = \beta \left[ C_0(t, T) e^{-\lambda t} - \frac{V_a}{V_w} C_a(t, T) - \alpha(T) \times C_a(t, T) \right] \quad (26)$$

where  $C_0(t, T)$  and  $C_a(t, T)$  are the initial radon-in-water and the radon-in-air concentrations respectively,  $\lambda$  is the decay constant of radon and  $\alpha(T)$  is the Ostwald's solubility coefficient, which is dependent on temperature as discussed in Chapter 3.

### Measurement of radon flux across different diffusion areas

The radon water samples are decanted into a small 250 mL vial with a small opening, a 500 mL aluminium can and a 2000 mL beaker. The experiments were conducted at different times and all start with different initial radon concentrations. The opening area of the vial is about  $1.8 \times 10^{-4} \text{ m}^2$ ; that of the aluminium can is about  $4.24 \times 10^{-3} \text{ m}^2$  and for the beaker, it is about  $0.011 \text{ m}^2$ . These investigations are conducted using water samples of 250 mL in the vial and 450 mL in the aluminium can.

Three sets of experiments were conducted for each of the above-mentioned containers. The experiments were repeated with different initial radon activity concentrations. The aim was to evaluate the correlation among the curves for each diffusion area and the radon flux from each container.

### Results

The figures 4.4(a) to 4.8 show the data based on the three experimental sets for each water-air interface area. The presented graphs are for the radon concentration and their respective fluxes across the diffusion area.

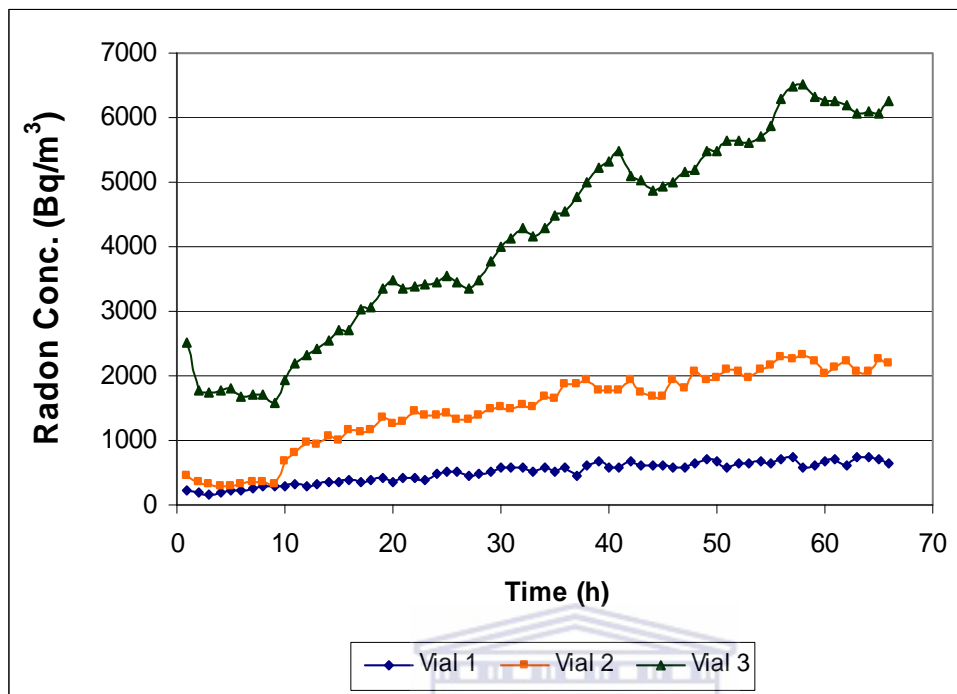


Figure 4.4 (a): The radon activity concentration in the air above a vial versus time.

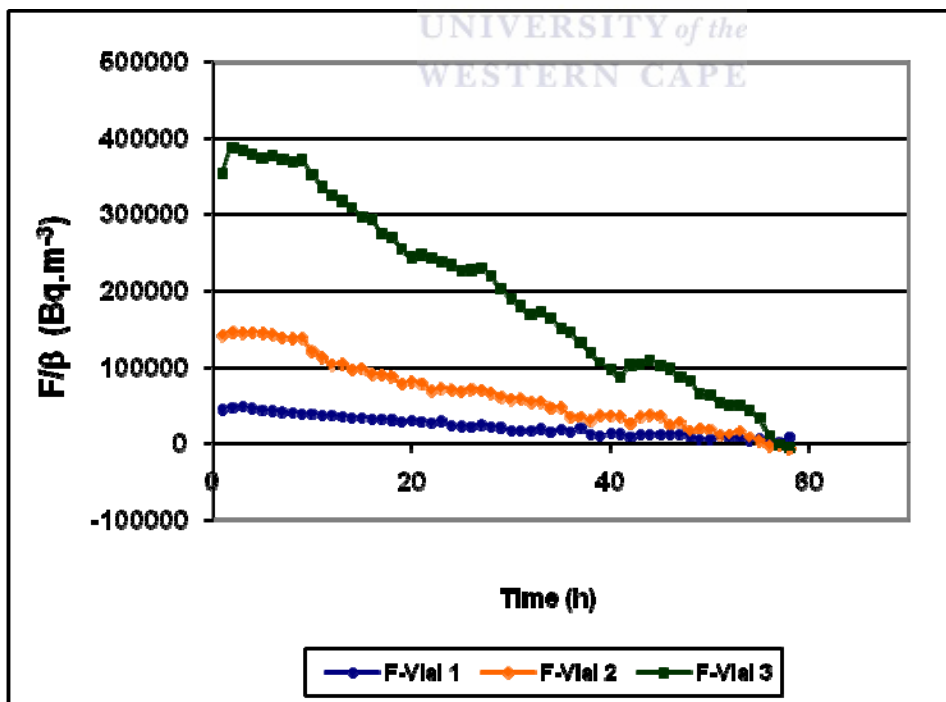
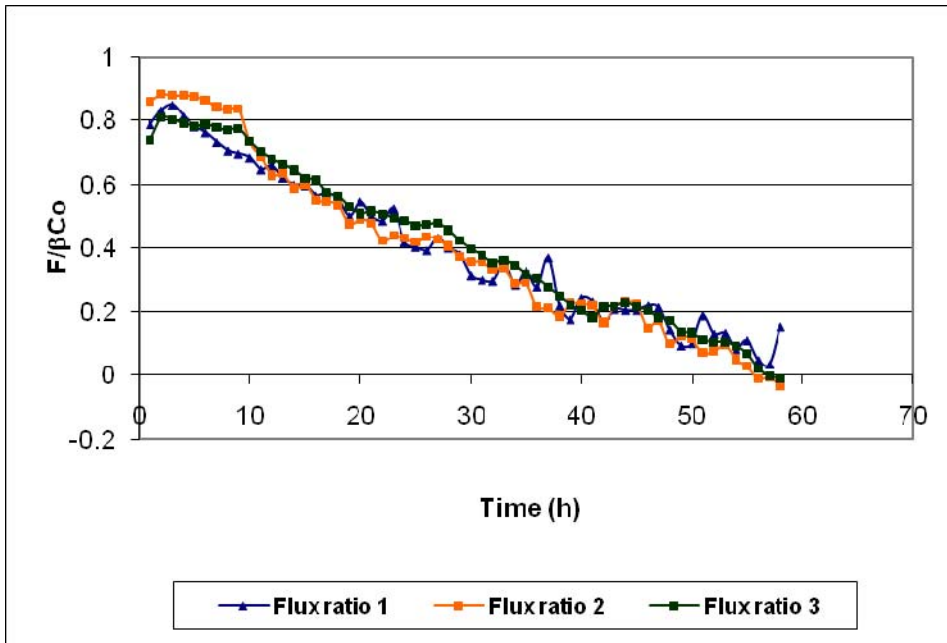
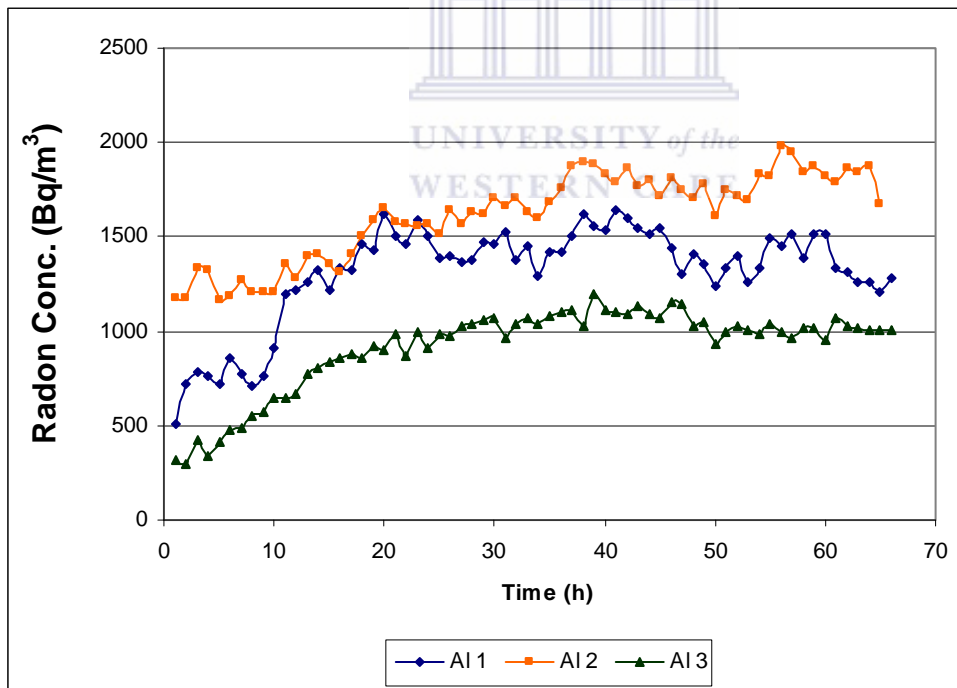


Figure 4.4 (b): The ratio of the radon flux ( $F/\beta$ ) from the vial versus the time.





**Figure 4.4 (c):** The radon flux divided by  $\beta C_0$  versus time for escape from the vial.



**Figure 4.5 (a):** The radon activity concentration in the air above the 500 mL Al can versus the time.

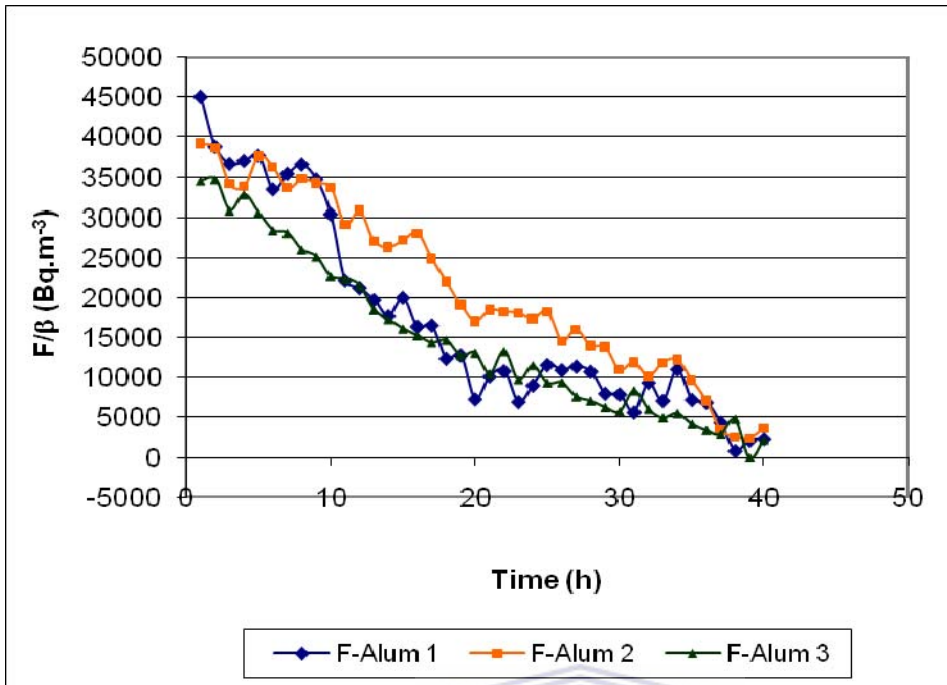


**Figure 4.5 (b):** The ratio of the radon flux ( $F/\beta$ ) from the Al can versus time. The flux becomes undefined when the radon in the air reaches equilibrium with the radon in the water after about 40 hours.

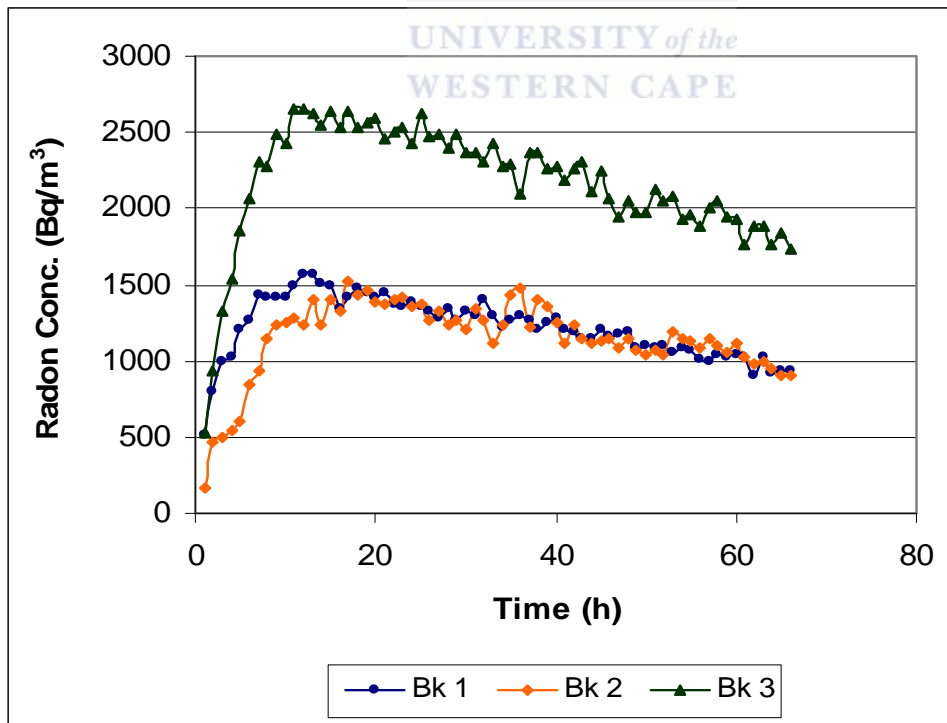


**Figure 4.6 (a):** The radon activity concentration in the air above a beaker versus time.

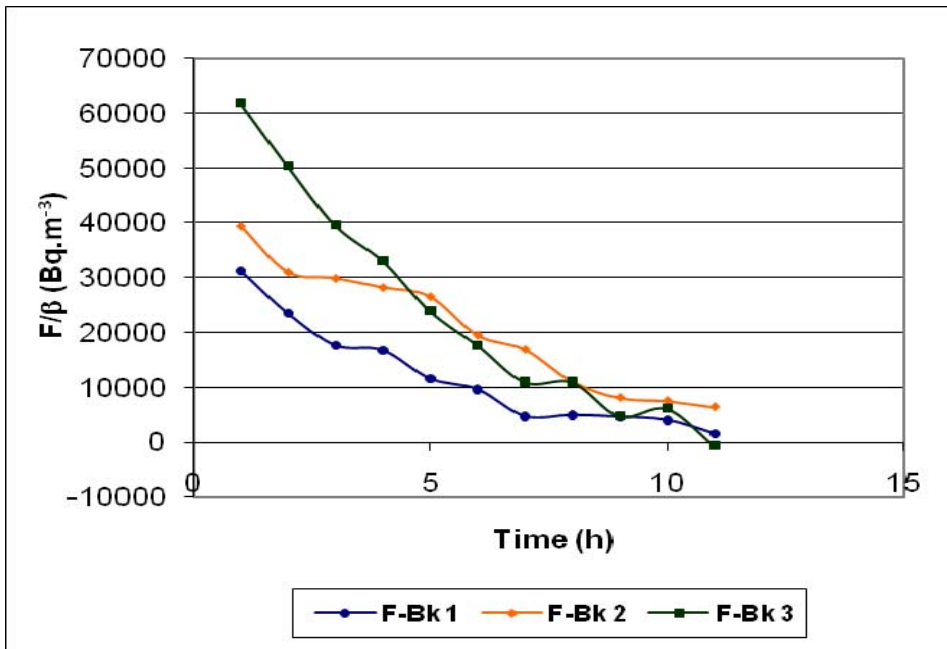


**Figure 4.6 (b):** The radon flux ( $\beta$ ) from the beaker versus the time for three initial concentrations. The flux becomes small when the radon in the air reaches equilibrium with the radon in the water after about 10 hours.

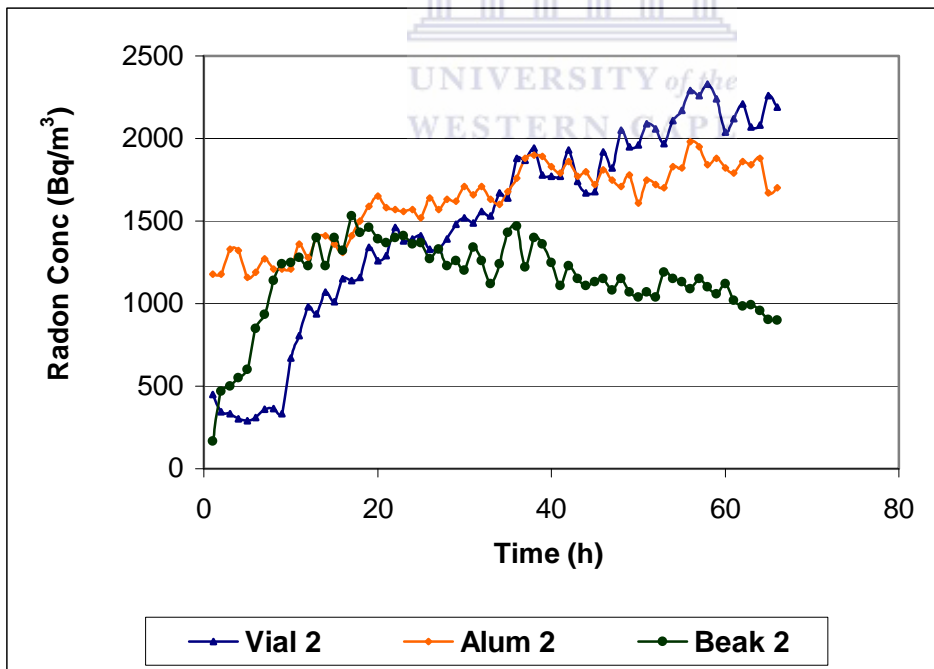


**Figure 4.7:** Examples of the radon activity concentration in air from each container versus time

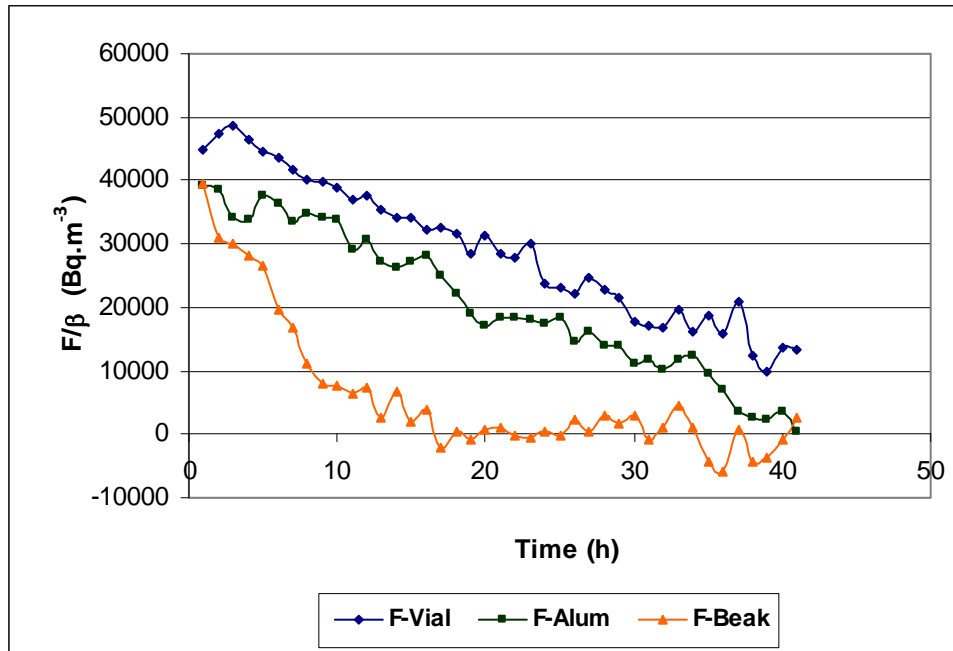


**Figure 4.8:** The ratio of radon flux to  $\beta$  from three containers versus time.

## Discussion and conclusion

The flux of radon atoms from water to air through the opening areas of three containers has been investigated. The radon atoms passing through the opening of the vial establishes the equilibrium only after about 50 hours. This happens because the vial has the smallest normal area through which radon atoms pass through per unit time and thus the vial releases the smallest number of radon atoms per unit time. The concentration is higher initially consequently; the flux is higher for the early hours and slowly decreases with time.

The transfer velocity coefficient of radon is a constant, unknown in the present case therefore; the flux of radon atoms divided by  $\beta$  as given in Eqn (26) is plotted on **Fig. 4.4(b)**. The resulting equation has the units of radon activity concentration. The radon flux in the vial is nearly linear for the first few hours but since the initial concentrations were different, the curves are far apart during early hours. However, if the fluxes are divided by the initial radon concentrations the curves come very close to each other as

shown on **Fig. 4.4(c)**. The flux is divided by the initial radon concentration to compare the flux without taking into account the initial radon activity concentrations differences between the water and the air.

For the aluminium can, the radon activity concentration reaches the equilibrium concentration quicker as compared to the case of the vial, after about 30 hours. This is expected because the aluminium can has a bigger normal area and therefore it has more radon atoms passing through the normal area per unit time to be pumped and counted by the RAD 7 detector. The radon atoms diffuse faster from the container because the normal area is bigger than that of vial. When comparing the  $1.8 \times 10^{-4} \text{ m}^2$  area of the vial and  $4.24 \times 10^{-3} \text{ m}^2$  of the aluminium can, we expect the can to release about 10 times more radon atoms than the vial.

In the case of the aluminium can, **Fig. 4.5 (a)**, the flux reduces faster as compared to the case of the vial. In the case of the beaker, the radon activity concentration reaches the equilibrium even faster than in both the cases of the aluminium can and vial. The normal area of the beaker is about  $0.011 \text{ m}^2$ , much larger than for the other containers. In this case, there are more radon atoms diffusing out easily from the container therefore more radon passes the normal area per unit time. Looking at the curves of radon measured from both the vial and the can, the escape of radon measured in the beaker is indeed much faster and equilibrium is reached after only around 12 hours.

All these curves show that the radon concentration approaches equilibrium as the experiment progresses with time. The studied curves also show that the normal area of the container, through which the gas escapes, plays an important role in the mass diffusion of materials. Since the diffusion of radon gas is expected to be proportional to the escape area, vessels with small openings are better when radon escape needs to be reduced.

### 4.1.3. The effect of temperature on radon escape from water

This section describes an experiment to test the effect which temperature can have on the diffusion of radon gas from water to air. From the kinetic theory of gases, the speed of gases increases with an increase in their temperatures. It is therefore expected that at lower temperatures the gases have less mobility. The radon escape at lower temperatures is studied in this section. The vacuum chamber, holding the radon water sample, is submerged in cold water with ice to study the change expected because of the temperature dependence of the Oswald coefficient.

#### Introduction

In this experiment, the water samples are measured for radon concentration using the vacuum chamber. The sample is placed inside the chamber and the  $^{222}\text{Rn}$  gas is expected to diffuse from water to air, thence transported to the desiccant where moisture is trapped. Radon in air is measured using the RAD7 and converted back into radon in water at equilibrium. The effect of temperature, specifically low temperature, to radon escape from water to air is tested by submerging the chamber in a bowl containing cold water. Ice blocks are introduced into the water in the bowl to maintain the system at low temperatures for a while. The chamber was removed from the water after a few hours.

#### Method

The radon water sample of about 450 mL is poured into a 2000 mL beaker with 12 cm mouth diameter. The radon sample is then immediately placed in the vacuum chamber. The vacuum chamber is sealed right away to limit radon loss. The experiment is started just after closing the vacuum chamber and it is initially conducted at room temperatures.

After a period of measurement, the vacuum chamber is put in the bowl with cold water and more ice is introduced into the bowl to observe temporal changes, as shown on **Fig.**

**4.9 (b).** An external thermometer is used to monitor the reduction in water temperature just after introducing the ice and to monitor the temperature as the ice starts melting. An electronic thermometer HOBO is also attached to the inside of the chamber. The experiment runs until all the ice blocks have melted and subsequently the vacuum chamber is removed from the bowl with water.

The program HOBOT Boxcar is installed in a PC operating with Windows 98 operation system for data acquisition. The data logger probe is submerged in the water sample inside the vacuum chamber to monitor the temperature of the water source during the measurement period. The program records the temperature hourly until the measurement period is over. The HOBOT Boxcar program is run on a PC to download the temperature readings from the data logger. The program takes a few minutes to download the entire memory from the logger, and displays it as a graph just after saving it. The information about HOBOT Boxcar program is available from RAD AQUA manual, DurrIDGE Company Inc. downloadable from the site of the company [www.durrIDGE.com](http://www.durrIDGE.com).



**Figure 4.9 (a):** The radon experiment before the introduction of the ice



**Figure 4.9 (b):** The whole Vacuum Chamber immersed in ice in bowl

## Results

The results of the experiment, conducted to study the effect of temperature on the escape of radon from water to air, are presented on **Fig. 4.10**. The radon activity concentrations that are recorded prior the introductions of ice and after are shown on the graph. After putting in the ice in the system, the temperature reduced from 30°C down to 11°C on the HOBO temperature logger as shown on the graph on **Fig. 4.10**.



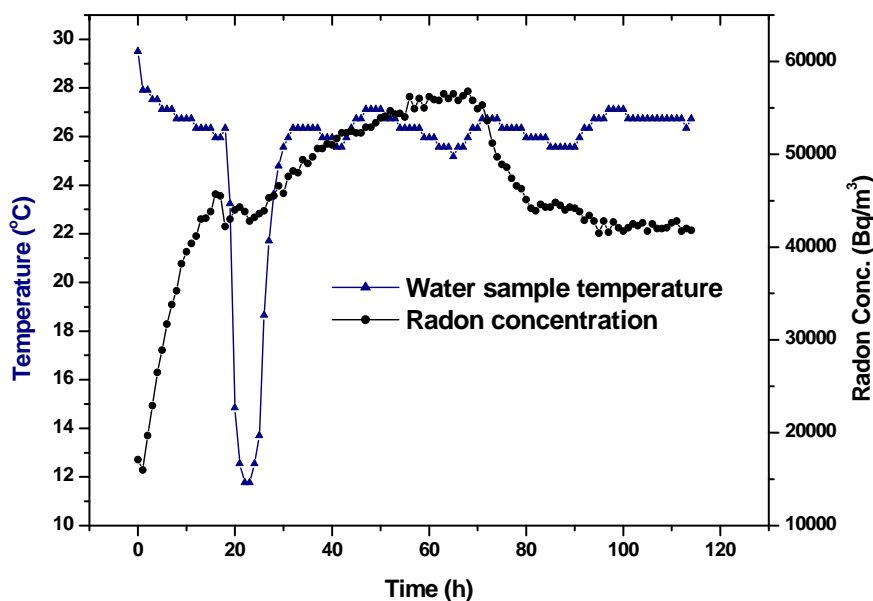


**Figure 4.10:** The water temperature and radon concentration versus time.

## Discussion and conclusion

Since radon behaves like other gases, then higher temperatures always increase the kinetic energy of the gas molecules. At lower temperatures, radon is more soluble in water. Eighteen hours after the experiment started, the ice was introduced to keep the system at lower temperatures for a while, and there is a perceptible alteration on the radon curve just after the 18<sup>th</sup> hour as it forms a valley before it reaches a crest again.

The concentration ebbs after the introduction of the ice blocks and rises again just after chamber is removed from the water. This is as expected. The conclusion drawn is that at lower temperatures, the radon mobilisation is reduced as radon remains in water. Therefore, the concentration goes into a valley instead of continuing rising up as happens at ordinary temperatures. This experiment gives results that agree in general with the temperature dependence of the Ostwald solubility coefficient because at low temperatures the solubility of radon in water is high therefore more radon is retained in water and less radon escapes from water to air.

## 4.2. Field water samples measured with the RAD-H<sub>2</sub>O

### Introduction

In this section, we present actual radon in water measurements to justify the importance of such measurements and hence the need to check on radon escape rate. The aim of the present investigation is to make use of the RAD-H<sub>2</sub>O radon measurement method to determine the dissolved activity concentration of radon in groundwaters and open surface waters. The groundwaters are borehole water and well water whereas the surface waters refer to the water samples from streams, river waters, dam and lakes. The water samples from a river and boreholes are analysed. In this text, these water samples are referred to as field water samples.

### Sample collection and preparation

The water samples were collected from different sources. Some were collected from the surface water while others were from groundwater. The groundwater samples were pumped from iThemba LABS and Strand boreholes while the surface water was fetched from Gevonden River. The Gevonden River is situated at Rawsonville. The Strand boreholes are about hundred metres away from the ocean whereas the iThemba LABS borehole is located a few kilometres away from the ocean.

The borehole, at iThemba LABS, was flushed for about 80 minutes to get rid of the water column where the radon has decayed; the sample was collected and filled in an airtight 5 L container. The water samples were filled in the clean 250 mL vials using a valve nozzle. The samples from Strand and Gevonden River were poured into 250 mL vials right away.

Since radon could be released from water during handling, transferring water from one container to another should be avoided and the water container should preferably be

closed while it is underwater during sampling. A sample that has been left open may have reduced activity. The water samples were filled in the clean containers directly from the sampling points while the containers were under water to avoid radon escape. The lids of the containers were tightly closed because there should preferably be no air bubble or air space between the water level and the lid.

### Analysis of the field water samples

The radon activity concentrations are obtained using the RAD H<sub>2</sub>O protocol where the radon in water concentration is obtained from the measurement of the radon in the gas bubbled through the water. An extra correction is made for the radon decay between the collection and analysis time using.

$$\Delta t = t_c - t_a \quad (27)$$

and

$$C(\Delta t, T) = C_0(t_0, T) e^{-\lambda \Delta t} \quad (28)$$

where the  $\Delta t$  term is the difference between the analysis time ( $t_a$ ) and collection time ( $t_c$ ) respectively. The  $C(\Delta t, T)$  is the radon concentration after time  $\Delta t$  and  $C_0(t_0, T)$  is the initial concentration at time  $t=0$

### Results and Discussion

The results of radon activity in water are presented in **Table 4**. The water samples after collection were taken to the University of the Western Cape Physics laboratory for analysis. The radon progeny was then analyzed for five minutes for four times as that is the protocol used by the RAD7 to measure radon in water using the RAD H<sub>2</sub>O method.

The four analysis results are then averaged. The average value represents the dissolved radon activity concentration in each sample.

The values presented here are the average values of the radon activity concentration in the waters collected in the sampling areas indicated. The field results of the measurements are presented in **Table 4**. The measured values are presented as averages,  $C_{Rn}$  and the radon corrected values are the average of the individual corrected values,  $C_o$ . the activities are expressed in units of Becquerel per litre (Bq/L). The activities are determined by making use of Eqn (28).

**Table 4: Radon concentration in water samples**

| Radon water Samples           | Collection Date | Analysis Date | Time between collection and measurement (Days) | Average Conc. $C_{Rn}$ (Bq/L) | Corrected Conc. $C_o$ (Bq/L) |
|-------------------------------|-----------------|---------------|--|-------------------------------|------------------------------|
| iThemba LABS borehole samples | 18-03-2009      | 19-03-2009    | 0.98   | 18±3                          | 22±4                         |
| Strand borehole samples       | 17-09-2009      | 17-09-2009    | 0.07   | 41±4                          | 42±4                         |
| Gevonden River samples        | 12-02-2010      | 16-02-2010    | 3.68   | 1.2±0.8                       | 2.4±1.3                      |

The field sample results shown on **Table 4**, show that the radon concentration in iThemba LABS groundwater is on average 22±4 Bq/L. The results show that on average the water sample from Strand borehole had an activity concentration of 42±4 Bq/L whereas the results of the surface water samples from Gevonden River show an average of 2.3±1.3 Bq/L.

The results for the water samples from Gevonden River (surface water) are within the range of the results reported for surface waters, which generally fall below 4 Bq/L (Cosma *et al.*, 2008; Rajashekara *et al.*, 2007; Marques *et al.*, 2004; Nazaroff *et al.*, 1987). These values are below the international recommended contaminant level of 11 Bq/L ((USEPA), 1999).

The activity concentration in groundwaters is high because of the presence of Radium-226 in soils and rocks through which water has seeped or has been contained (Singh *et al.*, 2008). The radon concentration is usually high in well water, intermediate in groundwater and lowest in surface water (Somlai *et al.*, 2007).



# CHAPTER 5 - MODELLING THE DIFFUSION OF RADON

In this section, a mathematical model is used to study numerically the behaviour of radon with time and the model is used to find an appropriate transfer velocity coefficient of radon from water to air. The concentrations are found using the models derived in section 3.5. Since the equations could not be solved analytically, a numerical model was employed. The numerical models were executed on a Microsoft Excel spreadsheet to deduce the transfer velocity coefficient of radon from water to air.

## 5.1. Modelling the experimental data

The numerical modelling results are compared to the measured data. This method helps to determine the value of the transfer velocity coefficient of radon movement from water to air. The volume is known and the value of the Ostwald solubility coefficient  $\alpha$  is the radon's solubility at equilibrium and is calculated by making use of the temperature dependence equation at equilibrium as given by Eqn (10).

### 5.1.1. The curves of the numerical model

When modelling the concentrations, the initial radon concentration in water is taken as equal to the maximum experimental value at equilibrium, corrected for decay. Thus, the initial radon concentration in water is known whereas radon in air is assumed initially negligible but nonzero. In this part of the study, the matching of the experimental radon data points and the modelled fit tests if the radon transfer velocity coefficient,  $\beta$ , values are similar in different experiments.

## 5.1.2. The results of the numerical modelling

The experimental radon curves are fitted with numerical model values. The results of the numerical modelling are presented on **Fig. 5.1** (a) to (e). The radon curves have different peak values since their individual initial radon concentrations were different. All parameters in Eqn (22a) and (22b) are known, except the initial radon concentration and the velocity transfer velocity.

The experiments were run when the temperatures were on average 25°C, thus the chosen value for the radon solubility coefficient is 0.22. The modelling fits were performed for different initial experimental concentrations.

The initial concentration in the water was measured or calculated from the concentration value at equilibrium ( $C_{0w} = (C_a^{eq} + C_w^{eq}) = C_e^{\lambda_{teq}} / V_w$ ). The transfer velocity coefficient of radon was then varied until a good fit to the data is obtained - see below.

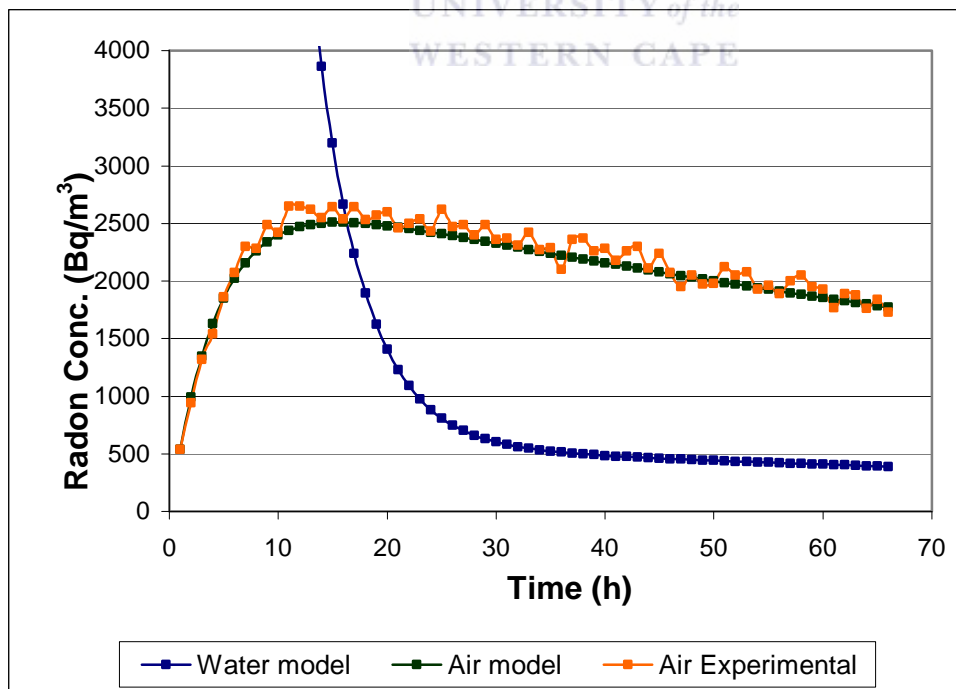


**Figure 5.1 (a):** The experimental and model radon concentration values for the  $\beta$  value that best fits the experimental data.

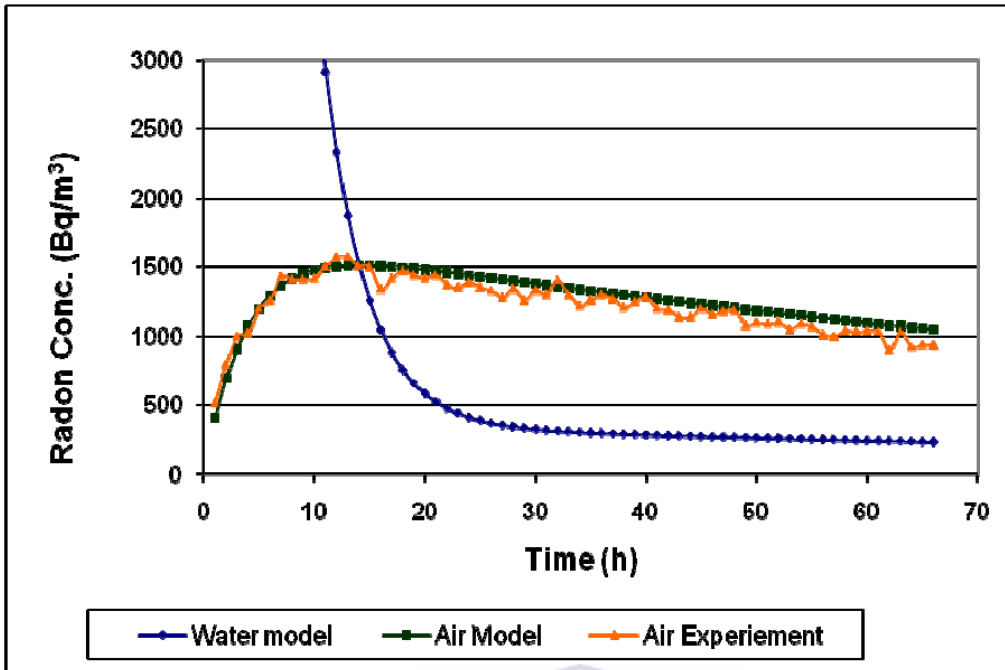


Figure 5.1 (b): Same as Fig. 5.1(a) for a different initial radon concentration.

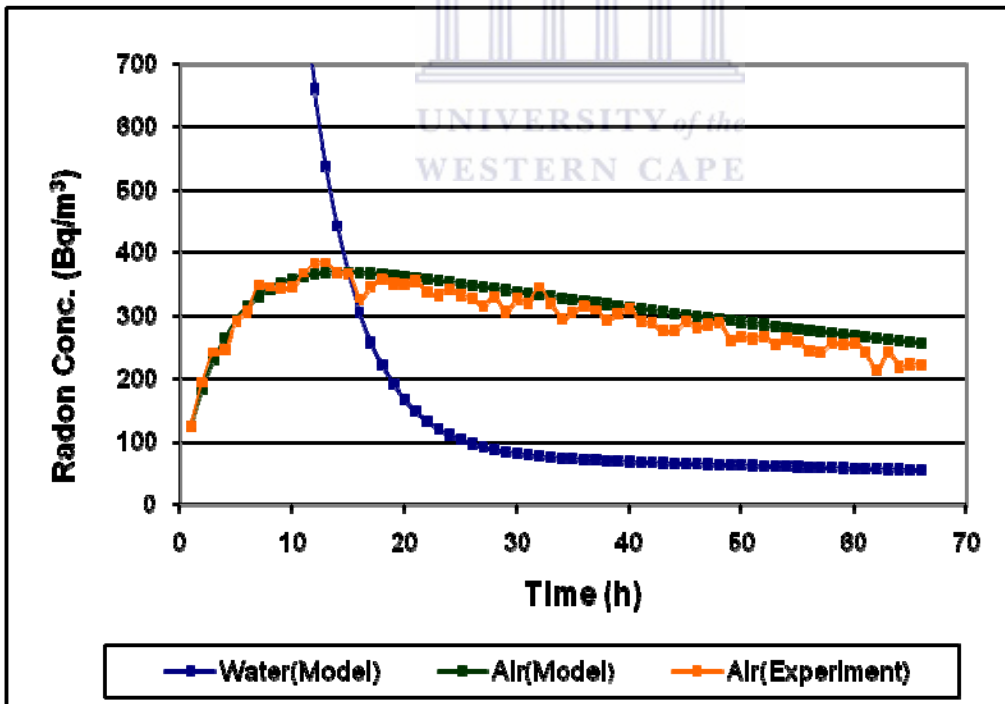


Figure 5.1 (c): Same as Fig. 5.1(a) for a different initial radon concentration.



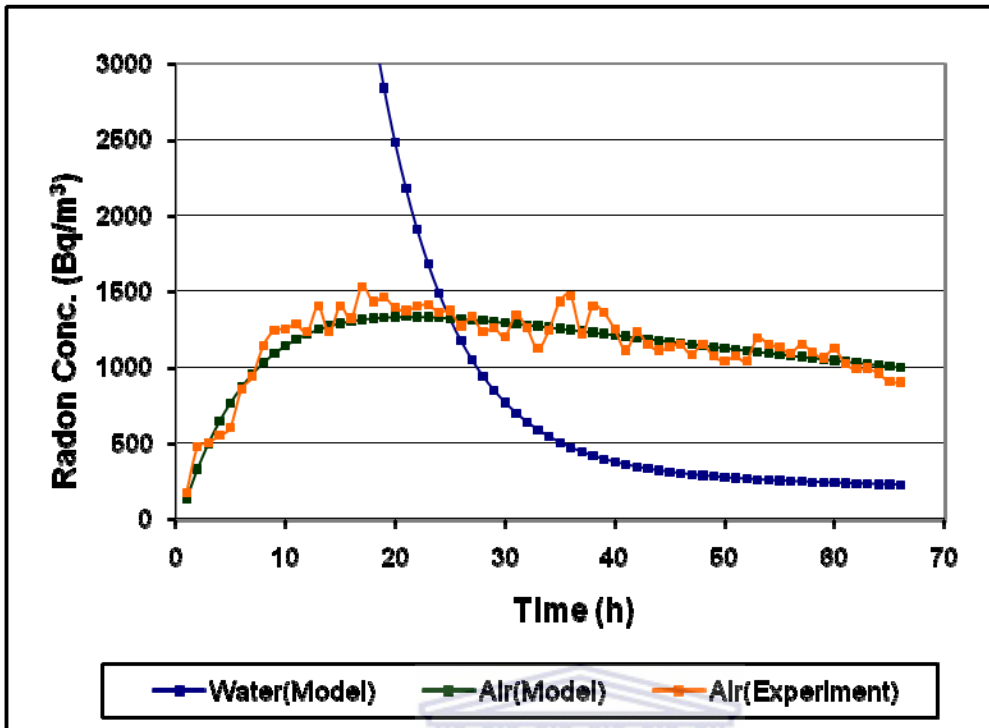


Figure 5.1 (d): Same as Fig. 5.1(a) for a different initial radon concentration.

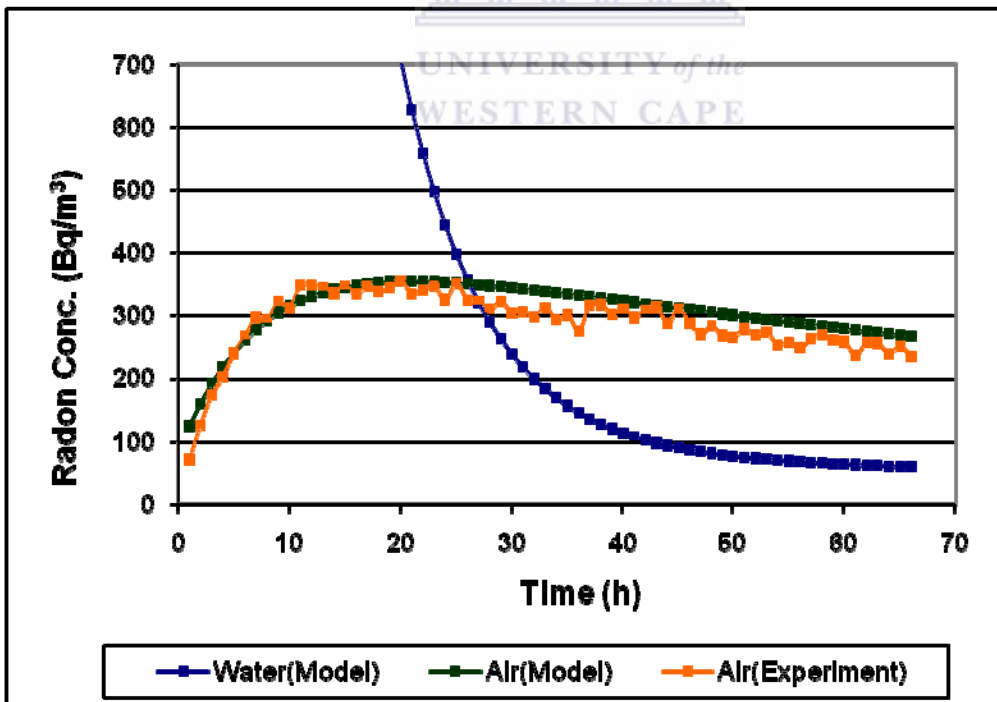


Figure 5.1 (e): Same as Fig. 5.1(a) for a different initial radon concentration.

The results deduced from the curves on **Fig. 5 (a)** to **Fig. 5 (e)** are presented on **Table 5**. **Table 5** presents the volume of the water sample, the maximum radon concentration at equilibrium, the average solubility coefficient of radon based on the average temperature and the transfer velocity coefficient of radon from water to air. The air volume is always the difference between the vacuum chamber and the sample volumes, which are about 0.01200 m<sup>3</sup> and 0.00045 m<sup>3</sup> respectively. The relative humidity was on average 5%.

**Table 5:** The parameters used in the numerical modelling and the results obtained. See discussion in section 5.2 on uncertainties.

| Graphs              | Water sample volume<br>( $\times 10^{-3} \text{ m}^3$ ) | Initial Rn in water<br>(Bq/L) | Ostwald coefficient | Transfer velocity $\beta$<br>( $\times 10^{-6} \text{ m/s}$ ) |
|---------------------|---|-------------------------------|---------------------|---|
| <b>Fig. 5.1 (a)</b> | 0.45  | 61.4                          | 0.22                | 2.2   |
| <b>Fig. 5.1 (b)</b> |   | 34.0                          |                     | 2.4   |
| <b>Fig. 5.1 (c)</b> |   | 7.8                           |                     | 2.3   |
| <b>Fig. 5.1 (d)</b> |   | 39.0                          |                     | 1.5   |
| <b>Fig. 5.1 (e)</b> |   | 8.1                           |                     | 1.3   |

## 5.2. Results and uncertainty analysis

The least square method offers a method to obtain unknown parameters in a fit. These parameters are fixed at values that minimize the sum of the squares of the difference between the measurements and the model (or predicted) values. The goodness of the fits shown on **Fig 5.1** were analyzed using this Chi-square method, which considers

$$\chi^2 = \sum_{i=1}^N \frac{(\hat{y}_i - y_i)^2}{\sigma_i^2} \quad (29)$$

where  $\hat{y}_i$  is the model (the fit) estimate,  $y_i$  is the actual observation,  $\sigma_i$  is the uncertainty in the individual measurement,  $N$  is the total number of observations, and  $\chi^2$  is the Chi-squared value.

The value of  $\beta$  was found that minimises  $\chi^2$  in Eqn (29) for the hours before the equilibrium was established.

The weighted average value of  $\beta$  will be calculated, and the final uncertainty evaluated with the following formula:

$$\sigma_{Tot} = \frac{1}{\left[ \sqrt{\sum_1^N \frac{1}{\sigma_i^2}} \right]} \quad (30)$$

where  $\sigma_{Tot}$  and  $\sigma_i$  are the total combined and individual uncertainties respectively.



## 5.3. Results and Discussion

### 5.3.1. Results

The modelling of the experimental curves and the results thereof are discussed in this section. The modelling fits were performed for different experimental curves with different initial radon concentrations, but the transfer velocity coefficients seem reasonably consistent as shown in Table 5.

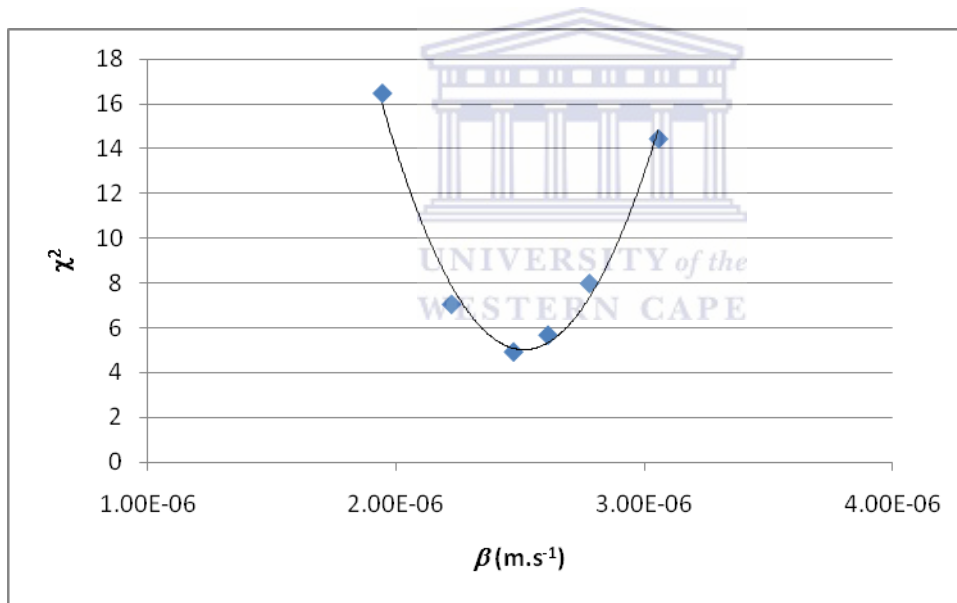
The modelling and the experiment data points compare well. To calculate the uncertainties in the transfer velocity coefficient of each curve, the concentration values of both the experimental and modelled curves are considered in the first few hours of the experiment before radon in water reaches equilibrium with radon in air.

The results of the transfer velocity coefficients and their relative uncertainties are evaluated by plotting the Chi-squared values against different beta values as presented on

**Fig 5.2.** The minimum value of Chi-square fixes the probable value of the transfer velocity coefficient presented on **Table 5**

The extracted  $\beta$  values give an average of  $1.9 \times 10^{-6}$  m/s. The uncertainty in the  $\beta$  values is estimated by considering the  $\chi^2$  values when one moves away from the minimum and using tables of  $\chi^2$  values for specific confidence intervals. Using this method, the uncertainties for the  $\beta$  values was found to be around  $0.3 \times 10^{-6}$  m/s.

Using the values found for  $\beta$  and calculating the standard deviation, gives a value of  $0.5 \times 10^{-6}$  m/s. Our best estimate of the transfer velocity coefficient is thus given by  $(1.9 \pm 0.5) \times 10^{-6}$  m/s.



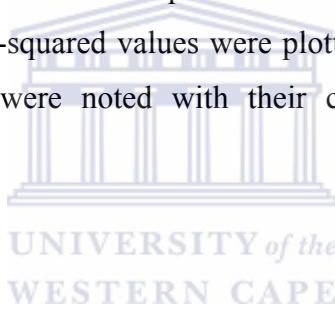
**Figure 5.2:** The total chi-square values plotted against the beta values for Fig. 5.1(b). The curve is a quadratic fit to the data.

Table 6 presents beta values and the uncertainties. For each of the mentioned figures the chi-squared values were plotted as shown on **Fig. 5.2** above to extract the uncertainty.

**Table 6:** The transfer velocity coefficient of radon deduced from model fits.

| <b>Graphs</b>  | <b>Fig. 5.1<br/>(a)</b> | <b>Fig. 5.1<br/>(b)</b> | <b>Fig. 5.1<br/>(c)</b> | <b>Fig. 5.1<br/>(d)</b> | <b>Fig. 5.1<br/>(e)</b> |
|--|-------------------------|-------------------------|-------------------------|-------------------------|-------------------------|
| <b><math>\beta</math> from fits<br/>(<math>10^{-6}</math> m/s)</b>                       | 2.2                     | 2.4                     | 2.3                     | 1.5                     | 1.3                     |
| <b>Full values<br/><math>\beta \pm \delta\beta</math><br/>(<math>10^{-6}</math> m/s)</b> | 2.2 $\pm$ 0.3           | 2.4 $\pm$ 0.4           | 2.3 $\pm$ 0.3           | 1.5 $\pm$ 0.3           | 1.3 $\pm$ 0.3           |

**Table 6** presents the results of the Chi-squared method for the beta,  $\beta$  values from different curves where the Chi-squared values were plotted against the beta values. The minimum Chi-square values were noted with their corresponding transfer velocity coefficient of radon.



### 5.3.2. Discussion

The values of the transfer velocity coefficient of radon from water to air that are given in Table 6 are averaged to give a final value. The combined uncertainty is evaluated by making use of the values reported in Table 6 above and using Eqn (30). The final value of the transfer velocity coefficient of radon from water is  $(1.9 \pm 0.5) \times 10^{-6}$  m/s. The uncertainty includes only statistical uncertainties. The value is dependent on several possible systematic uncertainties such as the measured area of the container and the calibration of the RAD7 monitor.

This value is of the same order of magnitude as the value Calugaru *et al.*, 2002 reports; it is two orders of magnitude smaller than the value reported by Kawabata *et al.*, 2003, but their value is not really comparable to the results found in this thesis. The study conducted by Kawabata *et al.*, 2003 is interesting because they also measured gas transfer

velocity using radon but in the presence of turbulence in the ocean. Kawabata *et al.*, 2003 reported the average value of the transfer velocity of radon from the ocean of  $(9.4 \pm 4.8)$  m day<sup>-1</sup>, a value that is equivalent to  $(1.1 \pm 0.6) \times 10^{-4}$  m/s. They measured the radon escape from the sea while we used still water in a container. A dimensionless transfer factor of radon from water to air for water in a house ( bath, shower, sink etc.) is reported by (Nazaroff *et al.*, 1987; Amrani *et al.*, 1999; Vinson *et al.*, 2008) but this is also not comparable to our measurement.

The value of  $\beta$  indicates that radon in water measurements are not affected much by radon escape. Consider for example a sample of one litre with a concentration of about 40 Bq/L as found in the sample in section 4.2. If the sample of one litre has an opening of area, A, of 10 cm<sup>2</sup> and left open to the atmosphere with negligible radon concentration for one minute, Eqn (19) predicts that the loss of radon due to radon flux will be

$$F(t) \times Area \times time = A \times t \times \beta (C_w(t) - 0)$$

$$= 10^{-3} \text{ m}^2 \times 60 \text{ s} \times 1.9 \times 10^{-6} \text{ m/s} \times 40 \times 10^3 \text{ Bq/m}^3$$

$$\sim 5 \times 10^{-3} \text{ Bq}$$

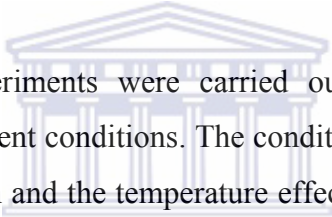
which is a very small part of the radon in the water.

# CHAPTER 6 - RESULTS AND DISCUSSION

This chapter summarizes the results from different experiments conducted in this study. This chapter is an overview of different radon measurement methods used. The results of the vacuum chamber and RAD-H<sub>2</sub>O measurement methods are discussed in this chapter. The results from the modelling fits of the radon escape from water are also considered in this chapter and their comparison with the results reported in the literature.

## 6.1. Results from measurements

### 6.1.1. Vacuum Chamber



The different laboratory experiments were carried out in order to investigate the behaviour of radon under different conditions. The conditions include the radon diffusion area, initial radon concentration and the temperature effects on radon escape. From these experiments, an understanding about the escape of radon gas from water to air is developed. Placing a radon enriched water sample in the vacuum chamber helped to measure radon escape from water in a partially quiescent environment. The water sample in the chamber can be regarded as a stagnant small water sample in a container exposed to a large volume of air but not to other external factors except the pumping air from detector and in the experiment to measure the temperature effect.

#### 6.1.1.1. The effect of the water-air interface area on radon escape

The flux of the atoms will be high during the early hours of the investigation when the water sample is highly enriched with radon compared to the concentration in air. For the samples placed in containers with large water-air interface area (e.g. beaker), the radon escape rate is high and the plotted radon graphs, see Fig. 4.6(a), peaks sooner meaning that the equilibrium between radon in air and water is established in a short time. For the

small water-air interface area, see Fig. 4.4(a) and 4.5(a), the radon takes very long to establish the equilibrium.

### 6.1.1.2. The effect of temperature on radon escape from water

As radon behaves like other gases, its mobility is influenced by temperature and pressure. At high temperatures, the atoms and or molecules are more mobile and collide more often. All the experiments were conducted at temperatures around 20 to 25°C. The only experiment conducted at lower temperature was the one where the objective was to observe the behaviour of radon escape rate at lower temperature. When the ice was introduced in the bowl, the lowest temperature that the whole system attained was 11°C. The radon graph plotted together with temperature shows that after introducing the ice, the temperature went down and the radon escape rate reduced. The escape rate went back to normal after the ice melted and the chamber was removed from the bowl. At lower temperatures, the equilibrium state has more radon in the water. The retaining of radon at lower temperatures is in agreement with the Ostwald solubility coefficient, which indicates that at low temperatures the radon gas dissolves in water more than at high temperatures.

### 6.1.2. RAD-H<sub>2</sub>O

In this study, the dissolved radon concentration was measured in groundwater and surface water samples. The RAD-H<sub>2</sub>O measurement method effectively measures radon in water. Using the RAD-H<sub>2</sub>O method, radon was measured in surface and groundwaters. The groundwaters have more radon than surface waters. The reason is that in surface waters the escape of radon is large as they are exposed to air whereas in groundwater, the radon is in a confined aquifer in contact with air in the soil that has a large concentration and the only way it escapes the water system is by decaying. Rocks cover groundwater and mud so that the production of radon is sustainable.



## 6.2. Results from numerical modelling

The models developed to estimate the radon diffusion from water to air help us to understand the radon escape. These models can provide values from the initial concentration and helps us to understand the underlying mechanisms and thus to perform more reliable interpretations and extrapolation of data. A thorough understanding of the models is helpful when making the final interpretation of the radon escape rate from water to air.

Despite the fact that the fits were implemented for different experiments with different initial radon concentrations, the radon escape rates in all the respective data sets are consistent. When comparing the model and experimental results, the model fits the experimental data sets very well. The radon data points of both the experimental and fitted graphs, sampled before the equilibrium was established, were used to calculate the uncertainties. The majority of the Chi-squared values per degree of freedom from all fits are below one, probably because the uncertainties of the RAD7 detector are overestimated.

The escape rate of radon from water to air was found to be in the order of  $10^{-6}$ . The value is on average,  $(1.9 \pm 0.5) \times 10^{-6}$  m/s. This value is of the same order of magnitude to the value Calugaru *et al.*, 2002 reports in their study. Their study is based purely on modelling whereas in this study, the values were determined by fitting experimental data points by numerical models.

The value this thesis reports is two orders of magnitudes smaller than the  $(1.1 \pm 0.6) \times 10^{-4}$  m/s reported by Kawabata *et al.*, 2003, but their value is for a very different physical situation. The only other value reported in the literature, that we found, was by the following authors (Nazaroff *et al.*, 1987; Amrani *et al.*, 1999; Vinson *et al.*, 2008; Radolic *et al.*, 2005) who consider the radon released into a house by radon-enriched groundwater. This value cannot be directly compared to our value.

# CHAPTER 7 - CONCLUSION

This chapter summarizes the findings of the study. The main objectives of this study were to measure dissolved radon concentration in water, and to model the escape of radon to air in order to find the transfer velocity coefficient for radon from water to air.

## 7.1. Experimental results

The objectives of the study were to measure the activity concentration of radon in the groundwater samples, surface water samples, and mainly the laboratory-prepared samples and to measure and model numerically the radon escape rate as the radon diffuses out of water sample to air. The radon concentrations in groundwater and surface water are different as the literature reports. This difference is based mainly in the escape of radon from water to air. The radon is present in higher concentrations in groundwaters than in surface waters as reported in this thesis and other literature reports. These concentration differences can be used to assess the exchange of groundwater and surface water. In such assessments, a good understanding of the radon escape from water to air during sampling and measurement is vitally important.

From the knowledge of radon concentration distribution in groundwater and surface water, the locations and discharges of groundwater to surface water can be identified precisely. The pathway of fresh water that discharges into open water bodies like seas and oceans can be determined. The radon concentrations in groundwater and surface waters found in this work are similar to the concentration values reported in the literature.

Radon measurement in a chamber is a good method for studying the radon escape rate from water to air because the water in the container inside the chamber is not disturbed by external factors. The radon gas that has escaped from a water phase to air phase is pumped through the pipes to the RAD7 radon continuous monitor.

## 7.2. Modelling result

The equations governing the diffusion of particles were developed to form a mathematical model. The model was further developed and written in terms of finite difference equations. In that case, it was simple to use the given parameters to fit the experimental data.

The experimental data fitted with the numerical models are reported in Chapter 4. The model fits were performed on the radon data measurements conducted to study the effect of area on the radon escape rate so that there were no experiments that were conducted specifically for modelling the data.

The models that were developed are very easy to use. While fitting the model graphs and experimental data points, different values of the parameter,  $\beta$ , were tried. The fitting of the experimental points was done by looking for the minimum  $\chi^2$  values. The results are reasonably consistent with each other, and the graphs fit the experimental data points well.

In this thesis, the value of the transfer velocity coefficient of radon was found to be  $(1.9 \pm 0.5) \times 10^{-6}$  m/s, which is comparable to the value used by Calugaru *et al.*, 2002 in their study.

The results of this thesis indicate that the escape velocity of radon from undisturbed water is a relatively slow process. This justifies the use of radon in practical applications where fast escape would have made all measurements unreliable.

## APPENDICES

### APPENDIX A: MEASUREMENTS OF THE CONTAINERS

The volume of the vacuum chamber is about 11 L whereas the volume of the beaker is 2 L but usually only 0.45 L was poured into the beaker. The volumes of the vial and aluminium can are 0.25 L and 0.5 L respectively, but again the Al can was only filled with 0.45 L.

**Table 7: The approximate areas and volumes of the containers used in the study.**

| <b>CONTAINERS USED IN THE STUDY</b> |                      |                       |               |                       |
|-------------------------------------|----------------------|-----------------------|---------------|-----------------------|
|                                     | <b>Vial</b>          | <b>Al Can</b>         | <b>Beaker</b> | <b>Vacuum Chamber</b> |
| <b>Area (m<sup>2</sup>)</b>         | 1.8×10 <sup>-4</sup> | 4.24×10 <sup>-3</sup> | 0.011         | -                     |
| <b>Volume (L)</b>                   | 0.25                 | 0.5                   | 2             | 11                    |

## APPENDIX B: TABULATED RAW EXPERIMENTAL DATA

The following tables represent the radon information where radon was measured in a beaker. The relative humidity (RH) inside the RAD 7 detector and the temperature of the water sample are also presented

**Table 8: Experimental data for graphs shown on Fig. 4.3**

| <b>Time (h)</b> | <b>Relative Humidity (%)</b> | <b>Temperature (°C)</b> | <b>Concentration (Bq/m<sup>3</sup>)</b> | <b>Uncertainty (Bq/m<sup>3</sup>)</b> |
|-----------------|------------------------------|-------------------------|---|---------------------------------------|
| 1               | 6                            | 23.24                   | 185                                     | 53                                    |
| 2               | 5                            | 22.09                   | 412                                     | 76                                    |
| 3               | 5                            | 22.09                   | 444                                     | 78                                    |
| 4               | 5                            | 22.48                   | 626                                     | 92                                    |
| 5               | 5                            | 22.48                   | 762                                     | 101                                   |
| 6               | 5                            | 22.09                   | 871                                     | 108                                   |
| 7               | 5                            | 22.09                   | 930                                     | 111                                   |
| 8               | 5                            | 22.09                   | 1080                                    | 120                                   |
| 9               | 5                            | 22.09                   | 1160                                    | 123                                   |
| 10              | 5                            | 22.09                   | 1270                                    | 129                                   |
| 11              | 5                            | 22.09                   | 1280                                    | 129                                   |
| 12              | 5                            | 22.09                   | 1590                                    | 143                                   |
| 13              | 5                            | 22.09                   | 1480                                    | 138                                   |
| 14              | 5                            | 22.09                   | 1540                                    | 141                                   |
| 15              | 5                            | 22.09                   | 1620                                    | 144                                   |
| 16              | 5                            | 21.71                   | 1760                                    | 151                                   |
| 17              | 5                            | 21.71                   | 1890                                    | 155                                   |
| 18              | 5                            | 21.71                   | 2050                                    | 162                                   |
| 19              | 5                            | 21.71                   | 2050                                    | 162                                   |
| 20              | 5                            | 21.71                   | 2150                                    | 166                                   |
| 21              | 5                            | 22.09                   | 2130                                    | 165                                   |
| 22              | 5                            | 22.09                   | 2190                                    | 167                                   |
| 23              | 5                            | 22.09                   | 2200                                    | 168                                   |
| 24              | 5                            | 22.48                   | 2120                                    | 165                                   |

|    |   |       |      |     |
|----|---|-------|------|-----|
| 25 | 5 | 22.48 | 2350 | 173 |
| 26 | 5 | 22.48 | 2300 | 171 |
| 27 | 5 | 22.48 | 2440 | 176 |
| 28 | 5 | 22.48 | 2300 | 171 |
| 29 | 5 | 22.48 | 2480 | 178 |
| 30 | 5 | 22.48 | 2500 | 179 |
| 31 | 5 | 22.48 | 2390 | 175 |
| 32 | 5 | 22.48 | 2680 | 184 |
| 33 | 5 | 22.48 | 2700 | 185 |
| 34 | 5 | 22.48 | 2680 | 184 |
| 35 | 5 | 22.48 | 2600 | 182 |
| 36 | 5 | 22.48 | 2630 | 183 |
| 37 | 5 | 22.09 | 2800 | 188 |
| 38 | 5 | 22.09 | 2540 | 180 |
| 39 | 5 | 22.09 | 2790 | 188 |
| 40 | 5 | 22.09 | 2670 | 140 |
| 41 | 5 | 22.09 | 2610 | 182 |
| 42 | 5 | 21.71 | 2700 | 185 |
| 43 | 5 | 21.71 | 2900 | 191 |
| 44 | 5 | 21.71 | 2700 | 185 |
| 45 | 5 | 21.71 | 2780 | 188 |
| 46 | 5 | 21.71 | 2840 | 190 |
| 47 | 5 | 21.71 | 2780 | 187 |
| 48 | 5 | 22.09 | 2770 | 187 |
| 49 | 5 | 22.09 | 2790 | 188 |
| 50 | 5 | 22.09 | 2810 | 189 |
| 51 | 5 | 22.09 | 2680 | 185 |
| 52 | 5 | 22.09 | 2670 | 184 |
| 53 | 5 | 22.09 | 2870 | 191 |
| 54 | 5 | 22.09 | 2690 | 185 |
| 55 | 5 | 22.09 | 2670 | 184 |
| 56 | 5 | 21.71 | 2730 | 186 |
| 57 | 5 | 21.71 | 2740 | 186 |
| 58 | 5 | 21.71 | 2830 | 189 |
| 59 | 5 | 21.71 | 2610 | 182 |
| 60 | 5 | 21.71 | 2810 | 189 |

|    |   |       |      |     |
|----|---|-------|------|-----|
| 61 | 5 | 21.71 | 2800 | 188 |
| 62 | 5 | 21.71 | 2770 | 188 |
| 63 | 5 | 21.33 | 2840 | 190 |
| 64 | 5 | 21.33 | 2680 | 185 |
| 65 | 5 | 21.33 | 2690 | 185 |
| 66 | 5 | 21.33 | 2790 | 188 |
| 67 | 5 | 20.95 | 2820 | 189 |
| 68 | 5 | 20.95 | 2680 | 185 |
| 69 | 5 | 21.33 | 2830 | 189 |
| 70 | 5 | 21.33 | 2810 | 189 |

**Table 9: Experimental data for use in modelling Fig. 5 (a)**

| <b>Time (h)</b> | <b>Relative Humidity (%)</b> | <b>Temperature (°C)</b> | <b>Concentration (Bq/m<sup>3</sup>)</b> | <b>Uncertainty (Bq/m<sup>3</sup>)</b> |
|-----------------|------------------------------|-------------------------|---|---------------------------------------|
| 1               | 5                            | 23.63                   | 535                                     | 86                                    |
| 2               | 5                            | 23.63                   | 941                                     | 111                                   |
| 3               | 5                            | 24.01                   | 1320                                    | 131                                   |
| 4               | 5                            | 24.01                   | 1540                                    | 141                                   |
| 5               | 5                            | 24.4                    | 1860                                    | 154                                   |
| 6               | 5                            | 24.4                    | 2070                                    | 163                                   |
| 7               | 5                            | 24.4                    | 2300                                    | 171                                   |
| 8               | 5                            | 24.4                    | 2280                                    | 170                                   |
| 9               | 5                            | 24.4                    | 2490                                    | 178                                   |
| 10              | 5                            | 24.4                    | 2420                                    | 176                                   |
| 11              | 5                            | 24.01                   | 2650                                    | 183                                   |
| 12              | 5                            | 24.01                   | 2650                                    | 183                                   |
| 13              | 5                            | 24.01                   | 2620                                    | 182                                   |
| 14              | 5                            | 24.01                   | 2550                                    | 180                                   |
| 15              | 5                            | 24.01                   | 2640                                    | 183                                   |
| 16              | 5                            | 24.01                   | 2540                                    | 179                                   |
| 17              | 5                            | 24.01                   | 2640                                    | 183                                   |
| 18              | 5                            | 23.63                   | 2530                                    | 180                                   |
| 19              | 5                            | 23.63                   | 2570                                    | 181                                   |
| 20              | 5                            | 23.24                   | 2600                                    | 182                                   |

|    |   |       |      |     |
|----|---|-------|------|-----|
| 21 | 5 | 23.24 | 2460 | 177 |
| 22 | 5 | 23.24 | 2500 | 178 |
| 23 | 5 | 23.24 | 2540 | 180 |
| 24 | 5 | 23.63 | 2430 | 176 |
| 25 | 5 | 23.63 | 2620 | 183 |
| 26 | 5 | 24.01 | 2470 | 177 |
| 27 | 5 | 24.4  | 2490 | 178 |
| 28 | 5 | 24.4  | 2400 | 175 |
| 29 | 5 | 24.4  | 2490 | 178 |
| 30 | 5 | 24.4  | 2360 | 173 |
| 31 | 5 | 24.4  | 2370 | 174 |
| 32 | 5 | 24.4  | 2310 | 171 |
| 33 | 5 | 24.4  | 2420 | 175 |
| 34 | 5 | 24.4  | 2270 | 170 |
| 35 | 5 | 24.01 | 2290 | 171 |
| 36 | 5 | 24.01 | 2100 | 164 |
| 37 | 5 | 23.63 | 2360 | 173 |
| 38 | 5 | 23.63 | 2370 | 174 |
| 39 | 5 | 23.63 | 2260 | 170 |
| 40 | 5 | 23.24 | 2280 | 170 |
| 41 | 5 | 23.24 | 2180 | 167 |
| 42 | 5 | 23.24 | 2260 | 170 |
| 43 | 5 | 23.24 | 2300 | 171 |
| 44 | 5 | 23.24 | 2110 | 165 |
| 45 | 5 | 22.86 | 2240 | 169 |
| 46 | 5 | 22.86 | 2070 | 163 |
| 47 | 5 | 22.86 | 1950 | 158 |
| 48 | 5 | 22.86 | 2050 | 162 |
| 49 | 5 | 23.24 | 1970 | 159 |
| 50 | 5 | 23.63 | 1980 | 159 |
| 51 | 5 | 24.01 | 2120 | 165 |
| 52 | 5 | 24.01 | 2050 | 162 |
| 53 | 5 | 24.01 | 2080 | 163 |
| 54 | 5 | 24.01 | 1930 | 157 |
| 55 | 5 | 24.01 | 1960 | 158 |
| 56 | 5 | 24.01 | 1890 | 155 |



|    |   |       |      |     |
|----|---|-------|------|-----|
| 57 | 5 | 24.01 | 2000 | 160 |
| 58 | 5 | 24.01 | 2050 | 162 |
| 59 | 5 | 23.63 | 1950 | 158 |
| 60 | 5 | 23.63 | 1930 | 158 |
| 61 | 5 | 23.63 | 1770 | 151 |
| 62 | 5 | 23.24 | 1890 | 155 |
| 63 | 5 | 23.24 | 1880 | 155 |
| 64 | 5 | 23.24 | 1760 | 150 |
| 65 | 5 | 23.24 | 1840 | 154 |
| 66 | 5 | 23.24 | 1730 | 149 |
| 67 | 5 | 23.63 | 535  | 86  |
| 68 | 5 | 23.63 | 941  | 111 |
| 69 | 5 | 24.01 | 1320 | 131 |
| 70 | 5 | 24.01 | 1540 | 141 |

**Table 10: Experimental data for use in modelling Fig 5 (b)**

| <b>Time (h)</b> | <b>Relative Humidity (%)</b> | <b>Temperature (°C)</b> | <b>Concentration (Bq/m<sup>3</sup>)</b> | <b>Uncertainty (Bq/m<sup>3</sup>)</b> |
|-----------------|------------------------------|-------------------------|---|---------------------------------------|
| 1               | 5                            | 21.5                    | 515                                     | 84                                    |
| 2               | 5                            | 21.5                    | 794                                     | 103                                   |
| 3               | 5                            | 21.5                    | 998                                     | 115                                   |
| 4               | 5                            | 21.5                    | 1020                                    | 80                                    |
| 5               | 5                            | 21.3                    | 1200                                    | 86                                    |
| 6               | 5                            | 21.3                    | 1260                                    | 88                                    |
| 7               | 5                            | 21.3                    | 1430                                    | 93                                    |
| 8               | 5                            | 21.3                    | 1410                                    | 93                                    |
| 9               | 5                            | 21.3                    | 1410                                    | 93                                    |
| 10              | 5                            | 21.3                    | 1420                                    | 93                                    |
| 11              | 5                            | 21.3                    | 1500                                    | 96                                    |
| 12              | 5                            | 21.3                    | 1570                                    | 98                                    |
| 13              | 5                            | 21.3                    | 1570                                    | 98                                    |
| 14              | 5                            | 21.3                    | 1510                                    | 96                                    |
| 15              | 5                            | 21.3                    | 1500                                    | 96                                    |
| 16              | 5                            | 21.3                    | 1340                                    | 90                                    |

|    |   |      |      |    |
|----|---|------|------|----|
| 17 | 5 | 21.3 | 1420 | 93 |
| 18 | 5 | 21.3 | 1470 | 95 |
| 19 | 5 | 21.3 | 1440 | 93 |
| 20 | 5 | 20.9 | 1420 | 93 |
| 21 | 5 | 20.9 | 1440 | 94 |
| 22 | 5 | 20.9 | 1370 | 91 |
| 23 | 5 | 20.9 | 1350 | 90 |
| 24 | 5 | 20.9 | 1390 | 92 |
| 25 | 5 | 20.9 | 1350 | 91 |
| 26 | 5 | 20.9 | 1330 | 90 |
| 27 | 5 | 20.9 | 1280 | 89 |
| 28 | 5 | 20.9 | 1340 | 90 |
| 29 | 5 | 21.3 | 1260 | 88 |
| 30 | 5 | 21   | 1330 | 90 |
| 31 | 5 | 21   | 1300 | 89 |
| 32 | 5 | 21   | 1400 | 93 |
| 33 | 5 | 21   | 1300 | 89 |
| 34 | 5 | 21.4 | 1220 | 87 |
| 35 | 5 | 21.4 | 1260 | 88 |
| 36 | 5 | 21.4 | 1300 | 89 |
| 37 | 5 | 21.4 | 1270 | 88 |
| 38 | 5 | 21.4 | 1210 | 86 |
| 39 | 5 | 21.4 | 1250 | 88 |
| 40 | 5 | 21.4 | 1280 | 89 |
| 41 | 5 | 21.4 | 1200 | 86 |
| 42 | 5 | 21.4 | 1190 | 86 |
| 43 | 5 | 21.4 | 1140 | 84 |
| 44 | 5 | 21.4 | 1140 | 84 |
| 45 | 5 | 21.4 | 1200 | 86 |
| 46 | 5 | 21.4 | 1160 | 84 |
| 47 | 5 | 21.4 | 1180 | 85 |
| 48 | 5 | 21.4 | 1190 | 85 |
| 49 | 5 | 21.4 | 1080 | 86 |
| 50 | 5 | 21.4 | 1100 | 82 |
| 51 | 5 | 21.4 | 1090 | 82 |
| 52 | 5 | 21.4 | 1100 | 82 |

|    |   |      |      |     |
|----|---|------|------|-----|
| 53 | 5 | 21.4 | 1050 | 81  |
| 54 | 5 | 21.4 | 1090 | 82  |
| 55 | 5 | 21.4 | 1070 | 81  |
| 56 | 5 | 21.4 | 1010 | 79  |
| 57 | 5 | 21.4 | 1000 | 79  |
| 58 | 5 | 20.7 | 1040 | 80  |
| 59 | 5 | 20.7 | 1030 | 80  |
| 60 | 5 | 20.7 | 1040 | 80  |
| 61 | 5 | 22.4 | 1030 | 80  |
| 62 | 5 | 22.4 | 901  | 75  |
| 63 | 5 | 22.4 | 1030 | 80  |
| 64 | 5 | 22.4 | 925  | 76  |
| 65 | 5 | 22.4 | 941  | 76  |
| 66 | 5 | 22.4 | 938  | 76  |
| 67 | 5 | 21.5 | 515  | 84  |
| 68 | 5 | 21.5 | 794  | 103 |
| 69 | 5 | 21.5 | 998  | 115 |
| 70 | 5 | 21.5 | 1020 | 80  |

**Table 11: Experimental data for use in modelling Fig. 5 (c)**

| <b>Time (h)</b> | <b>Relative Humidity (%)</b> | <b>Temperature (°C)</b> | <b>Concentration (Bq/m<sup>3</sup>)</b> | <b>Uncertainty (Bq/m<sup>3</sup>)</b> |
|-----------------|------------------------------|-------------------------|---|---------------------------------------|
| 1               | 5                            | 23.63                   | 125                                     | 20                                    |
| 2               | 5                            | 23.63                   | 193                                     | 25                                    |
| 3               | 5                            | 24.01                   | 242                                     | 28                                    |
| 4               | 5                            | 24.01                   | 247                                     | 19                                    |
| 5               | 5                            | 24.4                    | 293                                     | 21                                    |
| 6               | 5                            | 24.4                    | 307                                     | 21                                    |
| 7               | 5                            | 24.4                    | 349                                     | 23                                    |
| 8               | 5                            | 24.4                    | 344                                     | 23                                    |
| 9               | 5                            | 24.4                    | 344                                     | 23                                    |
| 10              | 5                            | 24.4                    | 347                                     | 23                                    |
| 11              | 5                            | 24.01                   | 366                                     | 23                                    |
| 12              | 5                            | 24.01                   | 383                                     | 24                                    |

|    |   |       |     |    |
|----|---|-------|-----|----|
| 13 | 5 | 24.01 | 383 | 24 |
| 14 | 5 | 24.01 | 368 | 23 |
| 15 | 5 | 24.01 | 366 | 23 |
| 16 | 5 | 24.01 | 327 | 22 |
| 17 | 5 | 24.01 | 347 | 23 |
| 18 | 5 | 23.63 | 359 | 23 |
| 19 | 5 | 23.63 | 351 | 23 |
| 20 | 5 | 23.24 | 351 | 23 |
| 21 | 5 | 23.24 | 355 | 23 |
| 22 | 5 | 23.24 | 338 | 23 |
| 23 | 5 | 23.24 | 333 | 22 |
| 24 | 5 | 23.63 | 343 | 23 |
| 25 | 5 | 23.63 | 333 | 23 |
| 26 | 5 | 24.01 | 328 | 22 |
| 27 | 5 | 24.4  | 316 | 22 |
| 28 | 5 | 24.4  | 331 | 22 |
| 29 | 5 | 24.4  | 307 | 21 |
| 30 | 5 | 24.4  | 327 | 22 |
| 31 | 5 | 24.4  | 320 | 22 |
| 32 | 5 | 24.4  | 345 | 23 |
| 33 | 5 | 24.4  | 320 | 22 |
| 34 | 5 | 24.4  | 297 | 21 |
| 35 | 5 | 24.01 | 307 | 21 |
| 36 | 5 | 24.01 | 316 | 22 |
| 37 | 5 | 23.63 | 309 | 21 |
| 38 | 5 | 23.63 | 294 | 21 |
| 39 | 5 | 23.63 | 304 | 21 |
| 40 | 5 | 23.24 | 311 | 22 |
| 41 | 5 | 23.24 | 292 | 21 |
| 42 | 5 | 23.24 | 290 | 21 |
| 43 | 5 | 23.24 | 277 | 20 |
| 44 | 5 | 23.24 | 277 | 20 |
| 45 | 5 | 22.86 | 292 | 21 |
| 46 | 5 | 22.86 | 282 | 21 |
| 47 | 5 | 22.86 | 287 | 21 |
| 48 | 5 | 22.86 | 290 | 21 |

|    |   |       |     |    |
|----|---|-------|-----|----|
| 49 | 5 | 23.24 | 263 | 20 |
| 50 | 5 | 23.63 | 268 | 20 |
| 51 | 5 | 24.01 | 265 | 20 |
| 52 | 5 | 24.01 | 268 | 20 |
| 53 | 5 | 24.01 | 255 | 20 |
| 54 | 5 | 24.01 | 265 | 20 |
| 55 | 5 | 24.01 | 260 | 20 |
| 56 | 5 | 24.01 | 246 | 19 |
| 57 | 5 | 24.01 | 243 | 19 |
| 58 | 5 | 24.01 | 258 | 20 |
| 59 | 5 | 23.63 | 256 | 20 |
| 60 | 5 | 23.63 | 258 | 20 |
| 61 | 5 | 23.63 | 244 | 19 |
| 62 | 5 | 23.24 | 213 | 18 |
| 63 | 5 | 23.24 | 244 | 19 |
| 64 | 5 | 23.24 | 219 | 18 |
| 65 | 5 | 23.24 | 223 | 18 |
| 66 | 5 | 23.24 | 222 | 18 |
| 67 | 5 | 23.63 | 125 | 20 |
| 68 | 5 | 23.63 | 193 | 25 |
| 69 | 5 | 24.01 | 242 | 28 |
| 70 | 5 | 24.01 | 247 | 19 |

**Table 12: Experimental data for use in modelling Fig 5 (d)**

| <b>Time (h)</b> | <b>Relative Humidity (%)</b> | <b>Temperature (°C)</b> | <b>Concentration (Bq/m<sup>3</sup>)</b> | <b>Uncertainty (Bq/m<sup>3</sup>)</b> |
|-----------------|------------------------------|-------------------------|---|---------------------------------------|
| 1               | 5                            | 23                      | 168                                     | 66                                    |
| 2               | 5                            | 22                      | 470                                     | 70                                    |
| 3               | 5                            | 22                      | 500                                     | 84                                    |
| 4               | 5                            | 23                      | 550                                     | 60                                    |
| 5               | 5                            | 23                      | 600                                     | 75                                    |
| 6               | 5                            | 23                      | 850                                     | 53                                    |
| 7               | 5                            | 23                      | 935                                     | 59                                    |
| 8               | 5                            | 23                      | 1140                                    | 51                                    |

|    |   |    |      |     |
|----|---|----|------|-----|
| 9  | 5 | 23 | 1240 | 62  |
| 10 | 5 | 22 | 1250 | 111 |
| 11 | 5 | 22 | 1280 | 122 |
| 12 | 5 | 22 | 1230 | 127 |
| 13 | 5 | 22 | 1400 | 128 |
| 14 | 5 | 22 | 1230 | 129 |
| 15 | 5 | 22 | 1400 | 127 |
| 16 | 5 | 22 | 1320 | 134 |
| 17 | 5 | 22 | 1530 | 127 |
| 18 | 5 | 22 | 1430 | 135 |
| 19 | 5 | 22 | 1460 | 131 |
| 20 | 5 | 22 | 1390 | 141 |
| 21 | 5 | 22 | 1370 | 136 |
| 22 | 5 | 22 | 1400 | 138 |
| 23 | 5 | 22 | 1410 | 134 |
| 24 | 5 | 22 | 1360 | 134 |
| 25 | 5 | 23 | 1370 | 134 |
| 26 | 5 | 23 | 1270 | 135 |
| 27 | 5 | 23 | 1330 | 135 |
| 28 | 5 | 23 | 1230 | 133 |
| 29 | 5 | 23 | 1260 | 134 |
| 30 | 5 | 23 | 1200 | 129 |
| 31 | 5 | 23 | 1340 | 131 |
| 32 | 5 | 23 | 1260 | 126 |
| 33 | 5 | 23 | 1120 | 128 |
| 34 | 5 | 23 | 1240 | 125 |
| 35 | 5 | 22 | 1430 | 132 |
| 36 | 5 | 22 | 1470 | 128 |
| 37 | 5 | 22 | 1220 | 121 |
| 38 | 5 | 22 | 1400 | 127 |
| 39 | 5 | 22 | 1360 | 136 |
| 40 | 5 | 23 | 1250 | 138 |
| 41 | 5 | 23 | 1110 | 126 |
| 42 | 5 | 22 | 1230 | 135 |
| 43 | 5 | 22 | 1150 | 133 |
| 44 | 5 | 22 | 1110 | 128 |

|    |   |    |      |     |
|----|---|----|------|-----|
| 45 | 5 | 22 | 1130 | 121 |
| 46 | 5 | 23 | 1150 | 122 |
| 47 | 5 | 23 | 1080 | 123 |
| 48 | 5 | 23 | 1150 | 119 |
| 49 | 5 | 23 | 1070 | 123 |
| 50 | 5 | 23 | 1040 | 119 |
| 51 | 5 | 23 | 1070 | 117 |
| 52 | 5 | 23 | 1040 | 119 |
| 53 | 5 | 24 | 1190 | 117 |
| 54 | 5 | 24 | 1150 | 125 |
| 55 | 5 | 24 | 1130 | 125 |
| 56 | 5 | 24 | 1090 | 123 |
| 57 | 5 | 24 | 1150 | 122 |
| 58 | 5 | 24 | 1100 | 120 |
| 59 | 5 | 24 | 1060 | 123 |
| 60 | 5 | 24 | 1120 | 120 |
| 61 | 5 | 23 | 1020 | 118 |
| 62 | 5 | 23 | 986  | 121 |
| 63 | 5 | 23 | 992  | 116 |
| 64 | 5 | 23 | 957  | 114 |
| 65 | 5 | 23 | 904  | 112 |
| 66 | 5 | 23 | 898  | 109 |
| 67 | 5 | 23 | 168  | 66  |
| 68 | 5 | 22 | 470  | 70  |
| 69 | 5 | 22 | 500  | 84  |
| 70 | 5 | 23 | 550  | 60  |

**Table 13: Experimental data for use in modelling Fig. 5(e)**

| <b>Time (h)</b> | <b>Relative Humidity (%)</b> | <b>Temperature (°C)</b> | <b>Concentration (Bq/m<sup>3</sup>)</b> | <b>Uncertainty (Bq/m<sup>3</sup>)</b> |
|-----------------|------------------------------|-------------------------|---|---------------------------------------|
| 1               | 5                            | 23.63                   | 72                                      | 12                                    |
| 2               | 5                            | 23.63                   | 126                                     | 15                                    |
| 3               | 5                            | 24.01                   | 174                                     | 17                                    |
| 4               | 5                            | 24.01                   | 203                                     | 19                                    |

|    |   |       |     |    |
|----|---|-------|-----|----|
| 5  | 5 | 24.4  | 241 | 20 |
| 6  | 5 | 24.4  | 268 | 21 |
| 7  | 5 | 24.4  | 298 | 22 |
| 8  | 5 | 24.4  | 295 | 22 |
| 9  | 5 | 24.4  | 322 | 23 |
| 10 | 5 | 24.4  | 313 | 23 |
| 11 | 5 | 24.01 | 349 | 24 |
| 12 | 5 | 24.01 | 349 | 24 |
| 13 | 5 | 24.01 | 345 | 24 |
| 14 | 5 | 24.01 | 336 | 24 |
| 15 | 5 | 24.01 | 348 | 24 |
| 16 | 5 | 24.01 | 335 | 24 |
| 17 | 5 | 24.01 | 348 | 24 |
| 18 | 5 | 23.63 | 339 | 24 |
| 19 | 5 | 23.63 | 345 | 24 |
| 20 | 5 | 23.24 | 355 | 25 |
| 21 | 5 | 23.24 | 336 | 24 |
| 22 | 5 | 23.24 | 342 | 24 |
| 23 | 5 | 23.24 | 347 | 25 |
| 24 | 5 | 23.63 | 326 | 24 |
| 25 | 5 | 23.63 | 352 | 25 |
| 26 | 5 | 24.01 | 326 | 23 |
| 27 | 5 | 24.4  | 322 | 23 |
| 28 | 5 | 24.4  | 311 | 23 |
| 29 | 5 | 24.4  | 322 | 23 |
| 30 | 5 | 24.4  | 306 | 22 |
| 31 | 5 | 24.4  | 307 | 23 |
| 32 | 5 | 24.4  | 299 | 22 |
| 33 | 5 | 24.4  | 313 | 23 |
| 34 | 5 | 24.4  | 294 | 22 |
| 35 | 5 | 24.01 | 302 | 23 |
| 36 | 5 | 24.01 | 277 | 22 |
| 37 | 5 | 23.63 | 317 | 23 |
| 38 | 5 | 23.63 | 318 | 23 |
| 39 | 5 | 23.63 | 303 | 23 |
| 40 | 5 | 23.24 | 311 | 23 |



|    |   |       |     |    |
|----|---|-------|-----|----|
| 41 | 5 | 23.24 | 298 | 23 |
| 42 | 5 | 23.24 | 309 | 23 |
| 43 | 5 | 23.24 | 314 | 23 |
| 44 | 5 | 23.24 | 288 | 23 |
| 45 | 5 | 22.86 | 311 | 23 |
| 46 | 5 | 22.86 | 288 | 23 |
| 47 | 5 | 22.86 | 271 | 22 |
| 48 | 5 | 22.86 | 285 | 23 |
| 49 | 5 | 23.24 | 269 | 22 |
| 50 | 5 | 23.63 | 266 | 21 |
| 51 | 5 | 24.01 | 279 | 22 |
| 52 | 5 | 24.01 | 270 | 21 |
| 53 | 5 | 24.01 | 274 | 21 |
| 54 | 5 | 24.01 | 254 | 21 |
| 55 | 5 | 24.01 | 258 | 21 |
| 56 | 5 | 24.01 | 249 | 20 |
| 57 | 5 | 24.01 | 264 | 21 |
| 58 | 5 | 24.01 | 270 | 21 |
| 59 | 5 | 23.63 | 262 | 21 |
| 60 | 5 | 23.63 | 259 | 21 |
| 61 | 5 | 23.63 | 237 | 20 |
| 62 | 5 | 23.24 | 258 | 21 |
| 63 | 5 | 23.24 | 257 | 21 |
| 64 | 5 | 23.24 | 240 | 20 |
| 65 | 5 | 23.24 | 251 | 21 |
| 66 | 5 | 23.24 | 236 | 20 |
| 67 | 5 | 23.63 | 72  | 12 |
| 68 | 5 | 23.63 | 126 | 15 |
| 69 | 5 | 24.01 | 174 | 17 |
| 70 | 5 | 24.01 | 203 | 19 |

## REFERENCES

Aghamiri S.M.R., Ghorbani Z., Darafsheh A., Torabzadeh H., Fathivand A.A., Minucheher A, Jalinoos A. <sup>226</sup>Ra concentration in the teeth of habitants of areas with high level of natural radioactivity in Ramsar. *Journal of Environmental Radioactivity* 89 (2006) 212-218.

Alavanja M.C.R. *Biologic damage resulting from exposure to tobacco smoke and from radon: implication for preventive interventions.* *Oncogene* (2002) 21, 7365 - 7375.

Al-Hamarneh I.F., Awadallah M.I. *Soil radioactivity levels and radiation hazard assessment in the highlands of northern Jordan.* *Radiation Measurements* 44 (2009) 102–110.

Al-Kazwini A.T., Hasan M.A. *Radon concentration in Jordanian drinking water and hot springs.* *J. Radiol. Prot.* 23 (2003) 439–448



Amrani D. and Cherouati D.E. *Health effects from radon-222 in drinking water in Algiers.* *J. Radiol. Prot.* 1999 Vol. 19 No 3 275–279.

Barros-Dios J.M., Barreiro M.A., Ruano-Ravina A., and Figueiras A. *Exposure to Residential Radon and Lung Cancer in Spain: A Population-based Case-Control Study.* *American Journal of Epidemiol* Vol. 156, No. 6, 2002.

Burnett W.C., Dulaiova H. *Radon as a tracer of submarine groundwater discharge into a boat basin in Donnalucata, Sicily.* *Continental Shelf Research* 26 (2006) 862–873.

Burnett, W.C., Santos, I.R., Weinstein, Y., Swarzenski, P.W., Herut, B., 2007. *Remaining uncertainties in the use of Rn-222 as a quantitative tracer of submarine groundwater discharge.* In: Sanford, W., Langevin, C., Polemio, M., Povinec, P. (Eds.), *A New Focus on Groundwater–Seawater Interactions.* IAHS Publ. 312, Perugia, Italy, pp. 109–118.

Burnett W.C., Peterson R.N., Santos I.R., Hicks R.W. *Use of automated radon measurements for rapid assessment of groundwater flow into Florida streams*. Journal of Hydrology 380 (2010) 298–304

Calugaru D.-G., Crolet J.-M. *Identification of radon transfer velocity coefficient between liquid and gaseous phases*. C. R. Mecanique 330 (2002) 377–382.

Carvalho F.P. and Oliveira J.M. *Polonium in Cigarette Smoke and Radiation Exposure of Lungs*. Czech. J. Phys. 56 (2006).

Chang B.U., Koh S.M., Kim Y.J., Seo J.S., Yoon Y.Y., Row J.W., Lee D.M. *Nationwide survey on the natural radionuclides in industrial raw minerals in South Korea*. Journal of Environmental Radioactivity 99 (2008) 455-460

Chen S.B., Zhu Y.G., Hu Q.H. *Soil to plant transfer of  $^{238}\text{U}$ ,  $^{226}\text{Ra}$  and  $^{232}\text{Th}$  on a uranium mining-impacted soil from south-eastern China*. Journal of Environmental Radioactivity 82 (2005) 223-236.

Cosma C., Moldovan M., Dicu T., Kovacs T. *Radon in water from Transylvania (Romania)*, Radiation Measurement (2008).

Davis S.N., DeWiest R.J. 1966, *Hydrogeology*, John Wiley & Sons, New York, pp. 44-46

Dimova N., Burnett W.C., Horwitz E.P., Lane-Smith D. *Automated measurement of  $^{224}\text{Ra}$  and  $^{226}\text{Ra}$  in water*. Applied Radiation and Isotopes 65 (2007) 428–434.

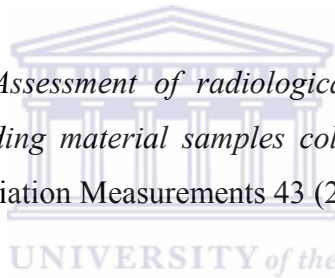
Dulaiova H., Gonenea M.E., Henderson P. B., and Charette M.A. *Geochemical and physical sources of radon variation in a subterranean estuary – Implications for groundwater radon activities in submarine groundwater discharge studies*, Marine Chemistry, **110**, 120-127.

Edson J.B., Degrandpre M.D., Frew N., and McGillis W.R. *Investigations of Air-Sea Gas Exchange*. Journal of the Oceanography Society Oceanography, Volume 21, Number 4. 2008

Eff-Darwich A, Viñas R., Soler V., de la Nuez J., Quesada M.L. *Natural air ventilation in underground galleries as a tool to increase radon sampling volumes for geologic monitoring*. Radiation Measurements 43 (2008) 1429–1436

Elmaghraby E.K., Lofty Y.A. *Differentiation between earthquake radon anomalies and those arising from nuclear activities*. Journal of Applied Radiation and Isotopes 67 (2009) 208-211.

Faheema M., Mujahid S.A. *Assessment of radiological hazards due to the natural radioactivity in soil and Building material samples collected from six districts of the Punjab province-Pakistan*. Radiation Measurements 43 (2008) 1443–1447.



Field R.W. *Radon Occurrence and Health Risk* (Adapted from Field RW, Occupational Medicine Secrets, Hanley and Belfus, Philadelphia, 1999).

Gainon F., Goldscheider N. & Surbeck H. *Conceptual model for the origin of high radon levels in spring waters—the example of the St. Placidus spring, Grisons, Swiss Alps*. Swiss j. geosci. 100 (2007) 251–262.

Ghose D., Paul D., Sastri R.C. *Radon as a tracer for helium exploration in geothermal areas*. Radiation Measurements 36 (2003) 375–377.

Jones E.R., and Childers R. L. 1990, *Contemporary College Physics*, Addison-Wesley Publishing. pp 832-848.

Kaplan I. 1955. *Nuclear Physics*, Addison-Wesley Publishing Company, Inc, United States of America, pp 208

Kawabata H., Narita H., Harada K., Tsunogai S. and Kusakabe M. *Air-Sea Gas Transfer Velocity in Stormy Winter Estimated from Radon Deficiency*, Journal of Oceanography, Vol. 59, pp. 651 to 661, 2003

Knoll G.F. 2000, *Radiation Detection and Measurement*, 3<sup>rd</sup> ed. John Wiley & Sons, New York, pp. 48-52.

Lapp R.E., Andrews H.L. 1972, *Nuclear Radiation Physics*, 4<sup>th</sup> Edition. pp 158-165.

Lauria D.C., Ribeiro F.C.A., Conti C.C., Loureiro F.A. *Radium and uranium levels in vegetables grown using different farming management systems*. Journal of Environmental Radioactivity 100 (2009) 176–183.

Lee J.-M, Kim G. *A simple and rapid method for analyzing radon in coastal and groundwaters using a radon-in-air monitor*. Journal of Environmental Radioactivity 89 (2006) 219-228.

Lehnert B.E. and Goodwin E.H. *A New Mechanism for DNA Alterations Induced by Alpha Particles Such as Those Emitted by Radon and Radon Progeny*. Environ Health Perspect 105 (Suppl. 5):1095-1101 (1997).

Lilley J.S. 2001, *Nuclear Physics, Principles and Applications*, John Wiley & Sons, New York. pp 13-15.

Loureiro C.O., and Abriola L.M., Martin J.E., Sextro R.G. *Three-Dimensional Simulation of Radon Transport into Houses with Basements under Constant Negative Pressure*. Environ. Sci. Technol. 1990, 24, 1338-1348.

Marques A.L., Dos Santos W., Geraldo L.P. *Direct measurements of radon activity in water from various natural sources using nuclear track detectors*. Applied Radiation and Isotopes 60 (2004) 801–804.

Masaro L., Zhu X.X. *Physical models of diffusion for polymer solutions, gels and solids*. Prog. Polym. Sci. 24 (1999) 731–775.

McCoy C.A., Corhert D.R. *Review of submarine groundwater discharge (SGD) in coastal zones of the Southeast and Gulf regions of the United States with management implications*. Journal of Environmental Management 90 (2009) 644-651.

Mohamed A., Ahmed A.A., Ali A.E., Yuness M. *Attached and Unattached Activity Size Distribution of Short-Lived Radon Progeny  $^{214}\text{Pb}$  and Evaluation of Deposition Fraction*. Journal of Nuclear and Radiation Physics, Vol. 3, No. 2, 2008, pp. 101-108.

Nain M., Chauhan R.P., Chakarvarti S.K. *Alpha radioactivity in tobacco leaves: Effect of fertilizers*. Radiation Measurements 43 (2008) S515–S519.

Nazaroff W.W., Doyle S.M., Nero A.V. and Sextro R.G. *Potable Water as a Source of Airborne  $^{222}\text{Rn}$  in U.S. Dwellings: A Review and Assessment*. Health Physics Vol. 52, No.3 (March), pp. 281-295, 1987

Othman M.R., Lee O.E and Fernando W.J.N. *Gas Adsorption and Surface Diffusion on 5Å Microporous Adsorbent in Transition and Turbulent Flow Region*. IIUM Engineering Journal, Vol. 7, No. 1, 2006.

Othman I., Al Masri M.S. *Impact of phosphate industry on the environment: A case study*. Applied Radiation and Isotopes 65 (2007) 131–141.

Papastefanou C. *Radioactivity of Tobacco Leaves and Radiation Dose Induced from Smoking*. Int. J. Environ. Res. Public Health 2009, 6(2), 558-567.

Picolo J.L., Pressyanov D., Blanchis P., Barbier M., Michielsen N., Grassin D., Voisin V., Turek K. *A radon 222 traceability chain from primary standard to field detectors*. Radiation and Isotopes 52 (2000) 427-434.

Prasad G., Prasad Y., Gusain G.S., Ramola R.C. *Measurement of radon and thoron levels in soil, water and indoor atmosphere of Budhakedar in Garhwal Himalaya, India*. Radiation Measurements 43 (2008) S375–S379.

Prueitt R.L., Goodman J.E., Valberg P.A. *Radionuclides in cigarettes may lead to carcinogenesis via p16<sup>INK4a</sup> inactivation*. Journal of Environmental Radioactivity 100 (2009) 157–161.

Radolic, V., Vukovic, B., Smit, G., Stanic, D., Planinic, J., 2005. *Radon in the spas of Croatia*. J. Environ. Radioact. 83, 191–198.

Rebour V., Billiotte J., Deveughele M., Jambon A., le Guen C. *Molecular diffusion in water-saturated rocks: A new experimental method*. Journal of Contaminant Hydrology 28 (1997) 71-93.

Savidou A., Kehagia K., Eleftheriadis K. *Concentration levels of <sup>210</sup>Pb and <sup>210</sup>Po in dry tobacco leaves in Greece*. Journal of Environmental Radioactivity 85 (2006) 94-102.

Schiavo M.A., Hauser S., and Povinec P.P. *Isotope distribution of dissolved carbonate species in south-eastern coastal aquifers of Sicily (Italy)*. Hydrol. Process. 21, 2690–2697 (2007).

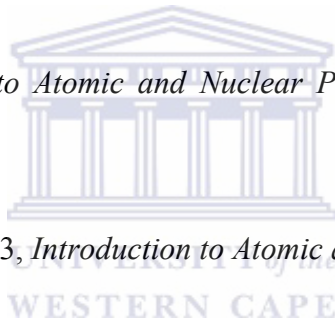
Schiavo M.A., Hauser S., Povinec P.P. *Stable isotopes of water as a tool to study groundwater–seawater interactions in coastal south-eastern Sicily*. Journal of Hydrology (2009) 364, 40– 49.

Schmidt A., Schlueter M., Melles M., Schubert M. *Continuous and discrete on-site detection of  $^{222}\text{Rn}$  in ground- and surface waters by means of an extraction module.* Journal of Applied Radiation and Isotopes 66 (2008) 1939–1944.

Schmidt A., Gibson J.J., Santos I.R., Schubert M., Tattrie K., and Weiss H. *The contribution of groundwater discharge to the overall water budget of two typical Boreal lakes in Alberta/Canada estimated from a radon mass balance.* Hydrol. Earth Syst. Sci., 14, 79–89, 2010.

Schubert M., Schmidt A., Paschke A., Lopez A., Balcázar M. *In situ determination of radon in surface water bodies by means of hydrophobic membrane tubing.* Radiation Measurements 43 (2008) 111–120.

Semat H. 1954, *Introduction to Atomic and Nuclear Physics*, 3<sup>rd</sup> Edition, New York, Chapman Hall, pp 306



Semat H. and Albright J.R. 1973, *Introduction to Atomic and Nuclear Physics*, 5<sup>th</sup> Edition, pp 457

Singh J., Singh H., Singh S., Bajwa B.S. *Estimation of uranium and radon concentration in some drinking water samples.* Radiation Measurements 43 (2008) S523–S526.

Somlai K., Tokonami S., Ishikawa T., Vancsura P., Gáspár M., Jobbágy V., Somlai J., Kovács T.  *$^{222}\text{Rn}$  concentrations of water in the Balaton Highland and in the southern part of Hungary, and the assessment of the resulting dose.* Radiation Measurements 42 (2007) 491–495

Stieglitz T. *Submarine groundwater discharge into the near-shore zone of the Great Barrier Reef, Australia,* Marine Pollution Bulletin 51 (2005) 51–59.



Surbeck H. *Dissolved gases as natural tracers in karst hydrogeology; radon and beyond*. Center of Hydrogeology (CHYN), University of Neuchâtel, Emile-Argand 11, CH-2007 Neuchâtel, Switzerland.

Taniguchi M., Turner J.V., and Smith A.J. *Evaluations of Groundwater Discharge Rates from Subsurface Temperature in Cockburn Sound, Western Australia*. Biogeochemistry 66: 111–124, 2003.

Thakre S.B., Bhuyar L.B., Deshmukh S.J. *Mathematical models for overall gas transfer coefficient using different theories and evaluating their measurement accuracy*. International Journal of Chemical and Biomolecular engineering 1:4 2008

United State Environmental Protection agency (USEPA), 1999. Office of ground water and drinking water rule: Technical fact sheet EPA 815-F-99-006, Washington, DC: USEPA.

Urosevic V., Nikezic D., Vulovic S. *A theoretical approach to indoor Radon and Thoron distribution*. Journal of Environmental Radioactivity 99 (2008) 1829–1833.

Van Giap T. *Use of Radon-222 as Tracer to Estimate Groundwater Infiltration Velocity in a River Bank Area*. Nuclear Science and Technology, Vol. 2, No. 2 (2003), pp. 12-17.

Vinson D.S., Campbell T.R., Vengosh A. *Radon transfer from groundwater used in showers to indoor air*. Applied Geochemistry 23 (2008) 2676–2685.

Walia V., Quattrocchi F., Virk H.S., Yang T.F., Pizzino L., and Bajwa B.S. *Radon, Helium and uranium survey in some thermal springs located in NW Himalayas, India: mobilization by tectonic features or by geochemical barriers?* Journal of Environmental Monitoring, 2005, 7, 850–855.

Wanninkhof R., Asher W. E., Ho D.T., Sweeney C, and McGillis W.R. *Advances in Quantifying Air-Sea Gas Exchange and Environmental Forcing*. Annu. Rev. Marine. Sci. 2009. 1:213-44.

Waska H., Kim S., Kim G, Peterson R.N., Burnett W.C. *An efficient and simple method for measuring <sup>226</sup>Ra using the scintillation cell in a delayed coincidence counting system (RaDeCC)*. Journal of Environmental Radioactivity 99 (2008) 1859–1862.

Williams-Jones G., Stix J., Heiligmann M., Charland A., Lollar B.S., Garzón N.A.G., Barquero V.J., Fernandez E.. *A model of diffuse degassing at three subduction-related volcanoes*. Bull Volcanol (2000) 62: 130-142.

Wu Y., Wen X., Zhang Y. *Analysis of the exchange of groundwater and river water by using Radon-222 in the middle Heihe Basin of northwestern China*. Environmental Geology (2004) 45:647–653.

Yngveson A., Williams C., Hjerpe A., Lundeberg J., Söderkvist P. and Pershagen G. *p53 Mutations in Lung Cancer Associated with Residential Radon Exposure*. Cancer Epidemiol Biomarkers Prev . Vol. 8, 433–438, May 1999.

Zhuo W., Guo Q., Chen B., Cheng G. *Estimating the amount and distribution of radon flux density from the soil surface in China*. Journal of Environmental Radioactivity 99 (2008) 1143-1148.

## NOMENCLATURE

|             |  |
|-------------|--|
| $C_{Rn}$    | Radon concentration (Bq/m <sup>3</sup> )                                     |
| $C_w(t,T)$  | Radon concentration in water (Bq/m <sup>3</sup> )                            |
| $C_a(t,T)$  | Radon concentration in air (Bq/m <sup>3</sup> )                              |
| $\alpha(T)$ | Ostwald solubility coefficient $\alpha = C_w/C_a$ , radon's water solubility |
| $N_a$       | Number of radon nuclei in air (moles)  |
| $V_a$       | Volume of air above the source (m <sup>3</sup> )                             |
| $N_w$       | Number of radon nuclei in water (moles)                                      |
| $V_w$       | Volume of water (radon source) (m <sup>3</sup> )                             |
| $J, F(t,T)$ | Radon flux (Bq/m <sup>2</sup> s)   |
| $A$         | Water-air interface area   |

### *Subscripts*

|     |                               |
|-----|-------------------------------|
| $i$ | an iterative index $i \geq 0$ |
| $w$ | water                         |
| $a$ | air                           |

### *Greek letters*

|             |                                     |
|-------------|-------------------------------------|
| $\alpha$    | Ostwald solubility coefficient      |
| $\beta$     | Transfer velocity coefficient (m/s) |
| $\gamma$    | Gamma ray                           |
| $\nu$       | Neutrino                            |
| $\bar{\nu}$ | Antineutrino                        |



# **GLOSSARY**

## **Absorbed Dose**

The amount of energy imparted to matter by ionizing radiation per unit mass of irradiated material. The unit of absorbed dose is the Rad.

## **Activity**

The number of nuclear disintegrations by radionuclide per unit time.

## **Alpha particle**

A positively charged particle (identical to the helium nucleus) composed of two protons and two neutrons that are emitted during decay of certain radioactive atoms. Several centimeters of air or a sheet of paper stops them. A strongly ionizing particle emitted from the heavy nucleus during radioactive decay.

## **Antineutrino**

The uncharged particles of zero rest mass but high energy, emitted in negative beta decay.

## **Aquifer**

A saturated layer of rock or soil below the ground surface that can supply usable quantities of groundwater to wells and springs. The aquifers can be a source of water for domestic, agricultural, and industrial uses.

## **Atom**

Smallest particle of an element, which is capable of entering into a chemical reaction.

## **Attenuation**

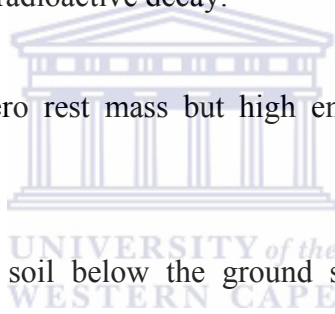
The process by which the radiation beam is reduced in intensity when passing through some material. It is the combination of absorption and scattering processes and leads to a decrease in flux density of the beam when projected through matter of high density.

## **Background Radiation**

Ionizing radiation arising from radioactive material other than the one directly under consideration.

## **Becquerel**

The SI unit of radioactivity that is equivalent to one disintegration per second.



**Beta Particle**

Beam of electrons emitted from the nucleus of an atom during radioactive decay.

**Cosmic Radiation**

Penetrating ionizing radiation, both particulate and photonic, originating in space.

**Charged Particle**

An ion. An elementary particle carrying a positive or negative electric charge.

**Compton Effect**

The Compton Effect (also called Compton scattering) is the result of a high-energy photon colliding with a target, which releases loosely bound electrons from the outer shell of the atom or molecule.

**Concentration**

The activity of radon gas in terms of decays per time in a volume of air. The unit of radioactivity concentration is given in Becquerel per cubic meter ( $\text{Bq}/\text{m}^3$ ).

**Cosmic Radiation**

Streams of highly penetrating radiations of charged particles bombarding the earth with the origin from outer space. It is made up mainly of protons, helium, and heavy ions with high kinetic energies.

**Curie**

The unit of radioactivity defined as  $3.7 \times 10^{10}$  nuclear transformation per second. The acronym of the curie unit is Ci.

**Daughter product, progenies**

The radioactive decay produces the isotopes. In the case of radium-226, for example, there are ten successive daughter products, ending in the stable isotope lead-206.

**Decay**

The disintegration of the nucleus of an unstable nuclide by the spontaneous emission of charged particulate and or photonic radiations.

**Diffusion**

The migration of particles from one region to another due to concentration gradient.

**Diffusion equation**

The partial differential equation that describes density fluctuations in a material undergoing diffusion.

**DNA**

Acronym of deoxyribonucleic acid, especially carrying genetic information in chromosomes.

**Electromagnetic Radiation**

A travelling wave motion resulting from changing electric or magnetic fields. Familiar electromagnetic radiations range from X-rays and gamma rays of short wavelength.

**Electron**

Negatively charged elementary particle that is a constituent of every neutral atom. Its unit of negative electricity equals  $1.9 \times 10^{-19}$  coulombs. Its mass is 0.000549 amu.

**Emission**

A gaseous waste discharged to the environment.

**Exposure**

The amount of time a person spends in any given radon concentration. It is determined by multiplying the radon concentration, measured in  $\text{Bq/m}^3$  of each area by the amount of time spent in that area. A measure of the ionization produced in air by X-ray or gamma radiation.

**External Radiation**

Radiation originating from a source outside the body. PE

**Gamma Radiation**

It is electromagnetic radiation of high frequency originating from the nucleus and possessing neither mass nor charge. Because of its short wavelength (high energy), gamma radiation can cause ionization.

**Groundwater**

Groundwater can be described as the water that occurs under the ground. It is a vast and slow moving resource, which greatly exceeds the volume of other available freshwater sources. The study of groundwater is known as hydrogeology.

**Half-Life, Radioactive**

Time it takes a radioactive substance to lose 50 percent of its activity by decay. Each radionuclide has a unique half-life.

**Ion**

An atom that has too many or too few electrons, causing it to be chemically reactive, such as an electron that is not associated (in orbit) with a nucleus. Ions may be positively or negatively charged, and vary in size.

**Ionization**

The process by which a neutral atom or molecule acquires either a positive or a negative charge.

**Ionizing Radiation**

Any radiation capable of displacing electrons from atoms or molecules, thereby producing ions. This may mean alpha particles, beta particles, high-speed electrons, high-speed protons, and or electromagnetic radiation capable of producing ions.

**Isotopes**

The nuclides having the same number of protons in their nuclei, and hence having the same atomic number, but differing in the number of neutrons, and therefore in the mass number. Almost identical chemical properties exist between isotopes of a particular element.

**Molecule**

A group of atoms held together by chemical forces. A molecule is the smallest unit of a compound that can exist by itself and retain all its chemical properties.

**Natural background radiation**

Ionizing radiation, not from artificial sources, arising from radioactive material other than the one directly under consideration. Natural radiation due to cosmic rays, soil, natural radiation in the human body and other sources of natural radioactivity are always present.

**Neutron**

An elementary particle with a mass nearly the same as that of a proton and electrically neutral. It has a half-life in minutes and decays into the proton and the electron. It is found in the nucleus of every atom heavier than hydrogen.

**Neutrino**

The uncharged particles of zero rest mass but high energy, emitted in positive beta decay.

**Nucleus**

The small central, positively charged region of an atom that carries essentially all the mass. With the exception of hydrogen, which has a single proton, all atomic nuclei contain both protons and neutrons.

**Numerical Modelling**

A simplified description of a system to assist calculations and predictions.

**Pair production**

The conversion of the entire photon of energy in the field of an atom into the creation of an electron-positron pair.

**Photoelectric Effect**

The transfer of energy from light rays that touch the electrons in a substance.

**Photon**

A quantum (or packet) of energy emitted in the form of electromagnetic radiation.

Gamma rays and X-rays are examples of photons.

**Positron**

A particle equal in mass, but opposite in charge, to the electron; a positive charge.

**Proton**

An elementary particle in the nucleus of all atoms, elementary particle with a positive electrical charge.

**Radioisotope**

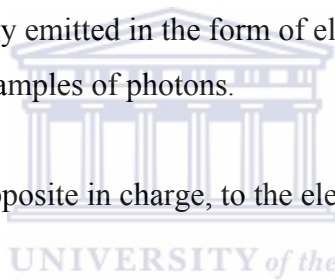
A nuclide with an unstable ratio of neutrons to protons placing the nucleus in a state of stress. In an attempt to reorganize to a more stable state, it may undergo various types of rearrangement that involve the release of radiation.

**Radiation**

Radiation is energy that is transported as waves or particles. The term mostly used for invisible energy.

**Radionuclide**

An unstable nuclide capable of spontaneous transformation into other nuclides through changes in its nuclear configuration or energy level. This transformation is accompanied by the emission of photons or particles.





**Shielding Material**

Any material used to absorb radiation falling on its surface and consequently reduces the intensity of radiation and in some cases eliminates it.

**Stable nuclide**

An element that does not undergo nuclear transformations.

**Terrestrial Radiation**

Radiation emitted by naturally occurring radionuclides such as potassium-40 ( $^{40}\text{K}$ ); the natural decay chains of uranium-235 ( $^{235}\text{U}$ ), uranium-238 ( $^{238}\text{U}$ ), or thorium-232 ( $^{232}\text{Th}$ ); or cosmic-ray-induced radionuclides in the soil.

**Tracer**

The isotope of an element which may be incorporated into a sample to make possible observation of the course of that element, alone or in combination, through a chemical, biological, or physical process. The observations may be made by measurement of radioactivity or of isotopic abundance.

**Uncertainty**

A process of identifying the errors in a measurement and quantifying their effects.

**Uranium**

Uranium is a radioactive element that occurs naturally in low concentrations in soil, rock, surface water, and groundwater. It is the predecessor of radon and its isotopes.

**Water Table**

The water level surface below the ground at which the unsaturated zone ends and the saturated zone begins.

**X-rays**

Penetrating electromagnetic radiations with wavelengths shorter than those of visible light. They are usually produced by bombarding a metallic target with fast electrons in a high vacuum.

